# USE OF PARTICLE SWARM OPTIMIZATION ALGORITHM TO REDUCE DRILLING COSTS BY FINDING OPTIMAL OPERATIONAL PARAMETERS

By

RYAN SELF

Bachelor of Science in Mechanical Engineering

Oklahoma State University

Stillwater, Oklahoma

2014

Submitted to the Faculty of the
Graduate College of the
Oklahoma State University
in partial fulfillment of
the requirements for
the Degree of
MASTER OF SCIENCE
July, 2016

USE OF PARTICLE SWARM OPTIMIZATION ALGORITHM TO REDUCE DRILLING COSTS BY FINDING OPTIMAL OPERATIONAL PARAMETERS

Thesis Approved:

Dr. Geir Hareland

Thesis Advisor

Dr. Brian Elbing

Dr. He Bai

# ACKNOWLEDGEMENTS

I would first like to thank my advisor, Dr. Geir Hareland, for his time and patience in guiding me through this research. His direction and expertise in the drilling area, allowed me to develop this research idea, and he consistently knew when to help guide me through my struggles and when to allow me to challenge myself when faced with difficulties through my research.

I would also like to thank all of my lab members working with me for their additional help throughout my master's program. In particular, Amin Atashnezhad, who worked countless hours with me, and gave me valuable advice throughout the entire process.

Additionally, I would like to thank my committee members; Dr. Brian Elbing and Dr. He Bai, for taking the time to review my thesis, and am very grateful for their valuable input.

Finally, I would like to thank my parents and my girlfriend for their continued support and patience over the years. They supported me through this entire time and I could not have accomplished this without them. Thank you.

Name: RYAN SELF

Date of Degree: JULY, 2016

Title of Study: USE OF PARTCILE SWARM OPTIMIZATION ALGORITHM TO REDUCE DRILLING COSTS BY FINDING OPTIMAL OPERATIONAL PARAMETERS

Major Field: MECHANICAL AND AEROSPACE ENGINEERING

Abstract: Oil and gas companies have played a major role in the energy sector, and constantly try to develop technology to maximize their overall revenue. One of the more substantial feats was the developed equipment that allowed for horizontal wells. These horizontal sections allow much more oil to reach the wellbore due to the extended length into reservoir supplies. However, as the wells continue to get drilled farther, the cost of drilling the wells continue to rise. Now more than ever, there is an increased need for better drilling optimization techniques, which could potentially reduce these drilling costs and increase the overall profit. Many individuals have researched optimizing constant operational parameters; however, these constant variables lead to wasted time and money for the operators. This is because formation variables constantly change throughout the drilling process; therefore, the concept of dynamic variables allow drillers to alter the drilling parameters to better adjust for changes in the formation. The research presented herein, incorporates a particle swarm optimization (PSO) algorithm to optimize operational parameters, weight on bit (WOB), revolutions per minute (RPM) of the bit, bit pull depth, and bit combination, with the goal to decrease the overall drilling cost per foot. A rate of penetration (ROP) model was incorporated with the PSO algorithm in order to calculate the drilling time and the associated costs from the given parameters. This research could be applied in numerous ways including as an artificial intelligence optimizer in an existing drilling simulator, or directly integrated by drilling engineers during the planning stage. Long term use for this algorithm is to be the foundation for an autonomous driller including being the real time optimal solver.

TABLE OF CONTENTS

Chapter Page

I. INTRODUCTION ..... 1

1.1 Motivation ..... 2
1.2 Drilling Today ..... 3

II. REVIEW OF LITERATURE ..... 5

2.1 Optimization Techniques ..... 5
2.2 Drilling Optimization ..... 6
2.3 Rate of Penetration Modeling ..... 8

III. METHODOLOGY ..... 11

3.1 Particle Swarm Optimization ..... 11
3.2 Rate of Penetration Model ..... 13
3.2.1 Model Correlation ..... 15

IV. RESULTS ..... 19

4.1 One Bit Optimization ..... 20
4.1.1 One Constant Rock Strength and Constant RPM ..... 21
4.1.2 Two Constant Rock Strengths and Constant RPM ..... 23
4.1.3 One Constant Rock Strength ..... 26
4.1.4 Two Constant Rock Strengths ..... 29
4.1.5 Three Constant Rock Strengths and Constant Abrasiveness ..... 31
4.1.6 Three Constant Rock Strengths and Changing Abrasiveness ..... 35
4.2 Two Bit Optimization ..... 38
4.2.1 Three Constant Rock Strengths, Increasing Left to Right ..... 39
4.2.2 Three Constant Rock Strengths, Decreasing Left to Right ..... 43
4.3 Field Case Validation ..... 46
4.3.1 WOB and RPM Optimization ..... 49
4.3.2 WOB, RPM, and Pull Depth Optimization ..... 51
4.3.3 WOB, RPM, Pull Depth, and Bit Selection Optimization ..... 54
4.3.4 Field Case Results ..... 56

Chapter Page

V. DISCUSSION .....59

VI. CONCLUSION.....64

6.1 Summary .....64
6.2 Future Work .....64

REFERENCES .....66

APPENDIX.....69

LIST OF TABLES

Table Page

Table 1: Data table for one rock strength scenario; 15,000 psi, and constant 150 RPM ..... 23
Table 2: Data table for two rock strength scenario; 10,000 and 20,000 psi, and constant 150 RPM ..... 26
Table 3: Data table for one rock strength scenario; 15,000 psi ..... 28
Table 4: Data table for two rock strength scenario; 10,000 and 20,000 psi ..... 31
Table 5: Data table for the three rock strength scenario; 10,000, 15,000, and 20,000 psi, with constant abrasiveness ..... 34
Table 6: Data table for the three rock strength scenario; 10,000, 15,000, and 20,000 psi, with changing abrasiveness ..... 37
Table 7: Two bit selection options for PSO algorithm ..... 38
Table 8: Data table for the three rock strength, multiple bit scenario; 10,000, 15,000, and 20,000 psi ..... 41
Table 9: Data table for the three rock strength, multiple bit scenario; 20,000, 15,000, and 10,000 psi ..... 45
Table 10: Two bits used in field case ..... 48
Table 11: Rotating time and cost for real field case data ..... 56
Table 12: Rotating time and cost for WOB and RPM Optimization ..... 57
Table 13: Rotating time and cost for WOB, RPM, and Pull Depth Optimization ..... 57
Table 14: Rotating time and cost for WOB, RPM, Pull Depth, and Bit Combination Optimization ..... 58
Table A-1: Data from WOB and RPM Optimization of Field Case ..... 69
Table A-2: Data from WOB, RPM, and Pull Depth Optimization of Field Case ..... 70
Table A-3: Data from WOB, RPM, Pull Depth, and Bit Combination Optimization of Field Case ..... 71

LIST OF FIGURES

Figure Page

Figure 1: Reported ROP data and calculated ROP vs. applied WOB in Limestone formation drill off test ..... 16
Figure 2: Reported ROP data vs. calculated ROP in Limestone formation drill off test ..... 16
Figure 3: Reported ROP data and calculated ROP vs. applied WOB in Shale formation drill off test ..... 17
Figure 4: Reported ROP data vs. calculated ROP in Shale formation drill off test ..... 17
Figure 5: Reported ROP data and calculated ROP vs. applied WOB in an additional Shale formation drill off test ..... 18
Figure 6: Reported ROP data vs. calculated ROP in an additional Shale formation drill off test ..... 18
Figure 7: Graph showing the one rock strength scenario; 15,000 psi, and constant 150 RPM ..... 21
Figure 8: Optimal WOB for one rock strength scenario; 15,000 psi, and constant 150 RPM ..... 21
Figure 9: Constant RPM input for one rock strength scenario; 15,000 psi ..... 22
Figure 10: Calculated ROP for one rock strength scenario; 15,000 psi, and constant 150 RPM ..... 22
Figure 11: Learning curve for one rock strength scenario; 15,000 psi, and constant 150 RPM ..... 23
Figure 12: Graph showing the two rock strength scenario; 10,000 and 20,000 psi, and constant 150 RPM ..... 24
Figure 13: Optimal WOB for two rock strength scenario; 10,000 and 20,000 psi, and constant 150 RPM ..... 24
Figure 14: Constant RPM input for two rock strength scenario; 10,000 and 20,000 psi ..... 24
Figure 15: Calculated ROP for two rock strength scenario; 10,000 and 20,000 psi, and constant 150 RPM ..... 25
Figure 16: Learning curve for two rock strength scenario; 10,000 and 20,000 psi, and constant 150 RPM ..... 25
Figure 17: Graph showing the one rock strength scenario; 15,000 psi ..... 26
Figure 18: Optimal WOB for one rock strength scenario; 15,000 psi ..... 27
Figure 19: Optimal RPM for one rock strength scenario; 15,000 psi ..... 27
Figure 20: Calculated ROP for one rock strength scenario; 15,000 psi ..... 27
Figure 21: Learning curve for one rock strength scenario; 15,000 psi ..... 28
Figure 22: Graph showing the two rock strength scenario; 10,000 and 20,000 psi ..... 29

Figure Page

Figure 23: Optimal WOB for two rock strength scenario; 10,000 and 20,000 psi ...29
Figure 24: Optimal RPM for two rock strength scenario; 10,000 and 20,000 psi ....30
Figure 25: Calculated ROP for two rock strength scenario; 10,000 and 20,000 psi .....30
Figure 26: Learning curve for two rock strength scenario; 10,000 and 20,000 psi ..31
Figure 27: Graph showing the three rock strength scenario; 10,000, 15,000, and 20,000 psi, with constant abrasiveness .....32
Figure 28: Optimal WOB for the three rock strength scenario; 10,000, 15,000, and 20,000 psi, with constant abrasiveness .....32
Figure 29: Optimal RPM for the three rock strength scenario; 10,000, 15,000, and 20,000 psi, with constant abrasiveness .....33
Figure 30: Calculated ROP for the three rock strength scenario; 10,000, 15,000, and 20,000 psi, with constant abrasiveness .....33
Figure 31: Learning curve for the three rock strength scenario; 10,000, 15,000, and 20,000 psi, with constant abrasiveness .....34
Figure 32: Graph showing the three rock strength scenario; 10,000, 15,000, and 20,000 psi, with changing abrasiveness .....35
Figure 33: Optimal WOB for the three rock strength scenario; 10,000, 15,000, and 20,000 psi, with changing abrasiveness .....35
Figure 34: Optimal RPM for the three rock strength scenario; 10,000, 15,000, and 20,000 psi, with changing abrasiveness .....36
Figure 35: Calculated ROP for the three rock strength scenario; 10,000, 15,000, and 20,000 psi, with changing abrasiveness .....36
Figure 36: Learning curve for the three rock strength scenario; 10,000, 15,000, and 20,000 psi, with changing abrasiveness .....37
Figure 37: Graph showing the three rock strength, multiple bit scenario; 10,000, 15,000, and 20,000 psi .....39
Figure 38: Optimal WOB for the three rock strength, multiple bit scenario; 10,000, 15,000, and 20,000 psi .....39
Figure 39: Optimal RPM for the three rock strength, multiple bit scenario; 10,000, 15,000, and 20,000 psi .....40
Figure 40: Calculated ROP for the three rock strength, multiple bit scenario; 10,000, 15,000, and 20,000 psi .....40
Figure 41: Learning curve for the three rock strength, multiple bit scenario; 10,000, 15,000, and 20,000 psi .....41
Figure 42: Graph for three rock strength, increasing left to right, showing optimal drilling cost with changing pull depth .....42
Figure 43: Graph showing the three rock strength, multiple bit scenario; 20,000, 15,000, and 10,000 psi .....43
Figure 44: Optimal WOB for the three rock strength, multiple bit scenario; 20,000, 15,000, and 10,000 psi .....43
Figure 45: Optimal RPM for the three rock strength, multiple bit scenario; 20,000, 15,000, and 10,000 psi .....44

Figure Page

Figure 46: Calculated ROP for the three rock strength, multiple bit scenario; 20,000, 15,000, and 10,000 psi ....44
Figure 47: Learning curve for the three rock strength, multiple bit scenario; 20,000, 15,000, and 10,000 psi ....45
Figure 48: Graph for three rock strength, decreasing left to right, showing optimal drilling cost with changing pull depth ....46
Figure 49: Graph of the 12.25 in. well real rock strength and averaged rock strength....47
Figure 50: Optimal WOB for field case WOB and RPM Optimization....49
Figure 51: Optimal RPM for field case WOB and RPM Optimization....50
Figure 52: Optimal ROP for field case WOB and RPM Optimization....50
Figure 53: Learning curve for field case WOB and RPM Optimization....51
Figure 54: Optimal WOB for field case WOB, RPM, and Pull Depth Optimization ....52
Figure 55: Optimal RPM for field case WOB, RPM, and Pull Depth Optimization ....52
Figure 56: Optimal ROP for field case WOB, RPM, and Pull Depth Optimization ....53
Figure 57: Optimal learning curve for field case WOB, RPM, and Pull Depth Optimization ....53
Figure 58: Optimal WOB for field case WOB, RPM, Pull Depth, and Bit Combination Optimization....54
Figure 59: Optimal RPM for field case WOB, RPM, Pull Depth, and Bit Combination Optimization....55
Figure 60: Optimal ROP for field case WOB, RPM, Pull Depth, and Bit Combination Optimization....55
Figure 61: Optimal learning curve for field case WOB, RPM, Pull Depth, and Bit Combination Optimization....56
Figure 62: Learning curve showing all three field case optimizations, along with the real data....58
Figure 63: Optimal WOB for the three rock strength, multiple bit scenario; 10,000, 15,000, and 20,000 psi with continuous trends....61
Figure 64: Optimal RPM for the three rock strength, multiple bit scenario; 10,000, 15,000, and 20,000 psi with continuous trends....62

# NOMENCLATURE

| | | |
|---|---|---|
| $a_1$, $a_2$, $a_3$, $a_4$ | Empirical Coefficient | - |
| ABR | Relative Abrasiveness | - |
| $b_1$, $b_2$, $b_3$, $b_4$ | Empirical Coefficient | - |
| b(x) | Function for the Effect of Number of Blades | - |
| ΔBG | Bit Grade | - |
| BR | Back Rake | degrees |
| $c_1$, $c_2$, $c_3$, $c_4$ | Empirical Coefficient | - |
| CCS | Confined Compressive Rock Strength | psi |
| $Cost_{Bit}$ | Cost of Bit | $ |
| $Cost_{Rig}$ | Cost of Drilling Rig | $ /day |
| ΔD | Depth Step Size | ft. |
| $D_{bit}$ | Bit Diameter | in. |
| $D_1$ | Start Drilling Bit Depth | ft. |
| $D_2$ | End Drilling Bit Depth | ft. |
| h(x) | Hydraulic Efficiency Function | - |
| HSI | Horsepower per Square Inch | HP /$in^2$ |
| JSA | Junk Slot Area | $in^2$ |
| $K_1$ | Calibrated Constant | - |
| k | Iteration | - |
| MD | Measure Depth | ft. |
| $N_b$ | Number of Blades | - |
| n | Number of Maximum Depths | - |
| OF | Objective Function | - |
| $P_{bit}$ | Pressure Drop across the Bit | psi |
| $p_g$ | Global Previous Best for each Particle | - |
| $p_i$ | Previous Best for each Particle | - |
| Q | Flowrate | GPM |
| $r_1$, $r_2$ | Random value from 0 to 1 | - |
| ROP | Rate of Penetration | ft. /hr. |
| RPM | Revolutions per Minute of the Bit | RPM |
| SR | Side Rake | degrees |
| SS | Sum of Squares | - |
| $t_{Rotating}$ | Rotating Time of Drill Pipe in Drilling Simulation | hr. |
| $t_{Tripping}$ | Tripping Time in Drilling Simulation | hr. |
| $t'_{Tripping}$ | Drill Pipe Tripping Rate Estimation | hr. /ft. |
| $v_i$ | Velocity of each Particle | - |
| WOB | Weight on Bit | lb. |
| $W_c$ | Wear Coefficient | - |
| $W_f$ | Wear Function | - |
| $x_i$ | Position of the Particle | - |
| $\phi_1$, $\phi_2$ | Cognitive and Social Components | - |
| ω | Weighted Inertia Component | - |

# CHAPTER I

## INTRODUCTION

Over the years, the oil and gas industry has played a key role in the US energy sector. Oil companies have continually worked to develop technology in order to maximize performance. Since oil well drilling is a complex procedure, in order to optimize it, the physical phenomenon must be modeled as represented by the primary governing equation (Kerkar et al., 2014). Before the early 1980s, most oil wells were mainly drilled vertically (Helms, 2008). These vertical wells were influenced by many physical control variables including: weight on bit (WOB), revolutions per minute of the bit (RPM), drilling fluid type, drilling fluid viscosity, bit type, bit wear, etc. For drill bits, there are many sub segments of this area; however, most all of them can be classified into three categories: Natural Diamond Bits (NDB), Polycrystalline Diamond Compact Bits (PDC), and roller cone bits. NDB's are bits that have natural diamonds that are set along the surface of the bit face and grind the rock. PDC's are bits that have polycrystalline diamond cutters set in the blades at the bit face and scrape or shear the rock. Roller cone bits are bits that have cones that roll along the rock face which crushes and gouges the rock as the bit teeth crush and penetrate into the rock. In this research, PDC bits will be incorporated since they are the most commonly used in industry.

In addition to the physical control variables, there are environmental variables including: rock strength, formation abrasiveness, formation pore pressure, fracture gradient, etc. These variables

then affect the rate of penetration (ROP), which is inversely proportional to the cost of drilling the well.

## 1.1 Motivation

In drilling optimization, reducing drilling time is a key factor that can minimize the total drilling cost and maximize the potential profits. This is especially true for offshore wells due to the large increase in operational costs per day (Kaiser, 2009). However, as technology has advanced, vertical wells have been mostly overtaken by horizontal directional wells, which now dominate the market. There are many reasons why most wells drilled today are horizontal wells. A couple of the main reasons for this switch are that oil companies can gather more oil from one well since the horizontal section will expose much more drainage area, along with the fact that the horizontal section allows for multiple wells to be drilled from the same setup location. However, all of the main reasons can be directly linked to the oil companies maximizing their overall profit. Yet, with this added lateral section, the length of the well can be drastically increased, along with horizontal wells having added complexity to them through the surface variables and down hole variables differing. The reason for this difference, is after the well passes the kick off point (KOP), which is the point in the well that it turns horizontal, friction now has to be taken into account. Friction is introduced because the drill pipe lies on the wellbore floor in the lateral section, and the loss due to friction can be described as the difference between the hook load at surface and the down hole weight on bit. This can be estimated through torque and drag analysis by taking small increment calculations starting at the bit and adding each segment up to surface. Once that is completed, a trial and error technique by adjusting the friction coefficient until the force calculated at surface matches the reported hook load. However, the results from this research only produce down hole measurements currently, and torque and drag analysis (Wu et al., 2011) will be incorporated into the future.

As previously mentioned, the horizontal section can substantially lengthen the well which is why the drilling industry has looked to find unique ways to maximize potential profits for drilling wells. In order to increase the efficiency in drilling performance, an artificial intelligence algorithm can be used. One of the biggest challenges in drilling optimization is to find the best operational drilling parameters in the infinite space of possible solutions. One of the reasons that the parameter search space is so large is due to the wearing of the drill bit. As the bit gets progressively more worn, variability in parameter selection decreases, thus, changing any of the sequences in drilling could result in a different search space towards the end of the bit run. Therefore, when beginning to optimize drilling a well, the entire length of the well needs to be taken into account. In this study, a new approach to drilling optimization will be introduced by incorporating a particle swarm optimization (PSO) technique on an ROP model in order to optimize one section of a well. The final goal will be to minimize the cost per foot of formation drilled by having the algorithm select the WOB and RPM combinations, as well as, drill bit selections and pull depths. It will then be validated by optimizing a field case.

## 1.2 Drilling Today

Oil and natural gas companies have continually worked to try and optimize the drilling process. As previously mentioned, the environmental conditions are a key factor affecting drilling performance. When planning a new well, unless the well is a wildcat, oil companies typically look at previously drilled adjacent wells, or offset wells, for data on rock strengths, formation pore pressure, and previous bit performance. It is common to correlate the seismic data before drilling to determine the rock formation tops of the newly planned well, and correlate these rock formations to the rock property profiles from adjacent wells. Next, the drilling engineer looks at the control variables used through these formations and the resultant ROP, to determine the best plan moving forward. Once drilling has begun, the rock cuttings that are brought back to the surface with the drilling mud can be used to verify that the rock formations originally anticipated

were correct. If the formation has changed unexpectedly, corrective actions may be taken into account for the unplanned change. These corrective actions may include varying some of the control variables in order ensure that the well is properly controlled and the well optimized. This research will hopefully alter the way that oil companies begin drilling plans in the future, not only offset wells, but also wildcat wells.

Portions of this thesis have been presented in previous publications (Self et al., 2016A, Self et al., 2016B).

# CHAPTER II

# REVIEW OF LITERATURE

## 2.1 Optimization Techniques

There are many advanced problems throughout multiple industries, and several complex problems are normally too difficult to find a simple analytical solution. When such problems are proposed, a numerical approach must be used. There are many methods developed to solve these numerical problems, and the two simplest methods are breadth first and depth first searches. Both of these approaches are very simple, easy to implement, and intuitively make sense. In addition, if both methods are executed exhaustively to a discrete problem, they will find the optimal solution. Both methods work in a similar way, in that they analyze every possible solution to the problem. The main difference between these two methods are how they search the possible solutions. Breadth first searches expand every node at the first layer and search the connections to the neighboring nodes before moving to the next layer of nodes. This can be done iteratively until the optimal solution is found. The depth first search starts at the first node and expands down one potential path until it reaches a stopping point, and this can also be iterated until the optimal solution is found. However with added dimensions, these two methods quickly become very inefficient to solve due to the time and memory challenges. These issues compound even further if the problem changes from a discrete problem to a continuous problem. At this point, these problems can no longer be solved by breadth first and depth first exhaustive searches, and more

intelligent algorithms must be employed. There have been numerous advanced optimization techniques designed to solve very complex problems throughout multiple industries. Some of these include; genetic algorithms (GE), simulated annealing (SA), ant colony optimization (ACO), particle swarm optimization (PSO), etc. All of these advanced algorithms are much more efficient in solving any problems, simple or complex, when compared to the exhaustive searches, depth based and breadth based. There has been work into determining which advanced algorithms perform best (Elbeltagi, et al., 2005). The research concluded that the particle swarm optimization algorithm performed the best when comparing the other methods in both success rate and the quality of the solution found. PSO is the optimization algorithm used for this research.

## 2.2 Drilling Optimization

As previously mentioned, the drilling industry is getting more complex as technology advances and with these added complexities, the price of drilling continues to increase. Therefore, a growing need for optimization in the drilling industry continues to develop.

Early optimization efforts began around 1958. Speer developed empirical relationships for weight on bit, rotary speed, formation drillability, and hydraulic horsepower effects on rate of penetration. The research combined all of these relationships into one chart for a specific drilling scenario, and the optimal combination could then be determined.

In 1959, Graham and Muench developed an analytical approach to determine optimal weight on bit and rotary speed. Their goal was to determine if there exists a possible combination of operational parameters that could minimize the cost of drilling a well. The three costs that they used include the cost of the rig for both drilling and tripping, along with the cost of the bit. They concluded that there are optimal WOB and RPM combinations that decrease the overall drilling time, and these can be calculated by varying a constant RPM iteratively while calculating the cost at various depths.

Galle and Woods in 1963, used mathematical models to determine the optimal combinations for constant drilling parameters, WOB and RPM, in order to find the lowest drilling cost for a drilling interval. They presented three different procedures for different applications depending on potential limiting factors for drilling scenarios.

In 1972, Reed developed a method to find the optimal WOB and RPM path by incorporating a Monte Carlo technique. To begin the method, a random path is initialized and the cost is calculated. Then an iterative method is introduced by selecting random numbers for every point along the path, and calculating new costs every time a point is moved. If this new cost is lower than the original, the new point is kept; however, if it is higher, the point is given a new random number. This process is repeated until convergence.

Once technology progressed even further, this led to the development of advanced drilling simulators. Techniques incorporating a simulator program to use manual input trial and error techniques to find the best parameters have been performed (Rastegar et al., 2008).

Eren (2010) found optimal drilling parameters through the use of a multiple regression technique. He incorporated an ROP model and used multiple regression to get a set of coefficients to represent the drilling data gathered. He then incorporated those coefficients found, and optimized WOB and RPM for a drilling interval by finding the roots of the first derivative of the ROP equation with respect to each variable, WOB and RPM.

Hamrick in 2011 took a different approach, and looked to analyze a method for finding optimal drilling parameters by minimizing mechanical specific energy (Teale 1965). He developed relationships for torque and penetration per revolution in terms of weight on bit. Therefore, optimization on the MSE equation was based purely on weight on bit and the minimum could be determined by finding the roots of the first derivative. Once the optimal weight on bit was found, the other parameters could be determined by the mathematical relationships developed.

There have been some other previous optimization efforts in the oil and gas industry outside of drilling performance. Atashnezhad et al. (2014) previously incorporated a swarm algorithm in order to find the optimal well path with the goal to minimize total measured depth of the well. Onwunalu and Durlofsky (2010), and Bangerth et al. (2004), have done research into optimizing the well location. The work outlined in this paper would work well in tandem with these algorithms and potentially provide significant improvement in performance.

## 2.3 Rate of Penetration Modeling

Any optimization algorithm must have a model in order to optimize a system. Therefore, many researchers have developed models that try to capture the physics of the drilling process for all types of bits. Below are some of the drill bit models developed, and the equations associated with them are directly below the explanations.

Bourgoyne and Young (1974) modeled the effects of formation strength, $a_1$ term, formation depth and formation compaction, $a_2$ term and $a_3$ term, pressure differential, $a_4$ term, weight on bit and bit diameter, $a_5$ term, speed of rotation, $a_6$ term, bit wear, $a_7$ term, and hydraulics, $a_8$ term.

$$\frac{dD}{dt} = Exp\left( a_1 + a_2\,(10{,}000 - D) + a_3\,D^{0.69}\left(g_p - 9\right) + a_4\,D\left(g_p - \rho_c\right) + a_5 \ln\left(\frac{\frac{w}{d} - \left(\frac{w}{d}\right)_t}{4 - \left(\frac{w}{d}\right)_t}\right) + a_6\,\ln\left(\frac{N}{100}\right) - a_7\,h + a_8\left(\frac{\rho\,q}{350\,\mu d}_n\right)\right)$$

Warren in 1981, developed an ROP model to relate weight on bit, W, revolutions per minute of the bit, N, bit diameter, D, rock strength, S, and bit type to rate of penetration, R.

$$R = \left(\frac{a\,S^2\,D^3}{N^b\,W^2} + \frac{c}{N\,D}\right)^{-1}$$

This model did not take into account hydraulic effects, and assumed perfect cleaning. Warren later added to this model by taking into account the hydraulics, and presented a new imperfect cleaning model incorporating a new term into the ROP equation (Warren, 1987). This term is a function of the diameter of the bit, D, density of the fluid, ρ, drilling fluid viscosity, μ, and modified jet impact force, $I_m$.

$$R = \left( \frac{a\, S^2\, D^3}{N\, W^2} + \frac{b}{N\, D} + \frac{c\, D\, \rho\, \mu}{I_m} \right)^{-1}$$

This model was again further developed to take into account roller cone offset and formation ductility which added an additional term to the ROP model (Winters, 1987), consisting of the cone offset coefficient, ϕ, rock compressive strength, σ, and rock ductility, ε.

$$R = \left( \frac{a\, S^2\, D^3}{N\, W^2} + \frac{b}{N\, D} + \frac{c\, D\, \rho\, \mu}{I_m} + \frac{\phi\, \sigma\, D^2}{N\, W\, \varepsilon} \right)^{-1}$$

A few years later, Warren's model was modified by adding another term for the chip hold down effect (Hareland and Hoberock, 1993). After this addition, the model now takes into account the position that the fluid is with respect to the mud overbalance (Charlez, 1999). This new term is a function of effective confining pressure, $P_e$, and lithology coefficients, $a_c$, $b_c$, and $c_c$.

$$R = \left( \left( c_c + a_c (P_e - 120)^{b_c} \right) \left( \frac{a\, S^2\, D^3}{N\, W^2} + \frac{b}{N\, D} \right) + \frac{c\, D\, \rho\, \mu}{I_m} \right)^{-1}$$

In 1994, Hareland and Rampersad, developed a new ROP model for drag bits. Their model incorporated wear and focused on modeling a single cutter's interaction with the rock. The developed model presented in the paper is for Natural Diamond Bits, and is a function of diamond cutter diameter, $d_s$, mechanical weight on bit, $W_{mech}$, and number of stones, $N_s$.

$$ROP = \frac{14.14\, N_s\, RPM}{D_B}\left(\left(\frac{d_s}{2}\right)^2 \cos^{-1}\left(1 - \frac{4\, W_{mech}}{N_s\, d_s^2\, \pi\, \sigma_c}\right) - \left(\frac{2\, W_{mech}}{N_s\, \pi\, \sigma_c} - \frac{4\, W_{mech}^2}{(N_s\, d_s\, \pi\, \sigma)^2}\right)^{\frac{1}{2}}\left(\frac{d_s}{2} - \frac{2\, W_{mech}}{N_s\, d_s\, \pi\, \sigma_c}\right)\right)$$

Hareland et al. 2010, developed a new model for roller cone bits. This model took a new approach by incorporating detailed bit cutting structure, while still integrating drilling operational effects and bit wear modeling. Some of the variables include number of insert in contact with rock, $n_t$, number of insert penetration per revolution, m, chip formation angle, $\psi$, and bit dull grade, DG.

$$ROP = K\frac{80\, n_t\, m\, RPM^a}{D_b^2\, \tan^2\psi}\left(\frac{1}{C_2}\left(\frac{WOB}{100\, n_t\, l\, \sigma_p} - C_1 w\right)\right)^b \left(1 - d\left(\frac{DG}{8}\right)^c\right)$$

In 2011, Arabjamaloei and Shadizadeh incorporated artificial neural network techniques to develop a new ROP model. They used data from an Iranian oilfield to develop the ROP model and compared the calculated ROP to reported ROP from the field.

In 2014, Kerkar et al., a PDC bit model was developed by incorporating bit wear, operational parameters, hydraulic effects, and bit specification effects, along with some formation factors. The model includes some experimental constants that can be altered to adjust for different drilling conditions and environments. This was the model selected for this research and explained in Section 3.2.

# CHAPTER III

# METHODOLOGY

Due to the fact that drilling process is highly dynamic, any basic gradient descent optimization algorithm will not be able to handle the sequential nature of the drilling process, meaning that any decisions made will likely affect any future decisions. This phenomenon shows up in the wear equation (Kerkar et al., 2014) due to the summation sign. Therefore, particle swarm optimization (PSO) was selected as the optimization algorithm.

## 3.1 Particle Swarm Optimization

Particle swarm optimization is a powerful and widely used optimization technique that covers a wide range of research areas (Blum and Li, 2008). PSO was first developed by Kennedy and Eberhart in 1995, and it was modeled to mimic how certain groups of animals move in the natural world; such as a school of fish, flock of birds, etc. For this algorithm, a group of animals is referred to as a "swarm," and each animal inside the group is considered a "particle." This algorithm uses a combination of information from the group as a whole and the information from each individual particle to search the space for the optimal solution. For each individual particle, the PSO algorithm uses the current velocity of each particle, along with the information from the best values found from both the individual particle and the best global from the swarm, to move the particle around the space. PSO starts initially by randomly selecting values for all dimensions corresponding to each particle inside a swarm. The swarm is evaluated and the new velocity of

each particle and position are updated. The velocity and position equations (Atashnezhad et al., 2014) are shown below, where $v_i$ represents the velocity of a particle, $p_i$ represents the previous best of the current particle, $x_i$ represents the current position of the particle, and $p_g$ represents the global previous best from the entire swarm. Each one of these variables is a vector of d in length, representing the number of dimensions in the problem. The other variables include; $\phi_1$ and $\phi_2$ which are considered acceleration constants, $\omega$ which is a weighted inertia constant, $r_1$ and $r_2$, are random values that are taken from the uniform distribution [0, 1].

$$v_i^{k+1} \leftarrow \omega v_i^k + \varphi_1 r_1^k \left(p_i^k - x_i^k\right) + \varphi_2 r_2^k \left(p_g^k - x_i^k\right) \quad (1)$$

$$x_i^{k+1} \leftarrow x_i^k + v_i^{k+1} \quad (2)$$

The velocity equation, Eq. 1, above is comprised of three components, social, cognitive and momentum (Blum and Li, 2008). The social component, $\phi_2$, forces the particles towards the global best solution found; the cognitive component, $\phi_1$, forces the particles back towards the previous best solution found by each particle; and the momentum component, $\omega$, forces the particle to continue on the current trajectory. All three components help the particle swarm optimization technique traverse the exploration/exploitation dilemma that surrounds all optimization problems (Rejeb et al., 2005).

The PSO algorithm incorporated in this study uses the ROP model by having the particles search the solution space and converge on the optimal WOB, RPM, bit selection, and pull depth. The inputs for this algorithm include; rock strength, WOB and RPM operational ranges, and available bit selections. The algorithm allows for a specified minimum bit wear, which forces the algorithm to select only potential solutions that satisfy this criteria. The bit wear begins at a value of one and decreases as the depth intervals increase, until the wear reaches the minimum allowable bit wear. In this study, the minimum allowable value for the bit wear function was 0.5, and can also be represented in equivalent IADC bit wear representation familiar in the drilling industry of 4.0.

3.2 Rate of Penetration Model

The main governing equation used in this research models the rate of penetration for a PDC bit and was developed by Kerkar et al. (2014). This model is a function of operational parameters, bit parameters, formation factors, and hydraulic effects

$$ROP = \left[\frac{K_1 WOB^{a_1} RPM^{b_1} \cos(SR)}{CCS^{c_1} D_{bit} \tan(BR)}\right] W_f h(x) b(x) \quad (3)$$

Eq. 3 above models the drilling process showing the parameters that affect drilling performance. The model above incorporates a wear function representative of the wear on the bit being drilled. This function is shown below

$$W_f = 1 - a_3 \left(\frac{\Delta BG}{8}\right)^{b_3} \quad (4)$$

Eq. 4 starts with a value of one and decreases as the bit gets progressively more worn. $W_c$ in Eq. 5, is the bit wear coefficient and represents the bits resistance to wear, resulting in a decreased bit wear with a lower value of $W_c$. This variable incorporates many factors including; the number of cutters, quality and wear resistance of the material of the cutters. The wear function changes as the depth increases and is a function of formation factors along with drilling parameters. The bit grade is modeled and changes according to Eq. 5

$$\Delta BG = W_c \sum_{i=2}^{n} \Delta D_i WOB_i^{a_4} RPM_i^{b_4} CCS_i ABR_i \quad (5)$$

In Eq. 5, CCS is the rock strength while the rock is subjected to confined pressure and it is a function of pore pressure and lithology (Rastegar et al., 2008). The CCS is measured by applying confined pressure to the rock samples tested in the lab. Equivalently the overbalance pressure, or the difference between hydrostatic mud pressure and pore pressure at depth in the field, is treated as the confined pressure while drilling. Different overbalance correlations exist for different rock

types. In this study, the overbalance is assumed integrated into the CCS value.

Abrasiveness (ABR) is representative for the coarseness of the rock, and related to the amount of quartz minerals in the rock. The higher the rock abrasivity, the higher the bit wear rate. A normalized table is applied for different rock types in which the relative value for sandstone of 1.0 is utilized. The abrasiveness relative value can also be obtained from the gamma ray log where a relative value of 1.0 is assigned to an equivalent 40 reading.

Efficiency in cutting removal can drastically effect drilling performance, therefore, the hydraulic effects on ROP are modeled below

$$h(x) = a_2 \left( \frac{HSI \frac{JSA}{2D_{bit}}}{ROP^{c_2}} \right)^{b_2} \tag{6}$$

$$HSI = \frac{\frac{QP_{bit}}{1714}}{\frac{\pi}{4} D_{bit}^2} \tag{7}$$

The last factor modeled in Eq. 3 that effects the ROP model, is the function representing the effect for the number of blades for the bit and is shown below

$$b(x) = \frac{RPM^{1.02-0.02N_b}}{RPM^{0.92}} \tag{8}$$

Assessing Eq. 8, a five bladed bit results in a value of one for b(x) for all RPM values. Additionally, it can be seen that b(x) increases with a decrease in blade number, resulting in a higher ROP value. Conversely, lower bladed bits generally have a lower wear resistance, which results in wearing the bit faster.

Analyzing the set of equations above, Eq. 3 – Eq. 8, WOB and RPM affect ROP performance both positively, Eq. 3, and negatively, Eq. 5. Additionally, there are an infinite number of possible solution combinations for WOB, RPM, bit selections, etc. Therefore, an optimization

algorithm must be used to find the best solution given the large number of variables included in the drilling process. More importantly, every value used for variables affect possible solutions in the future due to the summation in the wear equation, Eq. 5. Due to these conflicting affects, drilling optimization is required to help maximize overall drilling performance.

### 3.2.1 Model Correlation

Before beginning optimization on drilling scenarios, the experimental constants found in the ROP model, $a_1$, $b_1$, $c_1$, etc., need to be data correlated in order to get accurate numeric results. Therefore, drilling data was gathered using data from several drill off tests in both Shale and Limestone rock formations (Hareland, 1988). WOB, RPM, and ROP were just some of the data that was collected and recorded. Using the particle swarm optimization algorithm, a set of constants were found by incorporating the objective function (OF) below

$$\min \quad OF{:}SS = (ROP_{data} - ROP_{calc})^2 \tag{9}$$

Using the calculated ROP and the reported ROP, regression was performed on the dataset. It was determined that the datasets do have a strong correlation, $r^2 = 0.98$. After the set of constants were found that minimized Eq. 9, the calculated model and the real data were graphed for validation purposes. Fig. 1 and Fig. 2 show graphs for the Limestone data that was used for the correlations, and Fig. 3 and Fig. 4 show the Shale data used. In addition to the graphs incorporating the included data, an additional test's data was graphed to further prove the constants validity. Fig. 5 and Fig. 6, show graphs using the additional Shale drill off test data. As seen from Fig. 5 and Fig. 6, the set of constants found are closely representative of the actual drilling data. The valid set of experimental constants were determined and used for the drilling scenarios optimized.

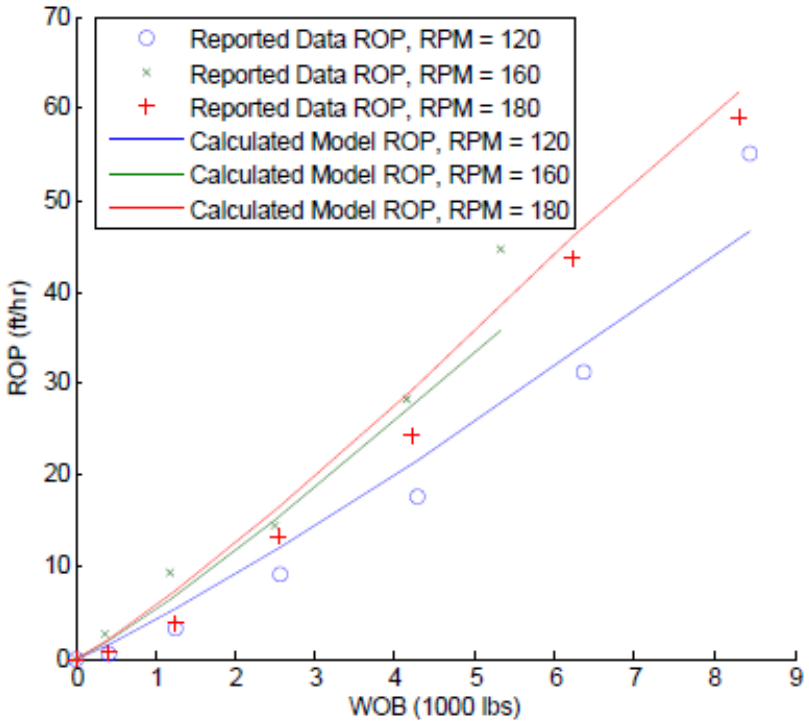


Figure 1: Reported ROP data and calculated ROP vs. applied WOB in Limestone formation drill off test

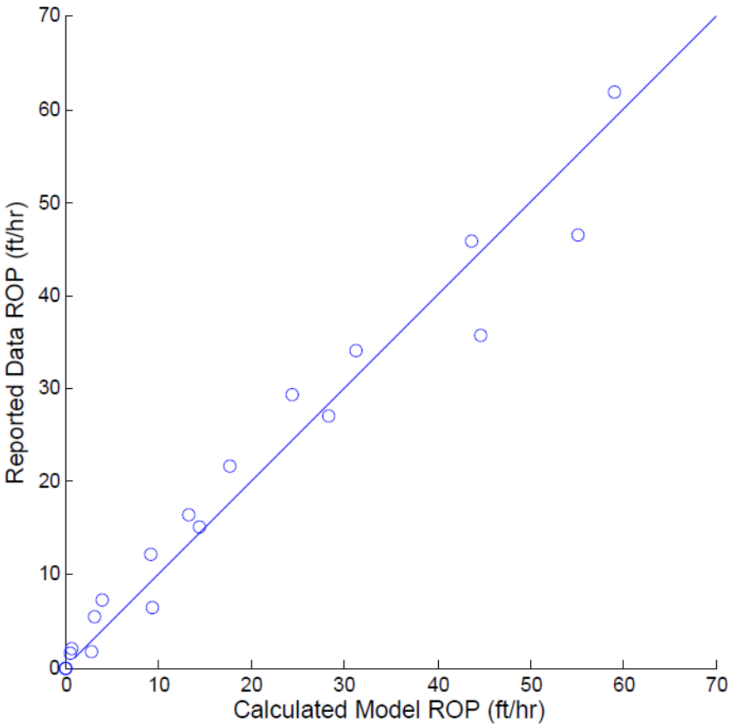


Figure 2: Reported ROP data vs. calculated ROP in Limestone formation drill off test

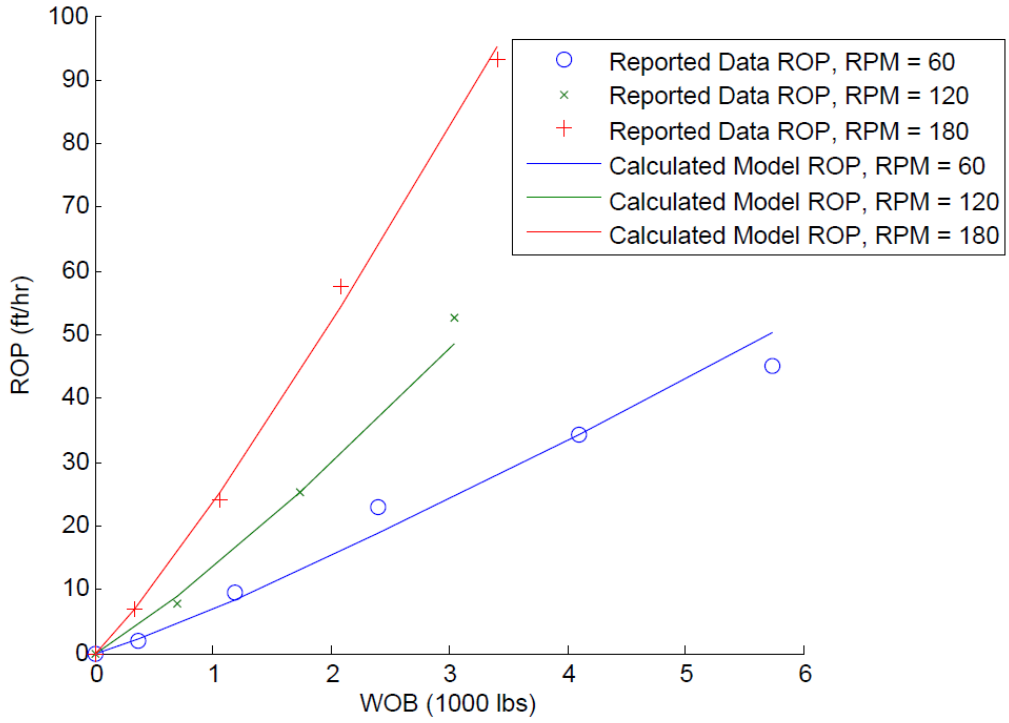


Figure 3: Reported ROP data and calculated ROP vs. applied WOB in Shale formation drill off test

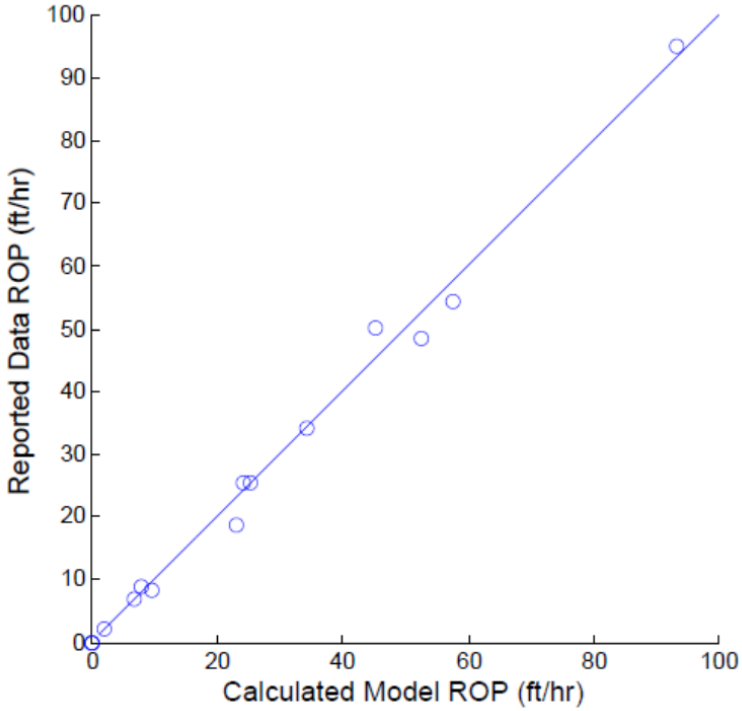


Figure 4: Reported ROP data vs. calculated ROP in Shale formation drill off test

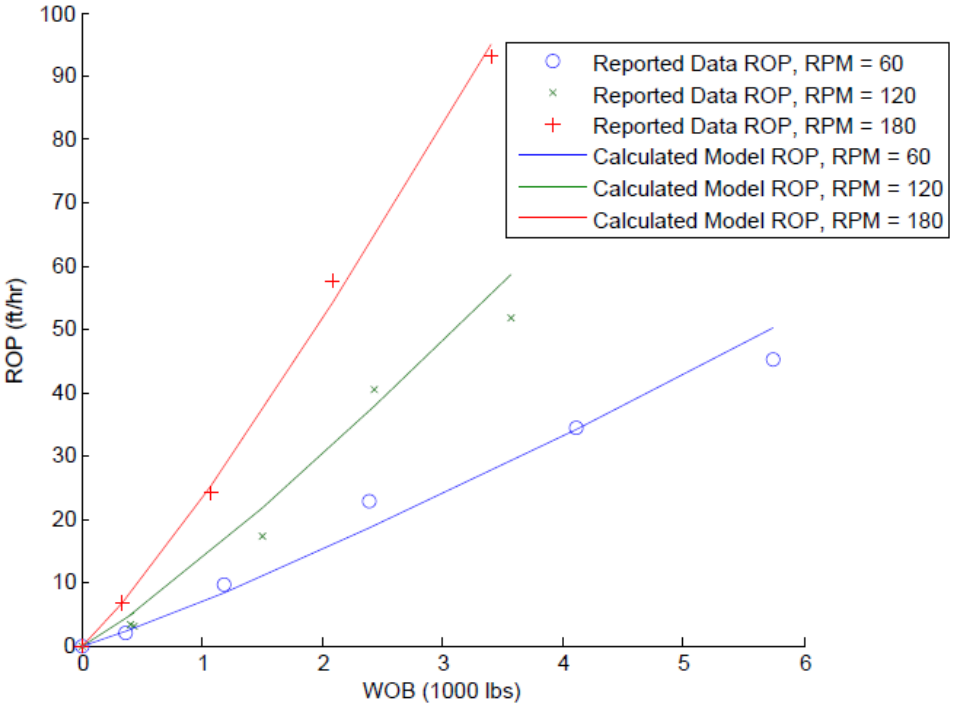


Figure 5: Reported ROP data and calculated ROP vs. applied WOB in an additional Shale formation drill off test

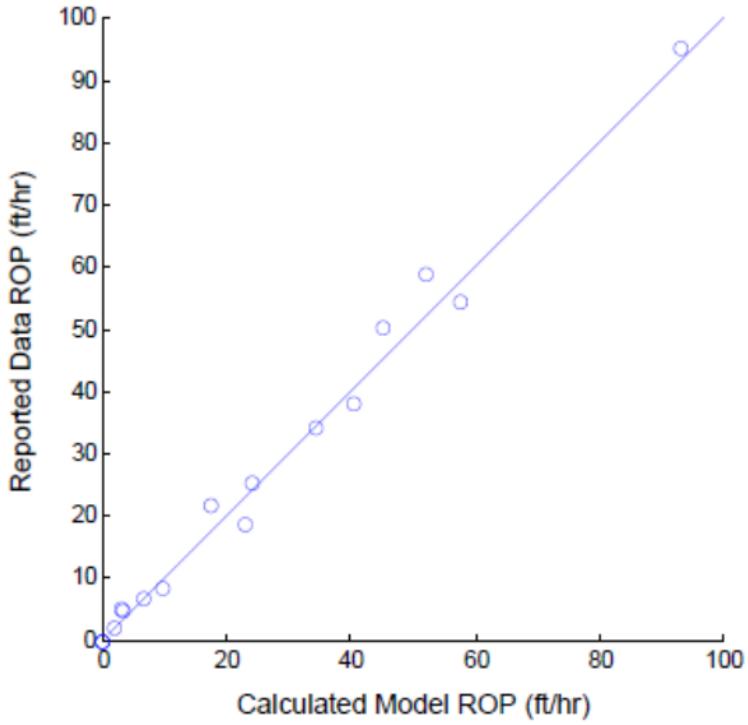


Figure 6: Reported ROP data vs. calculated ROP in an additional Shale formation drill off test

# CHAPTER IV

# RESULTS

The work presented in this thesis uses the PSO algorithm to optimize oil field drilling by incorporating a ROP model with the goal to find optimal operational drilling parameters. The results section is divided into two different optimization sections; one bit optimization and two bit optimization scenarios, and the objective function changes according to both sections and are detailed in both. Initial tests were designed to analyze how the optimization technique responds to various changes in both rock strength and operational parameters. The first eight test scenarios were designed to vary one aspect at a time, while maintaining similar values for all other parameters, in order to analyze these effects on the output. For these situations the confined compressive rock strength were chosen and input into the algorithm. For the field case validation, the rock strengths were averaged over specific depth intervals and discretized.

The PSO algorithm begins by selecting random values for WOB and RPM within the given operational ranges for each particle in the swarm. For every rock strength depth interval, there is one WOB value and one RPM value for that given interval. Each particle is evaluated through the specified objective function and the minimum parameters are recorded. In addition to calculating the OF, the algorithm has criteria that needs to be satisfied to ensure valid solutions. These include; not allowing bits to go below a specified minimum allowable bit wear, positive ROP, and nonnegative drilling time. If any one of these conditions are violated, the OF is defaulted to a

value of 1.0 x $10^{200}$ to ensure that this solution will not be selected. The position and velocity vectors for each particle are updated using Eq. 1 and Eq. 2, while maintaining values within given operational parameters. This process is iterated until the maximum number of iterations is obtained.

### 4.1 One Bit Optimization

The use of an advanced optimization algorithm for finding the best WOB and RPM combinations for a single bit run could potentially save numerous hours of drilling time. An initial round of simulations were ran incorporating the PSO algorithm.

For this optimization method, the inputs for the program include, rock strength, bit and fluid specifications, and WOB and RPM operational ranges. Included in the bit specifications, are whether the bit is new and has no wear before going into the hole, or if a worn bit is being used along with its' bit grade before drilling begins. The wear function, $W_f$, is equal to one if the bit is new and less than one but greater than zero if the bit is worn. Along with the bit wear before the run, the operator has the choice to establish a value for bit wear to go no lower than a given threshold. In this case, the optimization algorithm will not allow any solutions to go below the desired minimum bit wear level. This section assumes a brand new bit and set the minimum wear level to 0.5.

For any optimization problem, there must be a clear objective function to optimize, as given in Eq. 10.

$$\begin{aligned} \min \quad & OF: t_{Rotating} = \sum_{i=1}^{n} \frac{\Delta D_i}{ROP_i} \\ \text{where} \quad & t_{Rotating} > 0 \\ & ROP \geq 0 \end{aligned} \tag{10}$$

In this work, the OF was minimizing the total drilling time, as opposed to maximizing instantaneous ROP or average ROP. The reason for this is that the overall drilling time is the

factor that will directly affect the amount of time and eventually money being saved for one well. This section shows preliminary testing used for one bit drilling sections. The first two scenarios are used to test WOB and ROP by inputting rock strength and RPM. The next two scenarios have the algorithm find both WOB and RPM, along with resultant ROP. The last two are used to analyze the effect of abrasiveness (ABR), Eq. 5, for different rock strength values.

### 4.1.1 One Constant Rock Strength and Constant RPM

The first drilling scenario was used to test the simplest case. For this simulation, rock strength and RPM, Fig. 7 and Fig. 9, were both input and set to a constant value to analyze the effect on the outputs WOB and ROP, Fig. 8 and Fig. 10, found from the PSO algorithm.

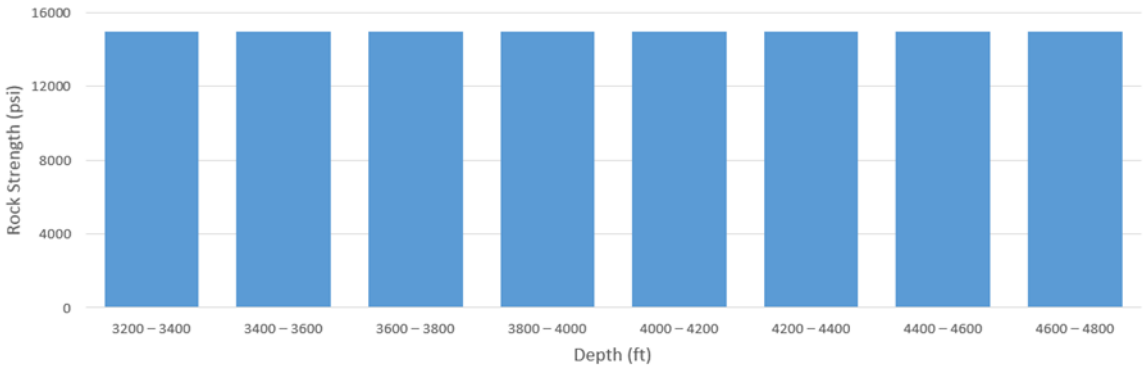


Figure 7: Graph showing the one rock strength scenario; 15,000 psi, and constant 150 RPM

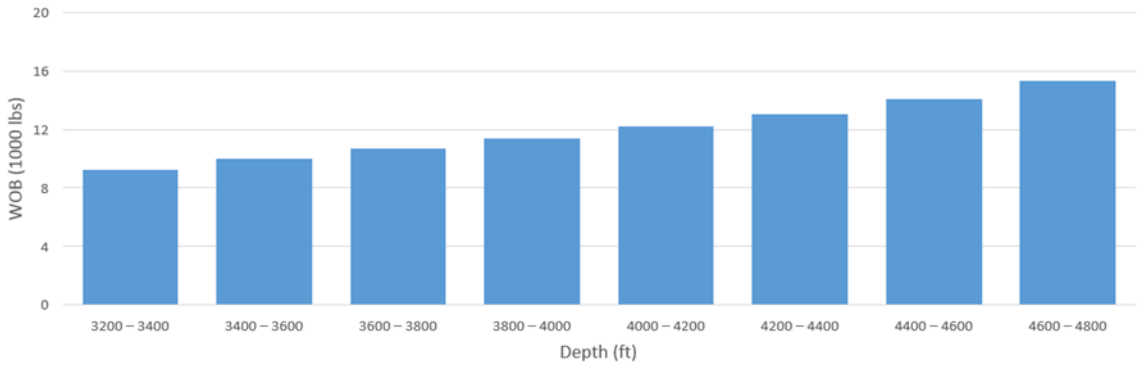


Figure 8: Optimal WOB for one rock strength scenario; 15,000 psi, and constant 150 RPM

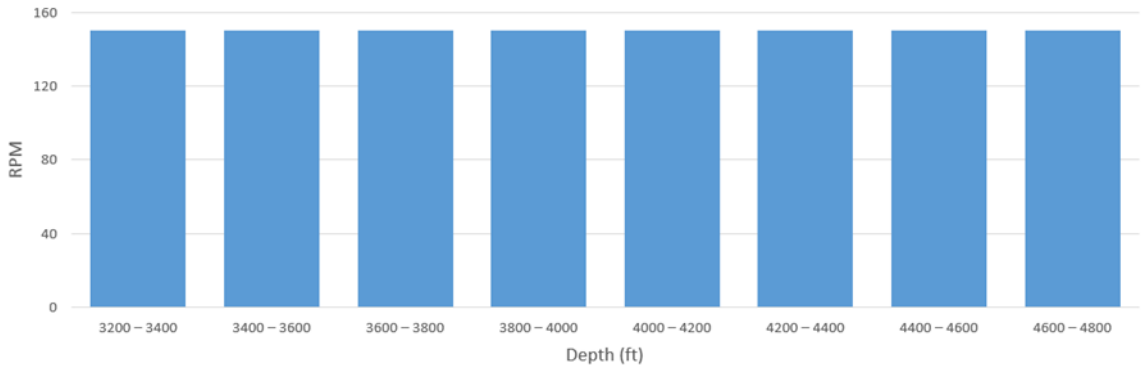


Figure 9: Constant RPM input for one rock strength scenario; 15,000 psi

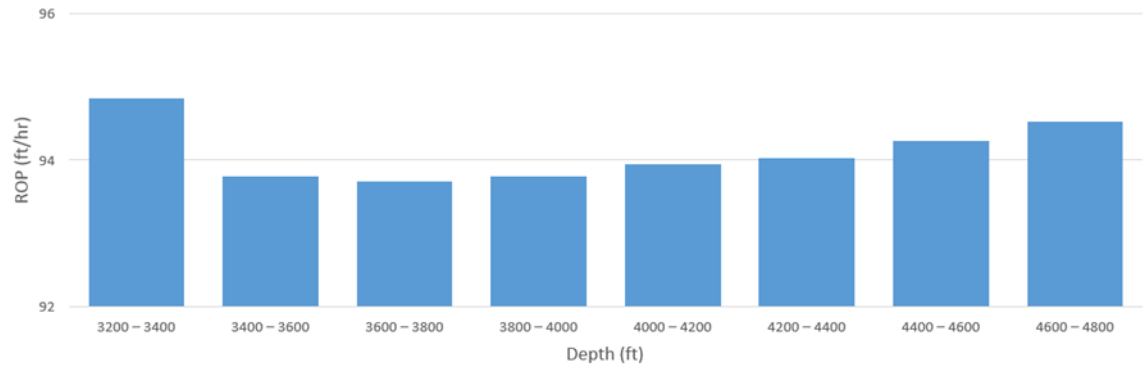


Figure 10: Calculated ROP for one rock strength scenario; 15,000 psi, and constant 150 RPM

As seen above, the algorithm found that the optimal WOB was to increase through the constant rock strength. This is due to the fact that the WOB needs to increase as the depth increases to overcome the progressing bit wear. Shown in Fig. 10, the optimal ROP found is nearly a constant value. Fig. 11 below shows the drilling time decrease as the number of iterations increase. For this simple scenario the code finds the optimal solution around iteration 25. All the values used for this simulation are shown in Table 1.

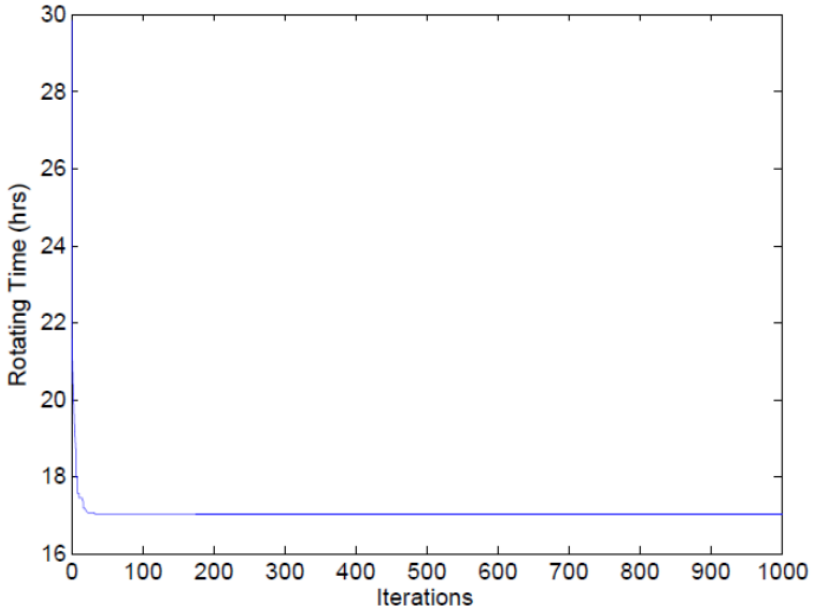


Figure 11: Learning curve for one rock strength scenario; 15,000 psi, and constant 150 RPM

| Depth (ft.) | Rock Strength (psi) | WOB (1000 lbs.) | RPM | ROP (ft. /hr.) | Wear | ABR |
|---|---|---|---|---|---|---|
| 3200 – 3400 | 15,000 | 9.26 | 150.0 | 94.8 | 0.90 | 0.3 |
| 3400 – 3600 | 15,000 | 10.02 | 150.0 | 93.8 | 0.84 | 0.3 |
| 3600 – 3800 | 15,000 | 10.69 | 150.0 | 93.7 | 0.78 | 0.3 |
| 3800 – 4000 | 15,000 | 11.40 | 150.0 | 93.8 | 0.72 | 0.3 |
| 4000 – 4200 | 15,000 | 12.18 | 150.0 | 93.9 | 0.67 | 0.3 |
| 4200 – 4400 | 15,000 | 13.06 | 150.0 | 94.0 | 0.61 | 0.3 |
| 4400 – 4600 | 15,000 | 14.10 | 150.0 | 94.3 | 0.56 | 0.3 |
| 4600 – 4800 | 15,000 | 15.35 | 150.0 | 94.5 | 0.50 | 0.3 |

Table 1: Data table for one rock strength scenario; 15,000 psi, and constant 150 RPM

4.1.2 Two Constant Rock Strengths and Constant RPM

The next rock scenario adds a change in rock strength, Fig. 12, while continuing to maintain the same constant RPM, Fig. 14. Fig. 13 shows the solution found for WOB and Fig. 15 shows the ROP values from the PSO algorithm.

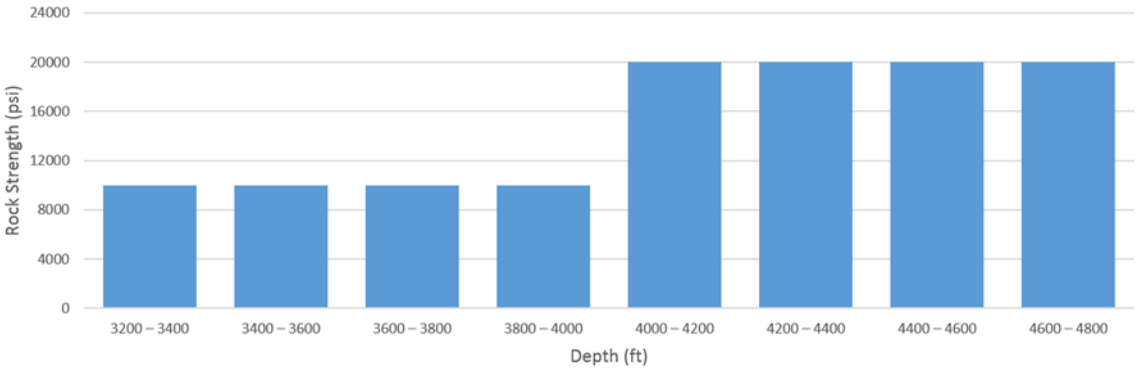


Figure 12: Graph showing the two rock strength scenario; 10,000 and 20,000 psi, and constant 150 RPM

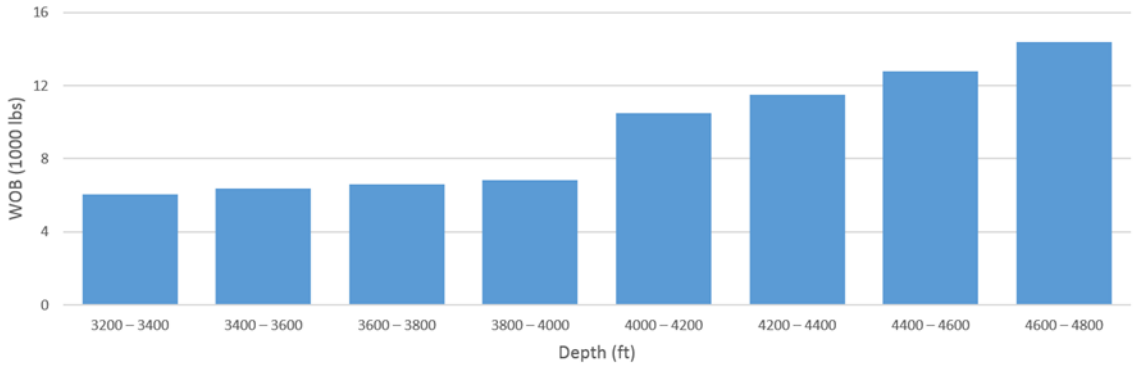


Figure 13: Optimal WOB for two rock strength scenario; 10,000 and 20,000 psi, and constant 150 RPM

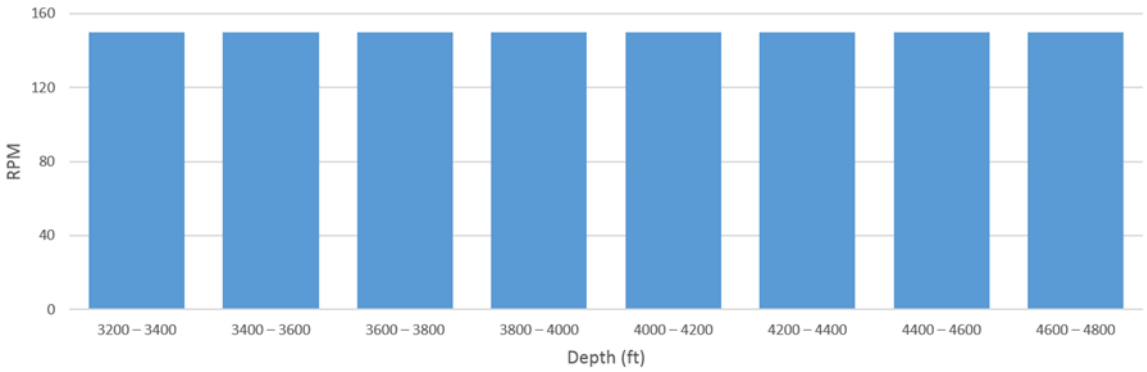


Figure 14: Constant RPM input for two rock strength scenario; 10,000 and 20,000 psi

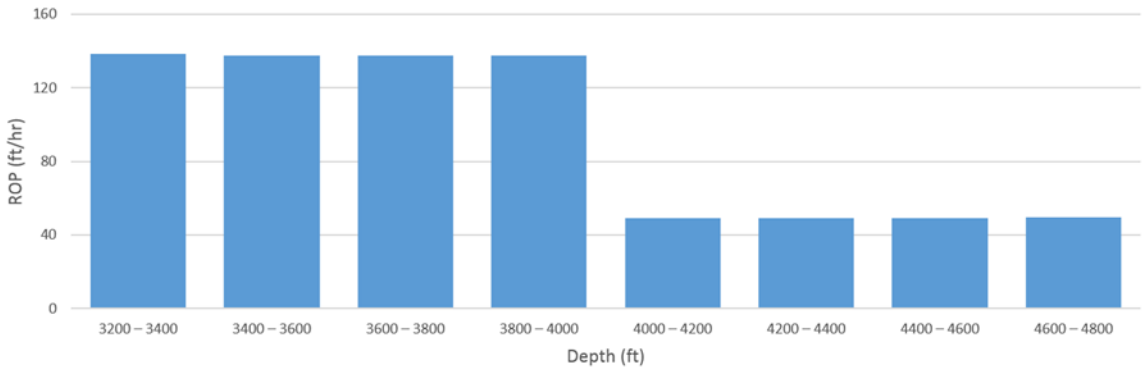


Figure 15: Calculated ROP for two rock strength scenario; 10,000 and 20,000 psi, and constant 150 RPM

Analyzing the graphs above, there is a clear shift at 4000 ft. in both WOB and ROP which is the point that the rock strength changes. The ROP clearly drops off significantly which makes since due to the rock strength doubling in value. Below in Fig. 16, the learning curve is shown along with Table 2 displaying the data for this simulation.

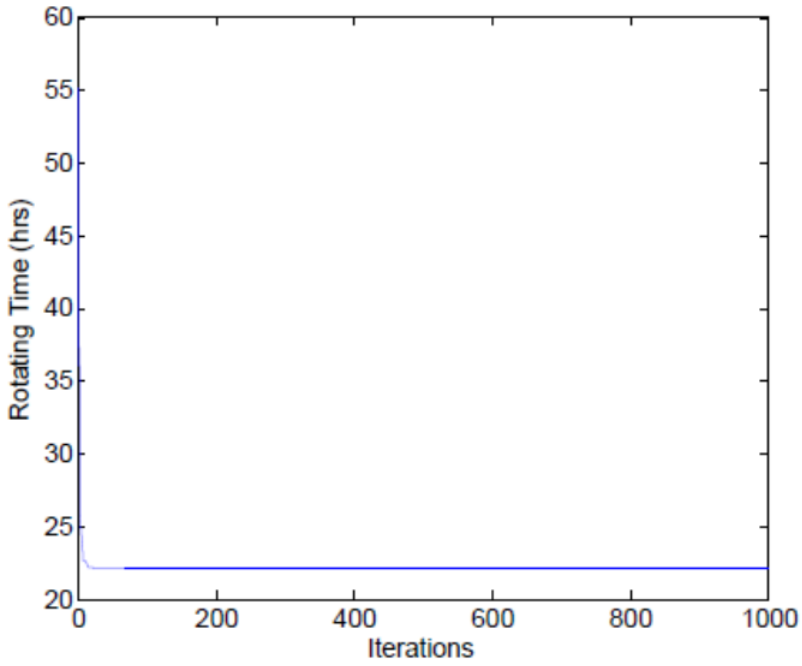


Figure 16: Learning curve for two rock strength scenario; 10,000 and 20,000 psi, and constant 150 RPM

| Depth (ft.) | Rock Strength (psi) | WOB (1000 lbs.) | RPM | ROP (ft. /hr.) | Wear | ABR |
|---|---|---|---|---|---|---|
| 3200 – 3400 | 10,000 | 6.05 | 150.0 | 138.5 | 0.94 | 0.3 |
| 3400 – 3600 | 10,000 | 6.34 | 150.0 | 137.5 | 0.90 | 0.3 |
| 3600 – 3800 | 10,000 | 6.58 | 150.0 | 137.3 | 0.87 | 0.3 |
| 3800 – 4000 | 10,000 | 6.81 | 150.0 | 137.4 | 0.83 | 0.3 |
| 4000 – 4200 | 20,000 | 10.46 | 150.0 | 49.2 | 0.75 | 0.3 |
| 4200 – 4400 | 20,000 | 11.51 | 150.0 | 49.2 | 0.67 | 0.3 |
| 4400 – 4600 | 20,000 | 12.76 | 150.0 | 49.3 | 0.58 | 0.3 |
| 4600 – 4800 | 20,000 | 14.36 | 150.0 | 49.6 | 0.50 | 0.3 |

Table 2: Data table for two rock strength scenario; 10,000 and 20,000 psi, and constant 150 RPM

4.1.3 One Constant Rock Strength

In this scenario, the rock strength is the same as in section 4.1.1, however, instead of manually inputting constant RPM values, the PSO will now find both WOB and RPM, Fig. 18 and Fig. 19. The resultant ROP is shown in Fig. 20.

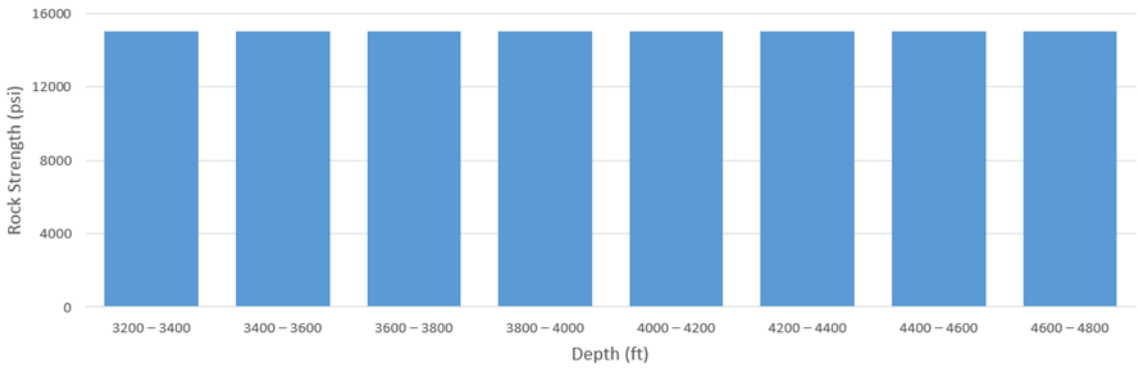


Figure 17: Graph showing the one rock strength scenario; 15,000 psi

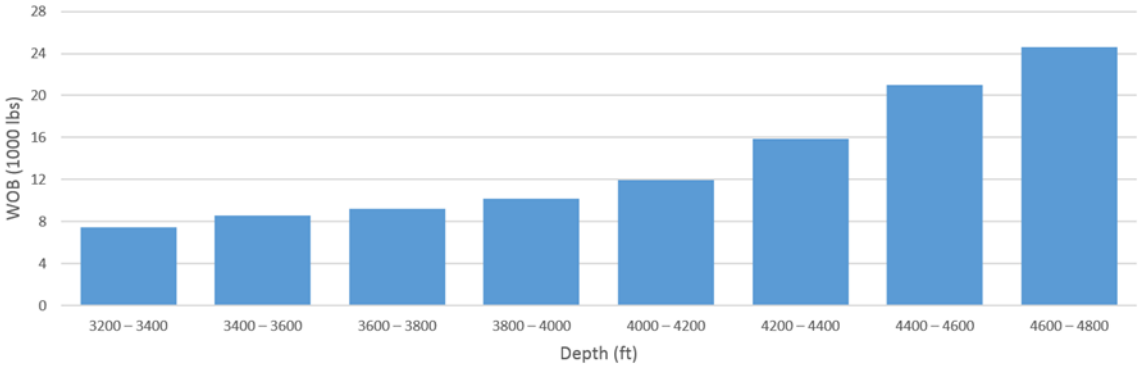


Figure 18: Optimal WOB for one rock strength scenario; 15,000 psi

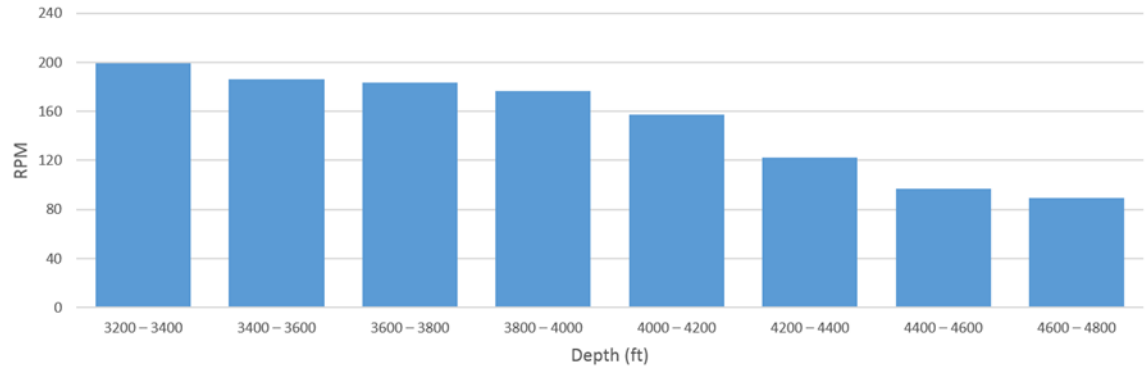


Figure 19: Optimal RPM for one rock strength scenario; 15,000 psi

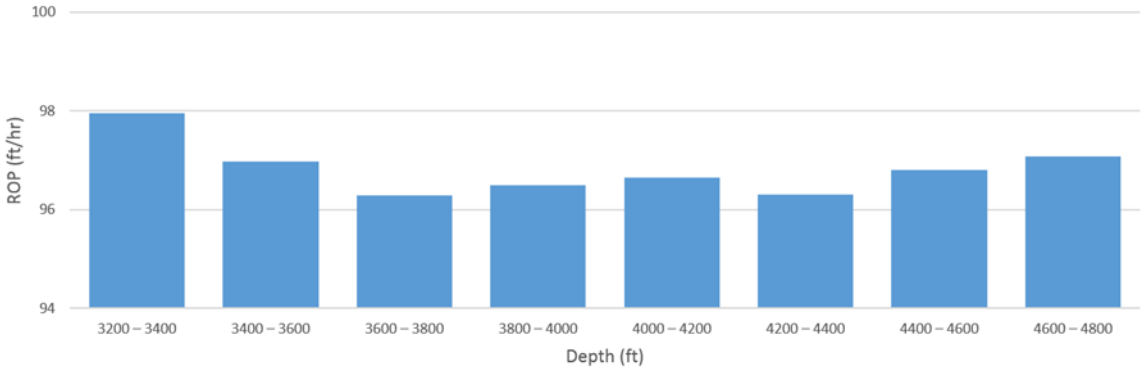


Figure 20: Calculated ROP for one rock strength scenario; 15,000 psi

Looking at the results shown above, similarly as explained in section 4.1.1, the optimal WOB was found to increase through the constant rock, along with the optimal ROP maintaining relatively constant. However, since the RPM was not input and allowed to change we can analyze the

optimal solution found. Differing from a constant RPM, the PSO algorithm found the best RPM values were to have an opposite trend from WOB, meaning RPM decreases through the constant rock. The learning curve, Fig. 21, and Table 3, showing the values from this simulation, are shown below.

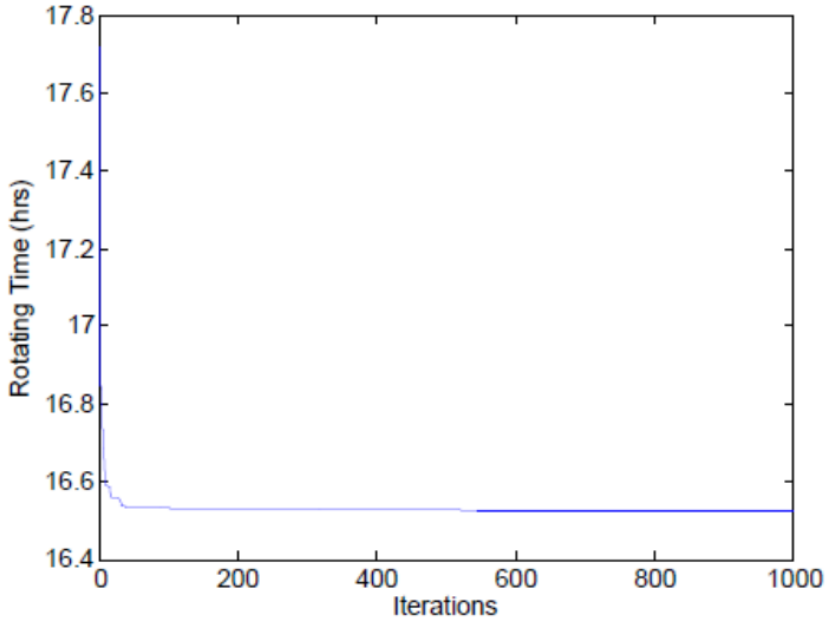


Figure 21: Learning curve for one rock strength scenario; 15,000 psi

| Depth (ft.) | Rock Strength (psi) | WOB (1000 lbs.) | RPM | ROP (ft. /hr.) | Wear | ABR |
|---|---|---|---|---|---|---|
| 3200 – 3400 | 15,000 | 7.45 | 199.6 | 98.0 | 0.90 | 0.3 |
| 3400 – 3600 | 15,000 | 8.58 | 186.1 | 97.0 | 0.84 | 0.3 |
| 3600 – 3800 | 15,000 | 9.21 | 183.5 | 96.3 | 0.78 | 0.3 |
| 3800 – 4000 | 15,000 | 10.15 | 176.9 | 96.5 | 0.72 | 0.3 |
| 4000 – 4200 | 15,000 | 11.97 | 157.7 | 96.6 | 0.67 | 0.3 |
| 4200 – 4400 | 15,000 | 15.89 | 122.3 | 96.3 | 0.61 | 0.3 |
| 4400 – 4600 | 15,000 | 20.97 | 97.1 | 96.8 | 0.56 | 0.3 |
| 4600 – 4800 | 15,000 | 24.58 | 89.1 | 97.1 | 0.50 | 0.3 |

Table 3: Data table for one rock strength scenario; 15,000 psi

### 4.1.4 Two Constant Rock Strengths

Similarly to section 4.1.2, this scenario has two different rock strengths, Fig. 22, but this situation the PSO is finding both WOB and RPM, Fig. 23 and Fig. 24. The output ROP is shown in Fig. 25.

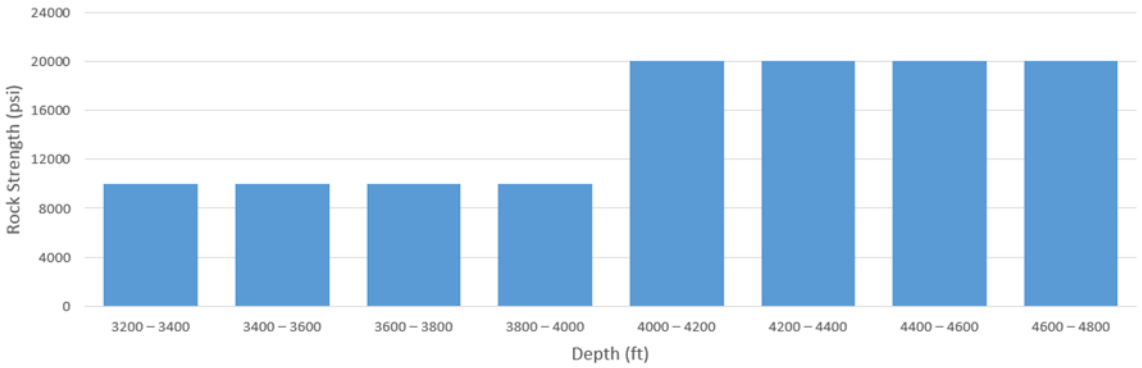


Figure 22: Graph showing the two rock strength scenario; 10,000 and 20,000 psi

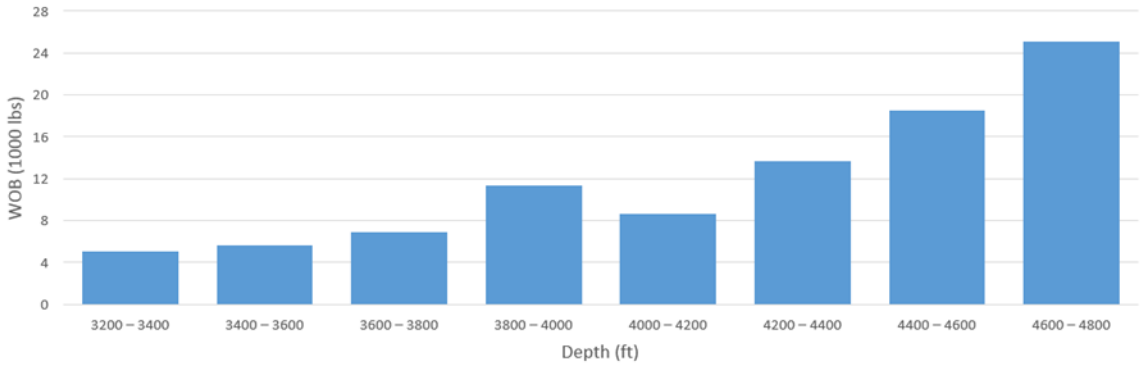


Figure 23: Optimal WOB for two rock strength scenario; 10,000 and 20,000 psi

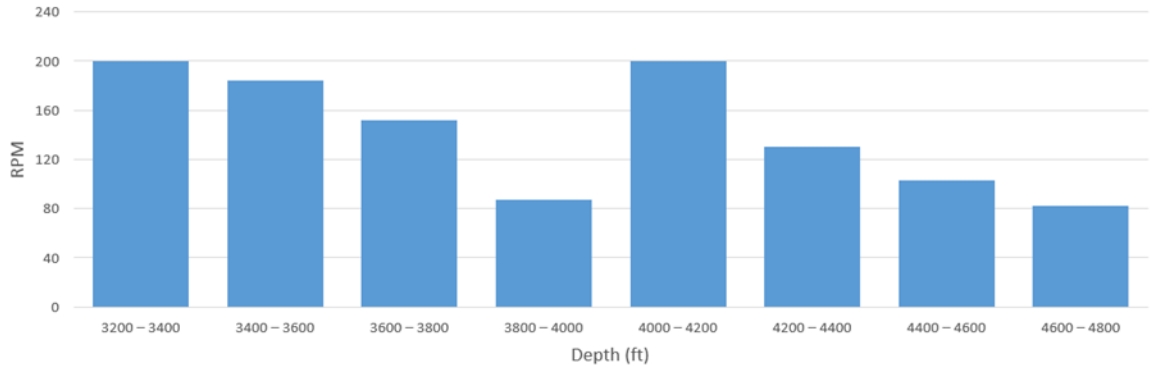


Figure 24: Optimal RPM for two rock strength scenario; 10,000 and 20,000 psi

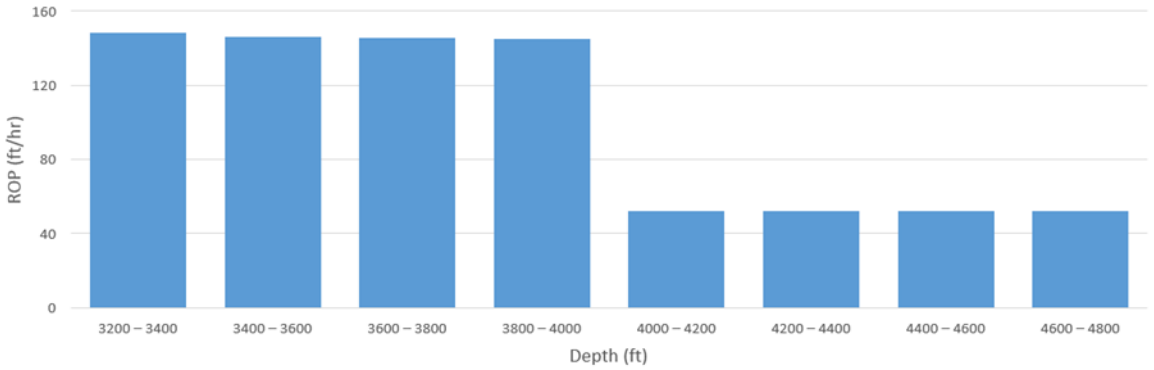


Figure 25: Calculated ROP for two rock strength scenario; 10,000 and 20,000 psi

As seen in Fig. 23 – Fig. 25, there is a clear shift in trends for WOB, RPM, and ROP at the point where the rock strength changes at depth 4000 ft. From Fig. 24, RPM is found from the code to be similar trends in both rock strengths, however, WOB is higher in the harder rock section, which agrees with section 4.1.2. Below is the learning curve, Fig. 26, and the simulation data, Table 4.

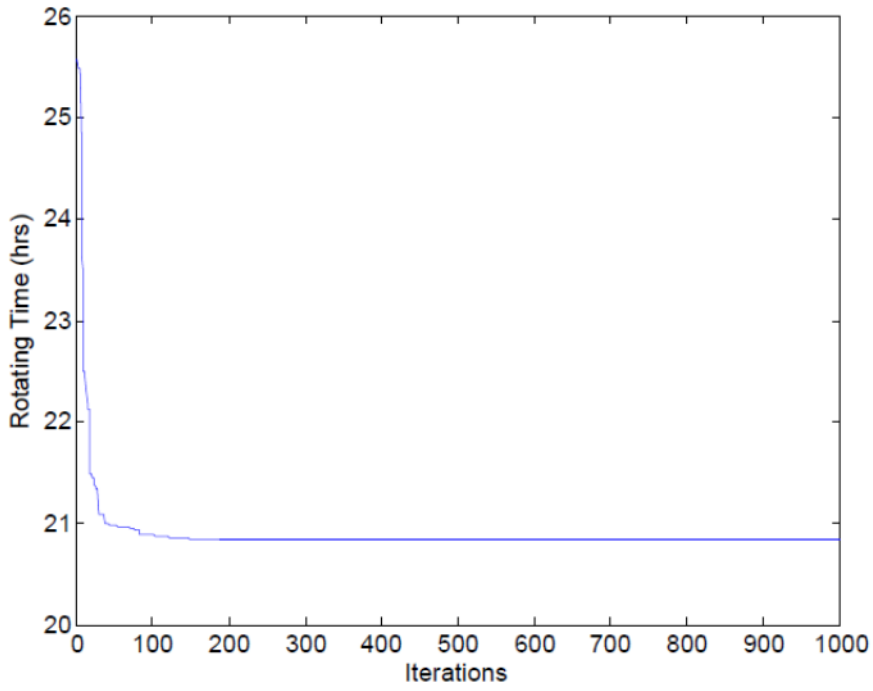


Figure 26: Learning curve for two rock strength scenario; 10,000 and 20,000 psi

| Depth (ft.) | Rock Strength (psi) | WOB (1000 lbs.) | RPM | ROP (ft. /hr.) | Wear | ABR |
|---|---|---|---|---|---|---|
| 3200 – 3400 | 10,000 | 5.02 | 200.0 | 148.3 | 0.94 | 0.3 |
| 3400 – 3600 | 10,000 | 5.62 | 183.8 | 146.2 | 0.90 | 0.3 |
| 3600 – 3800 | 10,000 | 6.86 | 151.5 | 145.4 | 0.87 | 0.3 |
| 3800 – 4000 | 10,000 | 11.37 | 87.2 | 145.0 | 0.83 | 0.3 |
| 4000 – 4200 | 20,000 | 8.59 | 200.0 | 52.1 | 0.75 | 0.3 |
| 4200 – 4400 | 20,000 | 13.67 | 130.3 | 52.1 | 0.67 | 0.3 |
| 4400 – 4600 | 20,000 | 18.49 | 102.9 | 52.0 | 0.58 | 0.3 |
| 4600 – 4800 | 20,000 | 25.12 | 82.2 | 52.1 | 0.50 | 0.3 |

Table 4: Data table for two rock strength scenario; 10,000 and 20,000 psi

4.1.5 Three Constant Rock Strengths and Constant ABR

The next two tests are to analyze the effects of rock abrasiveness. They consist of three rock

strengths, 10,000 psi, 15,000 psi, and 20,000 psi. Similarly to the first four simulations, this first test incorporates a constant value of 0.3 for abrasiveness in all three rock strengths. The graphs for rock strength, WOB, RPM, and ROP are shown in Fig. 27 – Fig. 30 below.

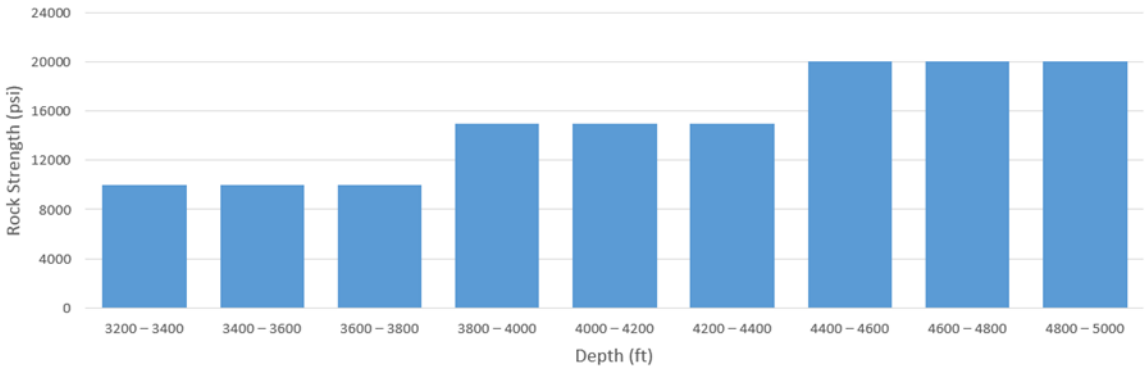


Figure 27: Graph showing the three rock strength scenario; 10,000, 15,000, and 20,000 psi, with constant abrasiveness

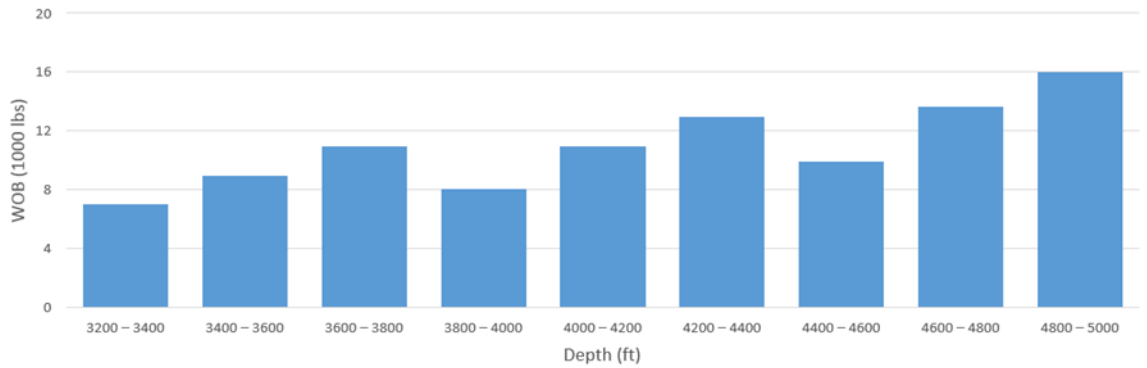


Figure 28: Optimal WOB for the three rock strength scenario; 10,000, 15,000, and 20,000 psi, with constant abrasiveness

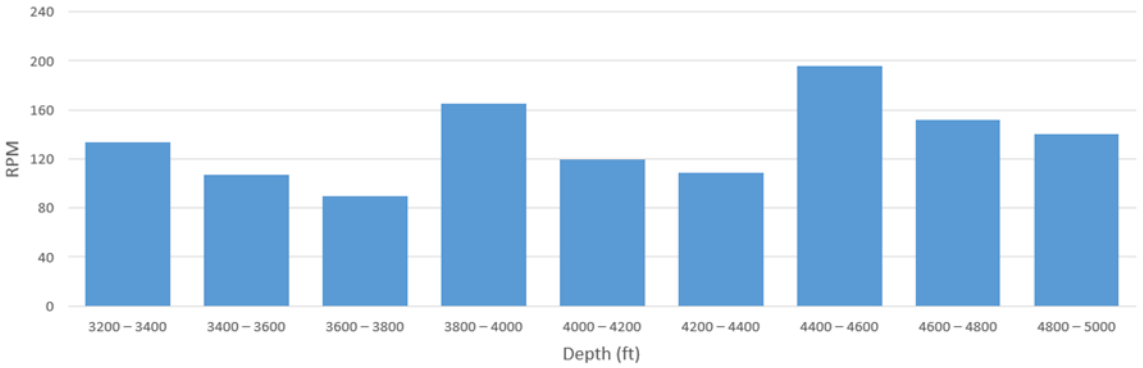


Figure 29: Optimal RPM for the three rock strength scenario; 10,000, 15,000, and 20,000 psi, with constant abrasiveness

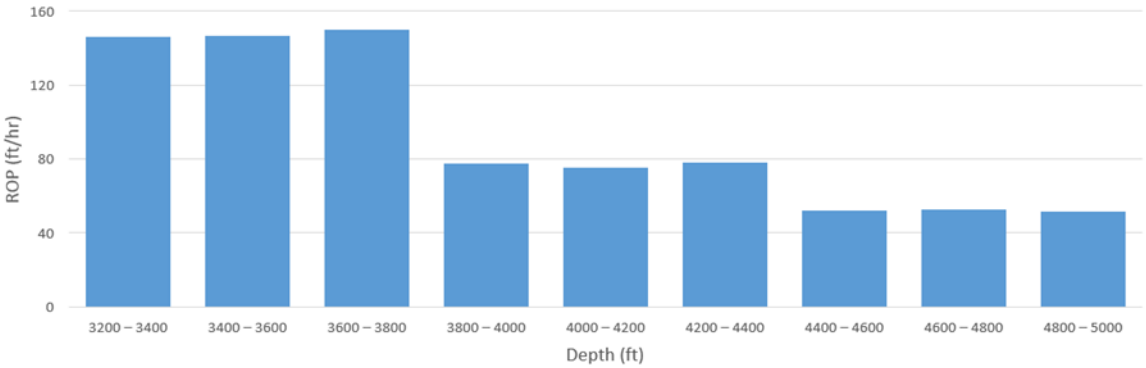


Figure 30: Calculated ROP for the three rock strength scenario; 10,000, 15,000, and 20,000 psi, with constant abrasiveness

Looking at the graphs above, ROP clearly decreases as the rock strength increases, however, both averages for WOB and RPM increase with increasing rock strength. The learning curve and the data for this simulation are shown in Fig. 31 and Table 5.

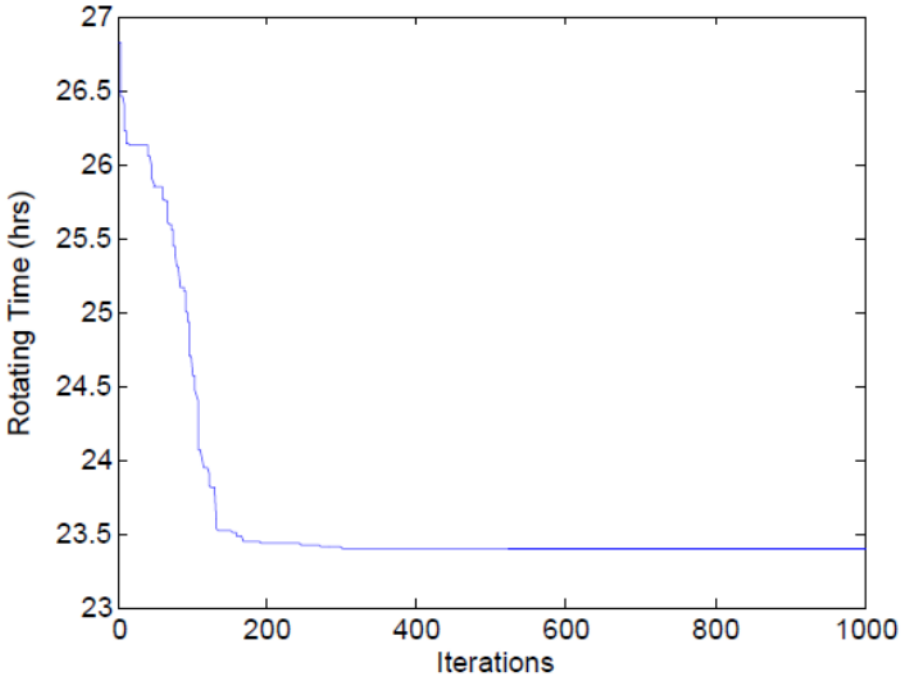


Figure 31: Learning curve for the three rock strength scenario; 10,000, 15,000, and 20,000 psi, with constant abrasiveness

| Depth (ft.) | Rock Strength (psi) | WOB (1000 lbs.) | RPM | ROP (ft. /hr.) | Wear | ABR |
|---|---|---|---|---|---|---|
| 3200 – 3400 | 10,000 | 7.00 | 133.5 | 146.1 | 0.94 | 0.3 |
| 3400 – 3600 | 10,000 | 8.94 | 106.9 | 146.5 | 0.91 | 0.3 |
| 3600 – 3800 | 10,000 | 10.94 | 90.0 | 149.9 | 0.87 | 0.3 |
| 3800 – 4000 | 15,000 | 8.04 | 165.3 | 77.5 | 0.82 | 0.3 |
| 4000 – 4200 | 15,000 | 10.96 | 119.2 | 75.4 | 0.77 | 0.3 |
| 4200 – 4400 | 15,000 | 12.91 | 108.7 | 78.0 | 0.72 | 0.3 |
| 4400 – 4600 | 20,000 | 9.87 | 196.1 | 52.0 | 0.65 | 0.3 |
| 4600 – 4800 | 20,000 | 13.65 | 151.7 | 52.6 | 0.58 | 0.3 |
| 4800 – 5000 | 20,000 | 15.95 | 140.0 | 51.5 | 0.5 | 0.3 |

Table 5: Data table for the three rock strength scenario; 10,000, 15,000, and 20,000 psi, with constant abrasiveness

### 4.1.6 Three Constant Rock Strengths and Changing ABR

This test is the same as section 4.1.5, except the abrasiveness values increase with increasing rock strength. The abrasiveness values used are 0.1, 0.3, and 0.8 for rock strengths 10,000, 15,000, and 20,000 psi, respectively. Fig. 32 – 35 show the rock strength, WOB, RPM and ROP results.

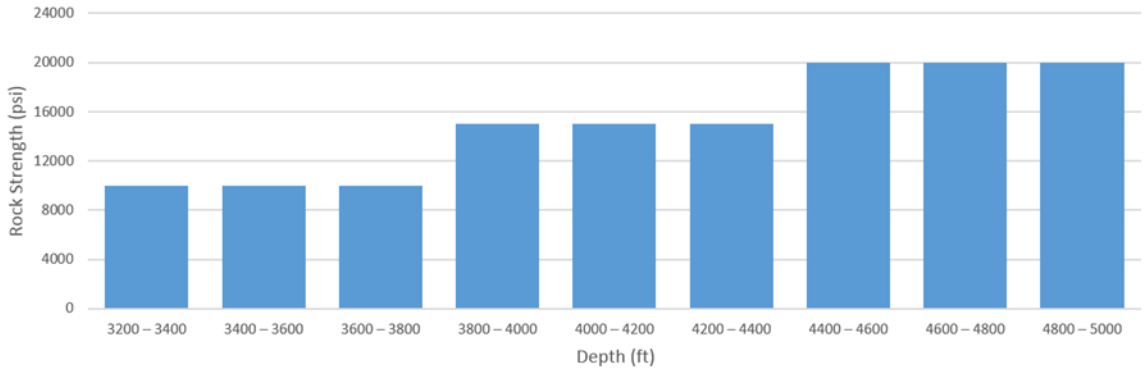


Figure 32: Graph showing the three rock strength scenario; 10,000, 15,000, and 20,000 psi, with changing abrasiveness

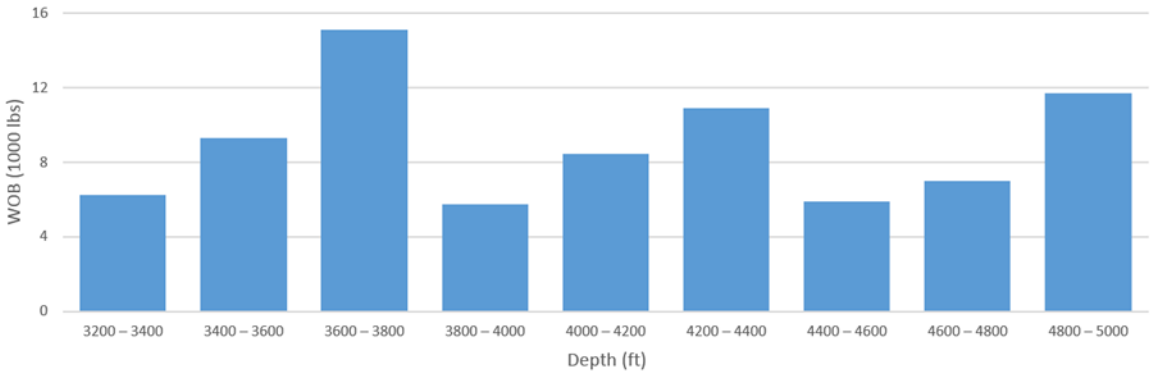


Figure 33: Optimal WOB for the three rock strength scenario; 10,000, 15,000, and 20,000 psi, with changing abrasiveness

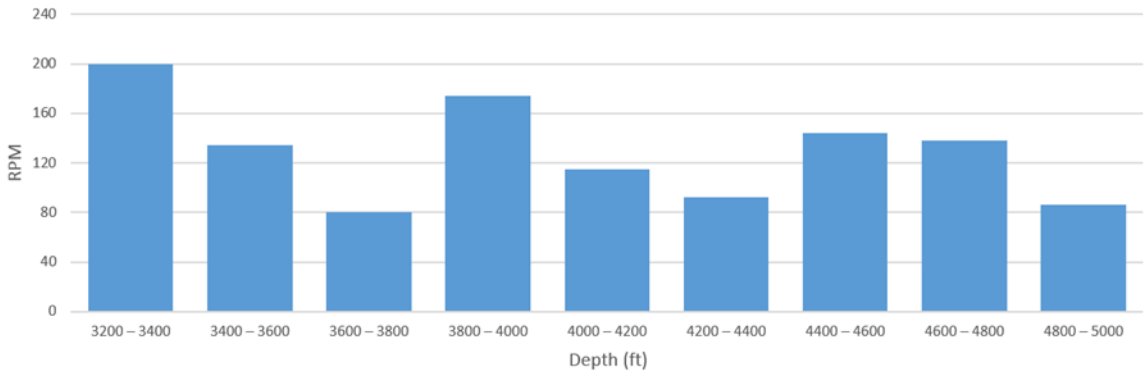


Figure 34: Optimal RPM for the three rock strength scenario; 10,000, 15,000, and 20,000 psi, with changing abrasiveness

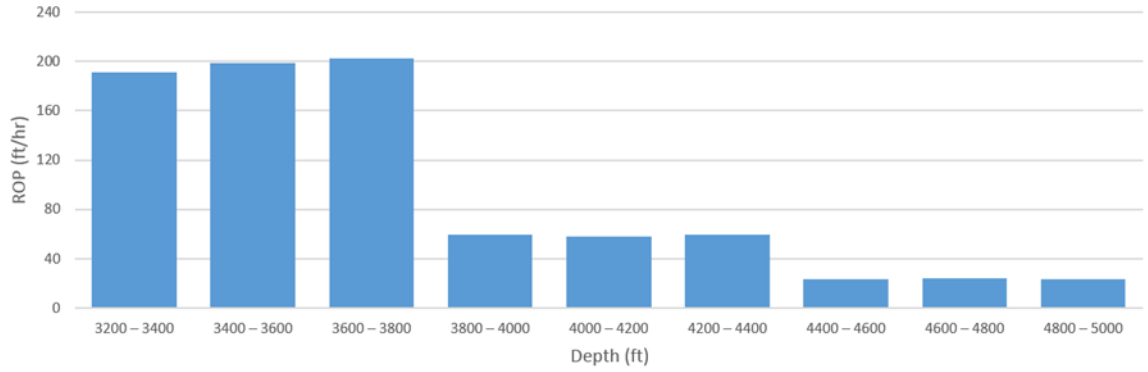


Figure 35: Calculated ROP for the three rock strength scenario; 10,000, 15,000, and 20,000 psi, with changing abrasiveness

Comparing the results from section 4.1.5 to Fig. 35, the ROP still decreases with an increase in rock strength, with Fig. 35 resulting in a much greater decrease. Looking at Fig. 33 and Fig. 34, in contrast to section 4.1.5, both the average WOB and RPM decrease with an increase in rock strength. This is significant since in the wear function, Eq. 5, there are two factors increasing, CCS and ABR, as opposed to just one variable as in the previous section. This is a better and more realistic representation of real world situations. This result also shows up in the optimal rotating time, Fig. 36. The times found here are much higher than in Fig. 36 since the effect of harder rock strengths are magnified with the changing ABR values. Table 6 shows the values from this simulation.

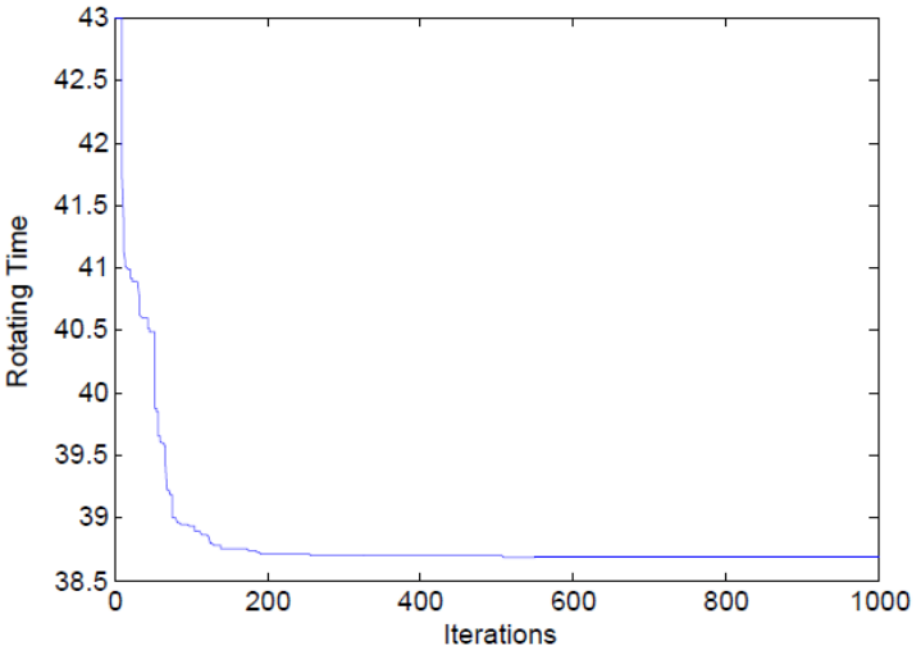


Figure 36: Learning curve for the three rock strength scenario; 10,000, 15,000, and 20,000 psi, with changing abrasiveness

| Depth (ft.) | Rock Strength (psi) | WOB (1000 lbs.) | RPM | ROP (ft. /hr.) | Wear | ABR |
|---|---|---|---|---|---|---|
| 3200 – 3400 | 10,000 | 6.25 | 200.0 | 190.9 | 0.97 | 0.1 |
| 3400 – 3600 | 10,000 | 9.32 | 134.6 | 198.4 | 0.95 | 0.1 |
| 3600 – 3800 | 10,000 | 15.09 | 80.1 | 202.5 | 0.93 | 0.1 |
| 3800 – 4000 | 15,000 | 5.77 | 174.0 | 59.3 | 0.88 | 0.3 |
| 4000 – 4200 | 15,000 | 8.48 | 115.0 | 58.2 | 0.84 | 0.3 |
| 4200 – 4400 | 15,000 | 10.89 | 92.2 | 59.3 | 0.80 | 0.3 |
| 4400 – 4600 | 20,000 | 5.91 | 144.3 | 23.5 | 0.70 | 0.8 |
| 4600 – 4800 | 20,000 | 7.01 | 138.1 | 24.0 | 0.60 | 0.8 |
| 4800 – 5000 | 20,000 | 11.69 | 86.0 | 23.2 | 0.5 | 0.8 |

Table 6: Data table for the three rock strength scenario; 10,000, 15,000, and 20,000 psi, with changing abrasiveness

## 4.2 Two Bit Optimization

This section is optimizing a drilling interval while incorporating two bits. For this optimization algorithm, the overall objective function (OF) determined to optimize upon differs from the one bit scenarios. In determining a successful well, one of the most important factors is the cost of drilling the well, therefore, the OF for optimization will be the cost per foot of drilling, Eq. 11. This classic cost equation, Eq. 11, is a function of the rig cost, the bit cost, the rotating time, Eq. 13, and tripping time, Eq. 12. In the trip time equation, $D_1$ is the depth when drilling starts for one bit and $D_2$ is the depth when the bit is finished drilling, and these are multiplied by the factor of how long it takes to trip the drill pipe, $t'_{Tripping}$, estimated as 0.75 hr. /1000 ft. The cost of the rig is assumed to be $100,000 per day. Eq. 11 is used to calculate the cost per foot for one bit. This equation will be used twice, and the overall cost per foot for the entire well will be determined.

$$\min \quad OF: Cost = \frac{Cost_{Rig}\left(t_{Rotating} + t_{Tripping}\right) + Cost_{Bit}}{Footage\ Drilled} \tag{11}$$

$$t_{Tripping} = (D_1 + D_2)t'_{Tripping} \tag{12}$$

$$t_{Rotating} = \sum_{i=1}^{n} \frac{\Delta D_i}{ROP_i} \tag{13}$$

Sections 4.2.1 and 4.2.2 used the two different bit proposals shown below in Table 7 for the PSO algorithm as the choice of possible bit selections.

| | Bit Proposal 1 | Bit Proposal 2 |
|---|---|---|
| Number of Blades | 5 | 6 |
| Number of Cutters | 32 | 38 |
| Cost | $ 35,000.00 | $ 40,000.00 |

Table 7: Two bit selection options for PSO algorithm

### 4.2.1 Three Constant Rock Strengths, Increasing Left to Right

The first two bit optimization scenario, Fig. 37, includes three different CCS values of rock; the three left columns (3200 ft. to 4400 ft.) correspond to 10,000 psi, the middle three (4400 ft. to 5600 ft.) are 15,000 psi, and the three right columns (5600 ft. to 6800 ft.) are 20,000 psi. Abrasiveness values corresponding to these three rock strengths are 0.1, 0.3, and 0.8, respectively. Below are the graphs for rock strength, WOB, RPM, and ROP, Fig. 37 - 40.

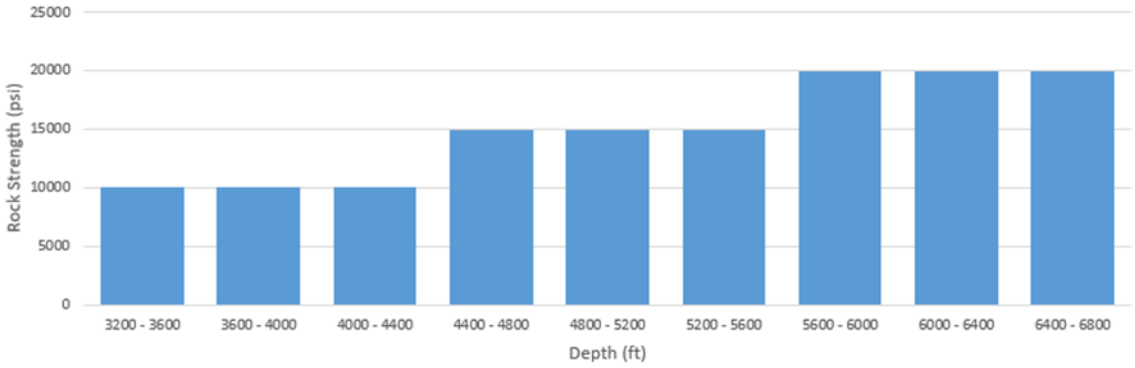


Figure 37: Graph showing the three rock strength, multiple bit scenario; 10,000, 15,000, and 20,000 psi

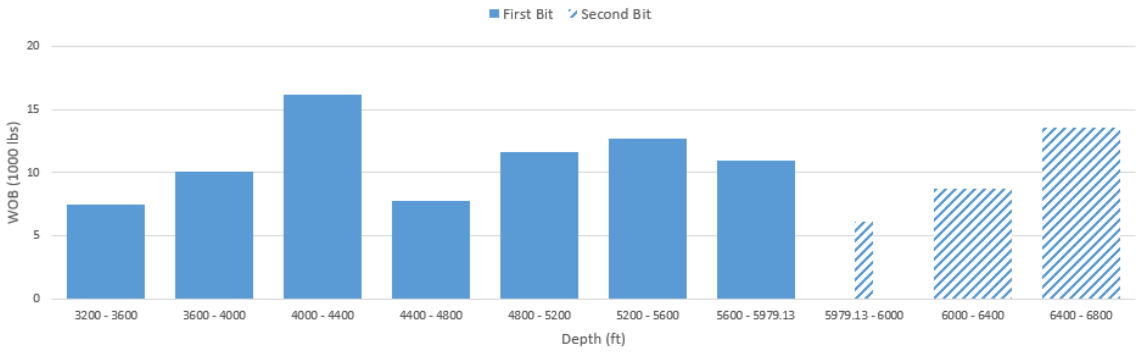


Figure 38: Optimal WOB for the three rock strength, multiple bit scenario; 10,000, 15,000, and 20,000 psi

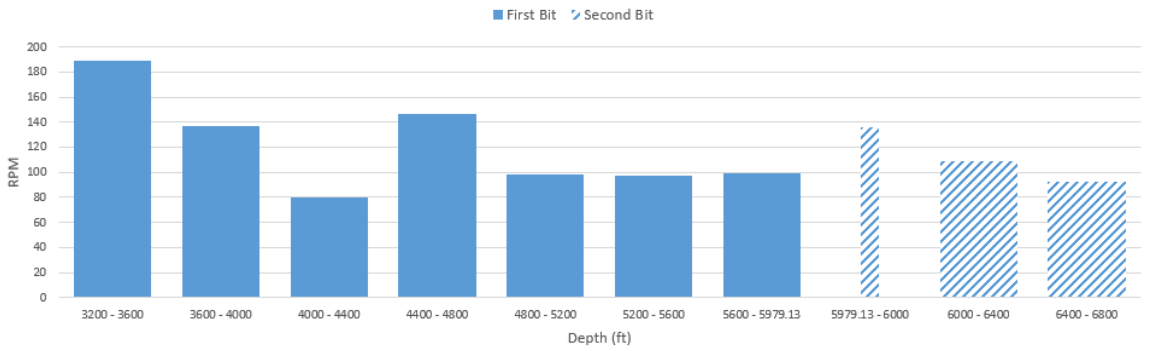


Figure 39: Optimal RPM for the three rock strength, multiple bit scenario; 10,000, 15,000, and 20,000 psi

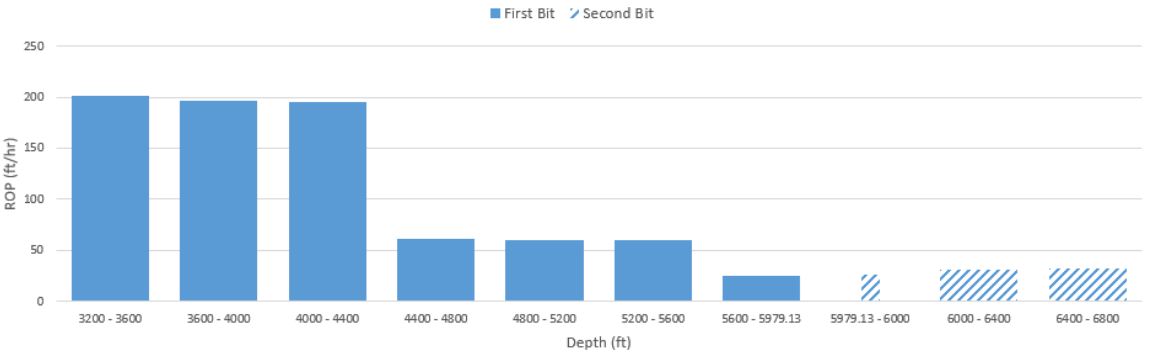


Figure 40: Calculated ROP for the three rock strength, multiple bit scenario; 10,000, 15,000, and 20,000 psi

Fig. 38 and Fig. 39 above show the optimized solution for the first two bit rock strength scenario, Fig. 37; including WOB and RPM combinations vs depth, along with the optimal depth that the bit was pulled out. Each column in Fig. 38 and Fig. 39 above represent the exact value used over the specified drilling intervals listed. The two different bits are illustrated with different textures, and both selected bits are bit proposal 2 from Table 7. The PSO algorithm found the best solution was to switch bits at 5979.13 ft. and that causes the column between 5600 ft. to 6000 ft. in Fig. 37 to divide into two different columns (from 5600 ft. to 5979.13 ft. and 5979.13 ft. to 6000 ft.) in Fig. 38 – 40. Below is the learning curve, Fig. 41, and the data table, Table 8.

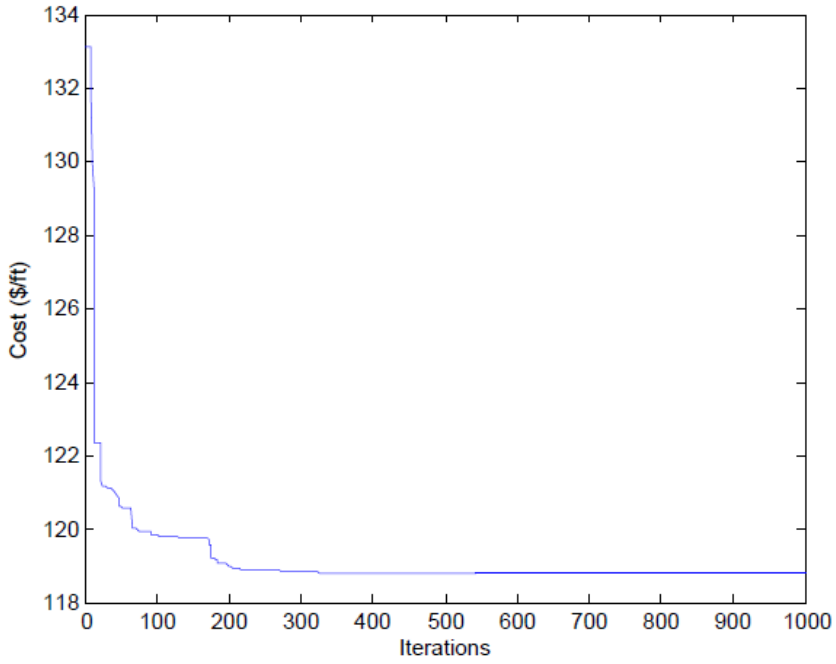


Figure 41: Learning curve for the three rock strength, multiple bit scenario; 10,000, 15,000, and 20,000 psi

| Depth (ft.) | Rock Strength (psi) | WOB (1000 lbs.) | RPM | ROP (ft. /hr.) | Wear | Bit |
|---|---|---|---|---|---|---|
| 3200 – 3600 | 10,000 | 7.49 | 189.5 | 200.8 | 0.95 | 2 |
| 3600 – 4000 | 10,000 | 10.11 | 137.0 | 197.1 | 0.92 | 2 |
| 4000 – 4400 | 10,000 | 16.20 | 80.0 | 194.8 | 0.89 | 2 |
| 4400 – 4800 | 15,000 | 7.73 | 146.9 | 61.1 | 0.81 | 2 |
| 4800 – 5200 | 15,000 | 11.58 | 98.8 | 60.3 | 0.74 | 2 |
| 5200 – 5600 | 15,000 | 12.66 | 97.4 | 60.2 | 0.67 | 2 |
| 5600 – 5979.13 | 20,000 | 10.94 | 99.2 | 25.4 | 0.50 | 2 |
| 5979.13 – 6000 | 20,000 | 6.10 | 136.4 | 26.2 | 0.97 | 2 |
| 6000 – 6400 | 20,000 | 8.68 | 108.9 | 30.6 | 0.72 | 2 |
| 6400 – 6800 | 20,000 | 13.56 | 92.7 | 32.6 | 0.50 | 2 |

Table 8: Data table for the three rock strength, multiple bit scenario; 10,000, 15,000, and 20,000 psi

Below shows a graph, Fig. 42, depicting how the cost of the well and selected bit combination changes with pull depth for the three rock strength scenario, increasing from left to right. This was achieved by manually inputting the bit pull depth and iteratively changing it through the well section. For each iteration, the algorithm was finding the optimal WOB, RPM, and bit combination associated with each specific pull depth. This graph agrees with the optimal solution found where the optimal depth to change bits found was 5979.13 ft., along with the optimal bit combination found to incorporate the second bit twice. The graph below shows three different sections of the graph representing the different order of possible combinations of the bits from Table 7 during the drilling process. These sections are associated with the different bit combinations including: use of the first bit followed by second bit, black dots; use of the second bit twice, green dots; and use of the second bit followed by the first bit, red dots. The bit combination of using the first bit twice never resulted in the optimal solution.

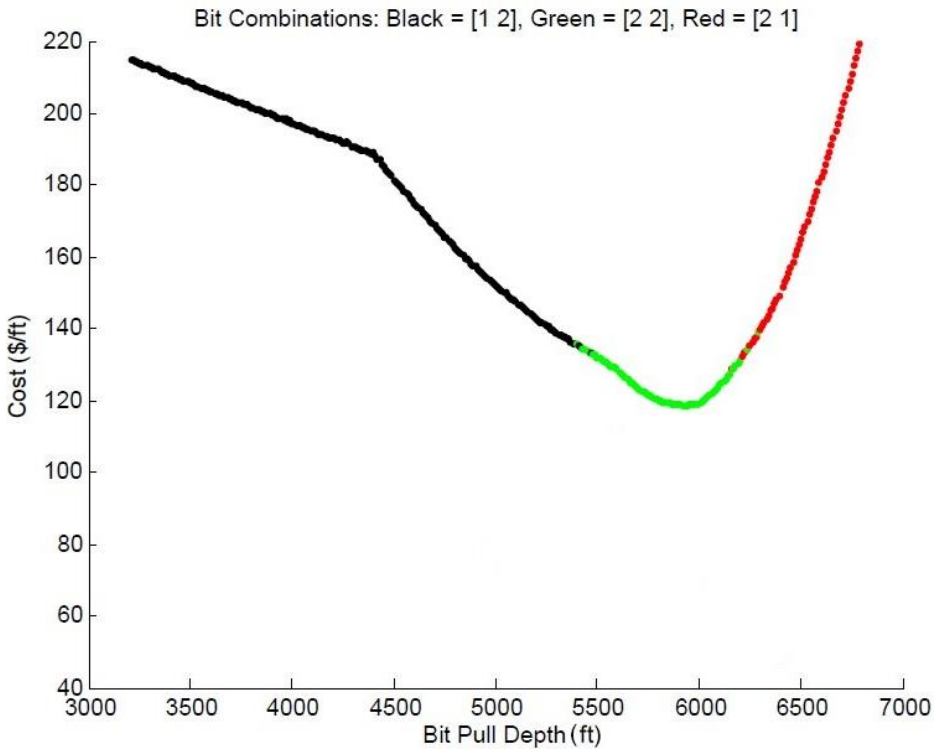


Figure 42: Graph for three rock strength, increasing left to right, showing optimal drilling cost with changing pull depth

### 4.2.2 Three Constant Rock Strengths, Decreasing Left to Right

The second rock strength scenario is the opposite from the first. Fig. 43 shows the second scenario including 20,000 psi in the three left columns (3200 ft. to 4400 ft.), the middle three columns (4400 ft. to 5600 ft.) are 15,000 psi, and the three right columns (5600 ft. to 6800 ft.) are 10,000 psi rock. Abrasiveness values corresponding to these three rock strengths are 0.8, 0.3, and 0.1, respectively. Below are the rock strength, WOB, RPM, and ROP graphs, Fig. 43 – 46, for this simulation.

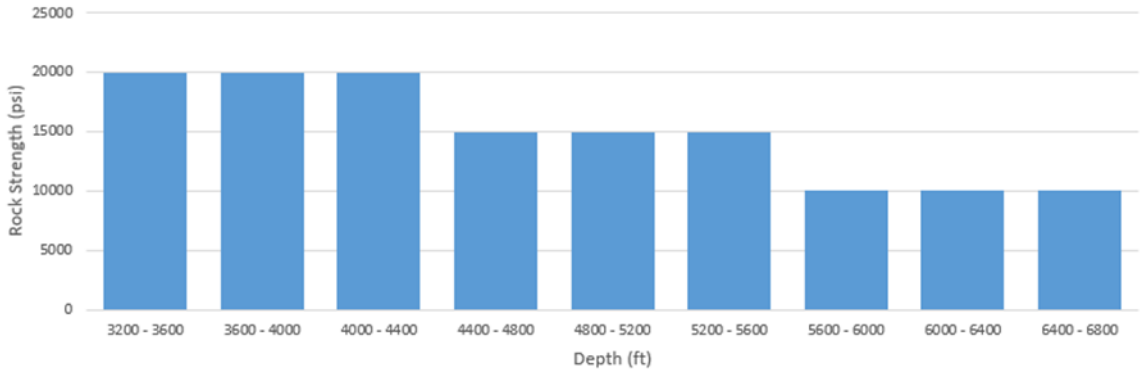


Figure 43: Graph showing the three rock strength, multiple bit scenario; 20,000, 15,000, and 10,000 psi

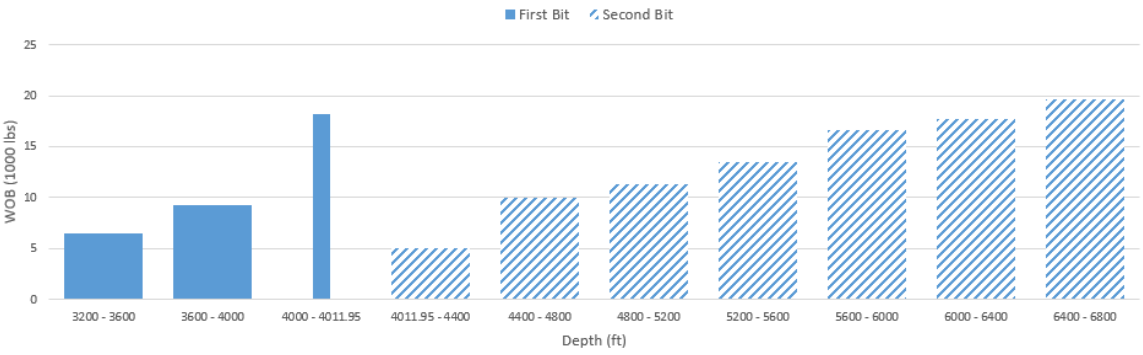


Figure 44: Optimal WOB for the three rock strength, multiple bit scenario; 20,000, 15,000, and 10,000 psi

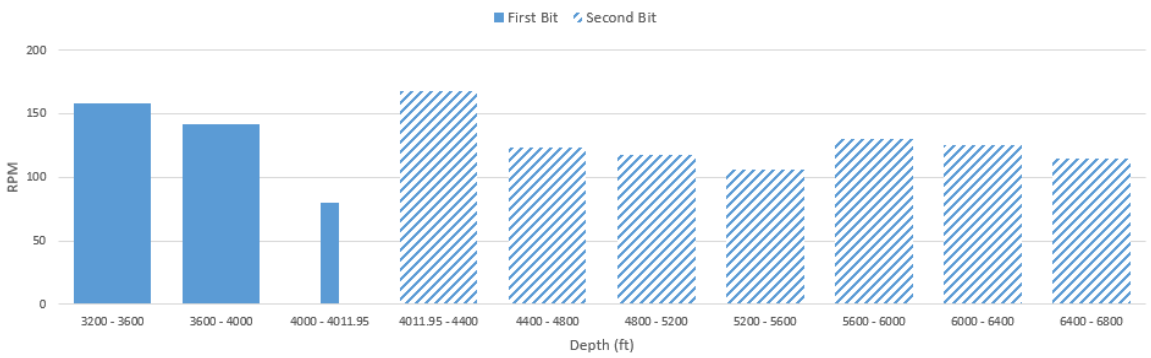


Figure 45: Optimal RPM for the three rock strength, multiple bit scenario; 20,000, 15,000, and 10,000 psi

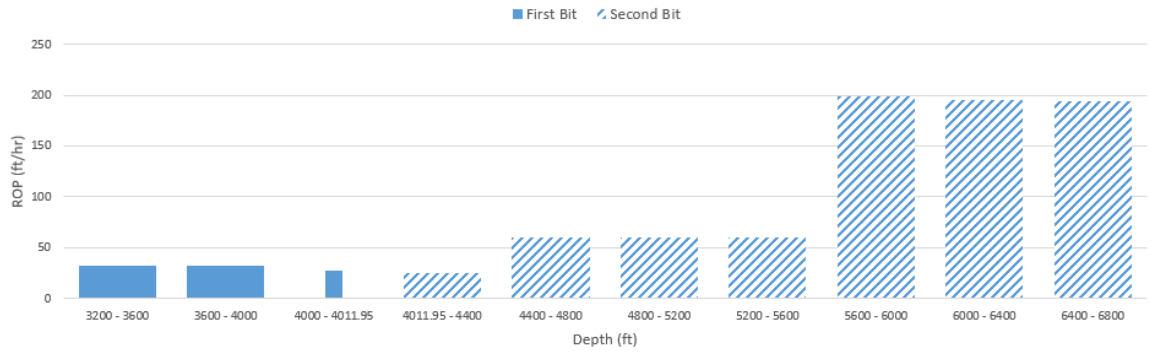


Figure 46: Calculated ROP for the three rock strength, multiple bit scenario; 20,000, 15,000, and 10,000 psi

Fig. 44 and Fig. 45 above show the optimal WOB and RPM combinations vs depth, along with the optimal pull depth for the second two bit rock strength scenario shown in Fig. 43. Similarly to section 4.2.1, the WOB and RPM values represented in Fig. 44 and Fig. 45 signify the exact value over the depth interval. The two different bits are again illustrated with different textures, both selected bits were bit proposal 2 from Table 7. The optimal bit pull depth was found to be 4011.95 ft. Likewise from the first scenario, the PSO algorithm split the column from 4000 ft. to 4400 ft. in Fig. 43 into two columns from 4000 ft. to 4011.95 ft. and from 4011.95 ft. to 4400 ft. Fig. 47 shows the learning curve and Table 9 is the data from this simulation.

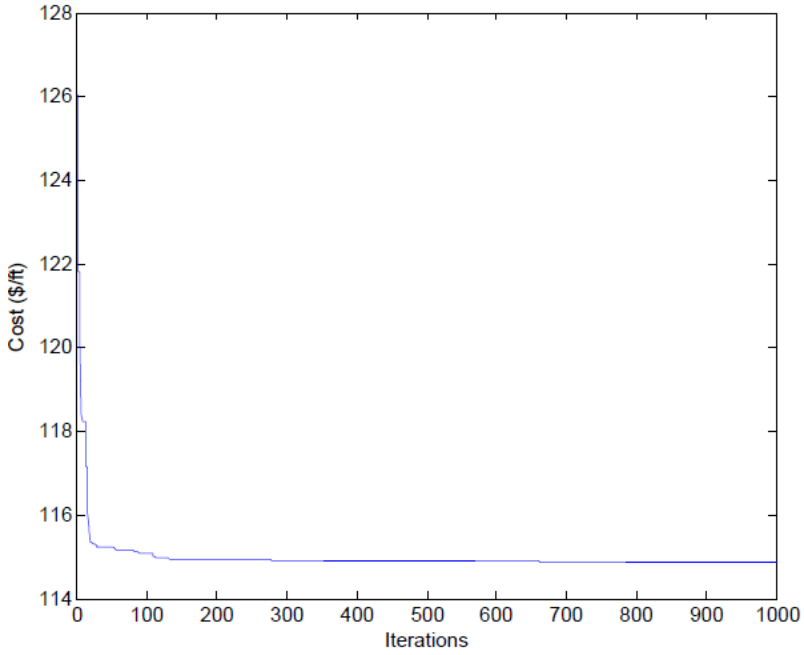


Figure 47: Learning curve for the three rock strength, multiple bit scenario; 20,000, 15,000, and 10,000 psi

| Depth (ft.) | Rock Strength (psi) | WOB (1000 lbs.) | RPM | ROP (ft. /hr.) | Wear | Bit |
|---|---|---|---|---|---|---|
| 3200 – 3600 | 20,000 | 6.53 | 158.0 | 32.6 | 0.72 | 2 |
| 3600 – 4000 | 20,000 | 9.31 | 142.1 | 32.1 | 0.51 | 2 |
| 4000 – 4011.95 | 20,000 | 18.18 | 80.0 | 27.8 | 0.50 | 2 |
| 4011.95 – 4400 | 20,000 | 5.00 | 167.5 | 25.4 | 0.77 | 2 |
| 4400 – 4800 | 15,000 | 9.97 | 123.7 | 59.6 | 0.70 | 2 |
| 4800 – 5200 | 15,000 | 11.35 | 117.7 | 60.1 | 0.63 | 2 |
| 5200 – 5600 | 15,000 | 13.54 | 106.4 | 60.3 | 0.56 | 2 |
| 5600 – 6000 | 10,000 | 16.70 | 130.5 | 198.5 | 0.54 | 2 |
| 6000 – 6400 | 10,000 | 17.70 | 125.0 | 196.0 | 0.52 | 2 |
| 6400 – 6800 | 10,000 | 19.64 | 114.3 | 194.5 | 0.50 | 2 |

Table 9: Data table for the three rock strength, multiple bit scenario; 20,000, 15,000, and 10,000 psi

Below shows a graph, Fig. 48, depicting how the cost of the well and selected bit combination changes with pull depth for the three rock strength scenario, decreasing from left to right. This graph was created in the same way as Fig. 42, and can be interpreted in a similar manner, except this represents the rock strength scenario shown in Fig. 43. This graph agrees with the optimal solution found where the optimal depth to change bits found was 4011.95 ft., along with the optimal bit combination found to incorporate the second bit twice.

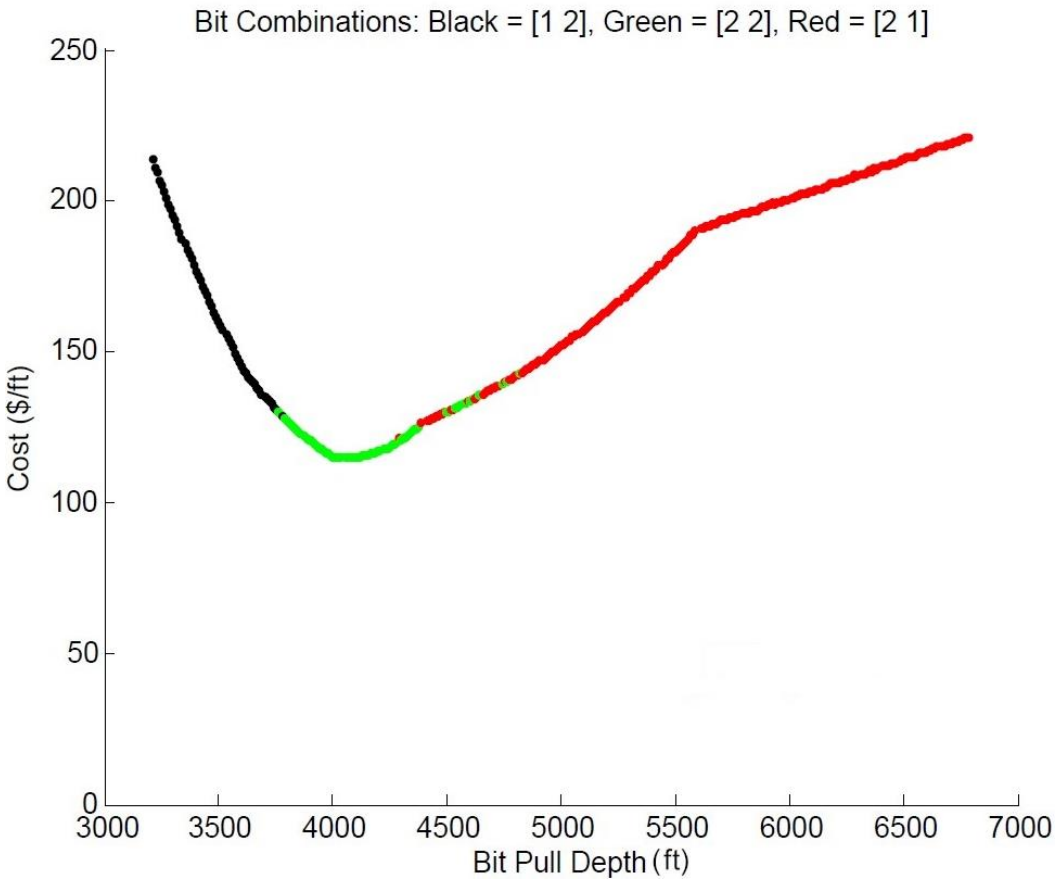


Figure 48: Graph for three rock strength, decreasing left to right, showing optimal drilling cost with changing pull depth

## 4.3 Field Case Validation

Field case data was used from a well in the North Sea and optimized to prove the validity of this program in more complex situations. The validation was shown using data from the first two bit

runs, 9379.92 ft. – 13832.02 ft., for the 12.25 in. well section (Gjelstad et al., 1998, Bratli et al., 1997). The rig rates and the estimate for tripping 1000 ft. of pipe were held the same as in Section 4.2.

Before optimizing, the data from the well had to be correlated to the constants found in Eq. 3 and Eq. 5. All of the constants found in the methodology section were held to the same value as in the previous results sections, except for K, $W_c$, $a_2$, $b_2$, and $c_2$. The constants found in Eq. 6, were taken from previous research done in modeling PDC bits (Rashidi, 2011), the other two were calibrated. Before finding the experimental constants, the confined rock strength for the well was calculated (Rastegar et al., 2008), and the well was discretized by taking averages of specific sections. Below is a graph showing the real rock CCS and the averaged rock values, Fig. 49.

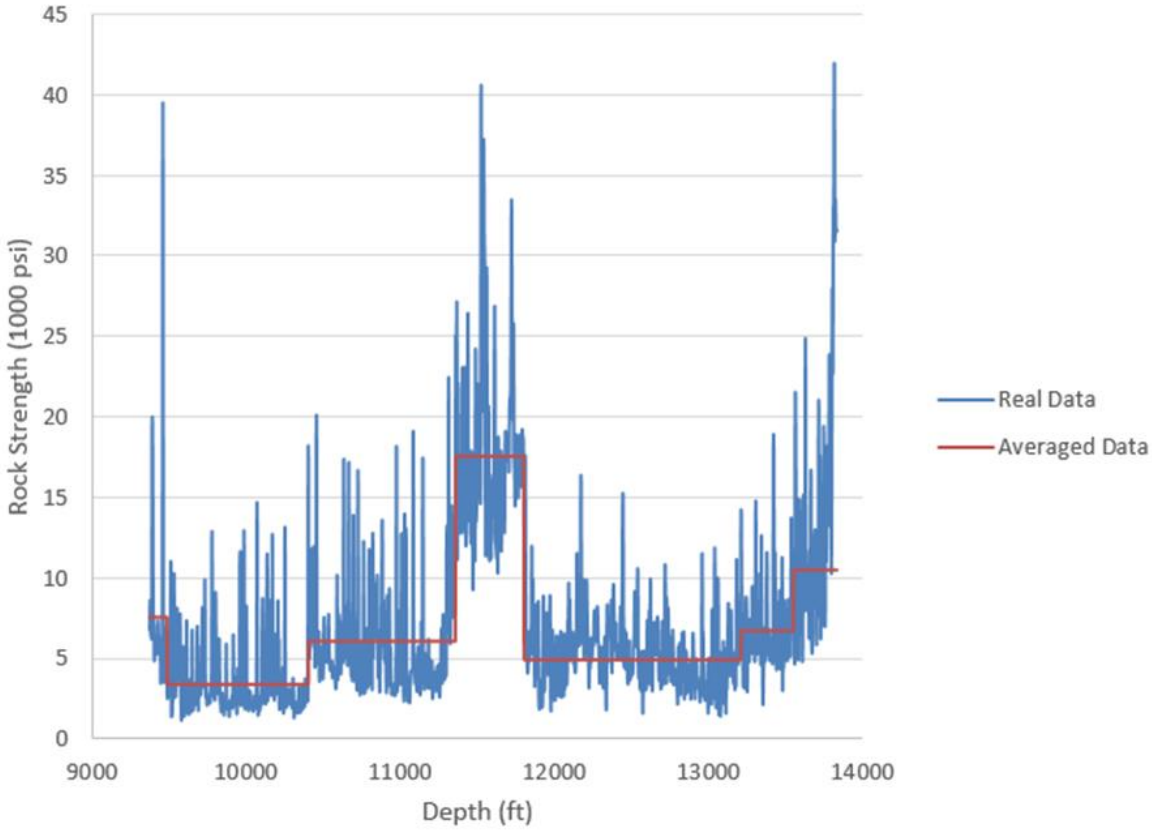


Figure 49: Graph of the 12.25 in. well real rock strength and averaged rock strength

The bit data that was used is shown below in Table 10.

| | Bit 1 | Bit 2 |
|---|---|---|
| Bit Type | PDC | PDC |
| Bit Diameter | 12.25 in. | 12.25 in. |
| Depth In | 9379.92 | 11814.30 |
| Depth Out | 11814.30 | 13832.02 |
| Wear In | 0.0 | 0.0 |
| Wear Out | 0.45 | 0.825 |
| Cost | $ 48,062 | $57,876 |
| Number of Cutter | 69 | 107 |
| Back Rake | 20° | 20° |
| Side Rake | 15° | 0° |
| Number of Blades | 6 | 6 |
| Junk Slot Area | 28 $in^2$ | 28 $in^2$ |

Table 10: Two bits used in field case

Both bit 1 and bit 2 will have different K and $W_c$ values, so calibrating both of the constants were done using only the data associated with each individual bit. The K constant from Eq. 3 was found by using the reported data from the well and altering the K value until the difference between the final calculated drilling time and the reported time for each bit was minimized. $W_c$ in Eq. 5, was calibrated iteratively by incorporating the drilling data and varying $W_c$ until the calculated wear out matched the field reported wear for each bit. There were three different optimizations done for this well and are detailed below. The abrasiveness (ABR) values for this well were determined by fitting an exponential curve fit through the rock strength vs. abrasiveness values used in Sections 4.1 and 4.2.

The objective function for the field case validation is same as in Section 4.2 and shown in Eq. 10. For these simulations, there were no ROP restrictions applied to the field case optimization and is therefore purely theoretical. A maximum ROP limit can be set from maximum handling capabilities of solid control equipment on the rig, annulus solid loading, hole cleaning or just controlled drilling with a set maximum ROP.

### 4.3.1 WOB and RPM Optimization

For this section, WOB and RPM were the only variables optimized, with the goal to reduce the overall cost per foot. The bit combination, pull depth, and final bit wear out were held the same as done in the field. Below are graphs showing the optimal WOB, RPM, ROP, and learning curve for this simulation, Fig. 50 – Fig. 53. Each bit is represented with different textures.

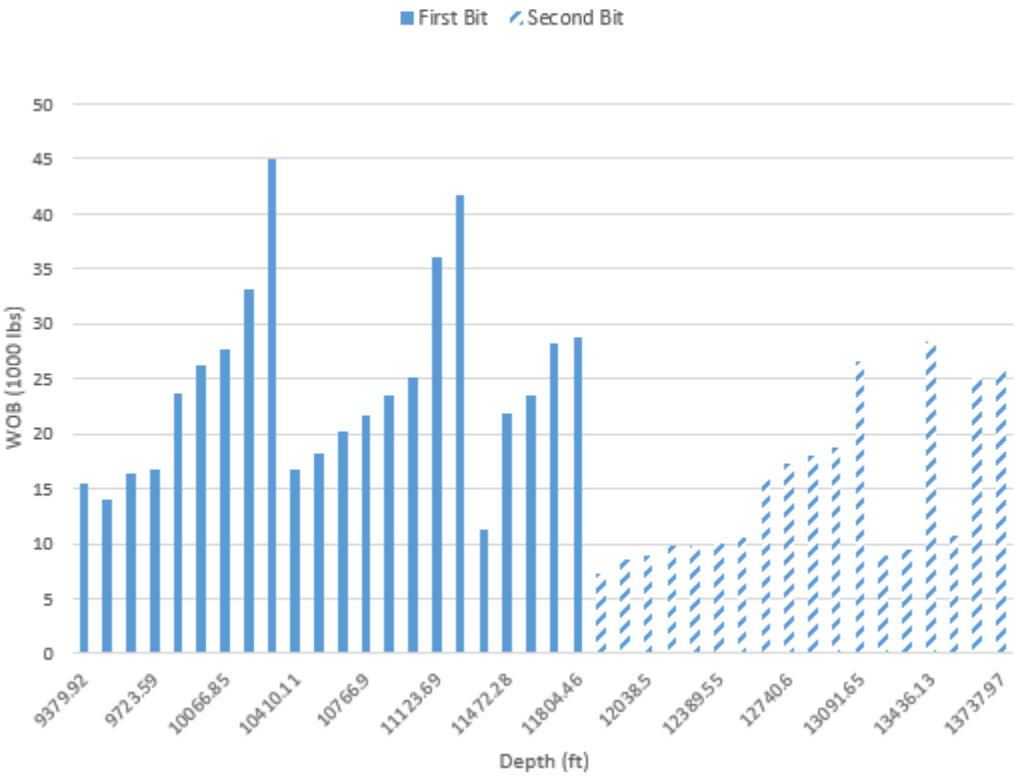


Figure 50: Optimal WOB for field case WOB and RPM Optimization

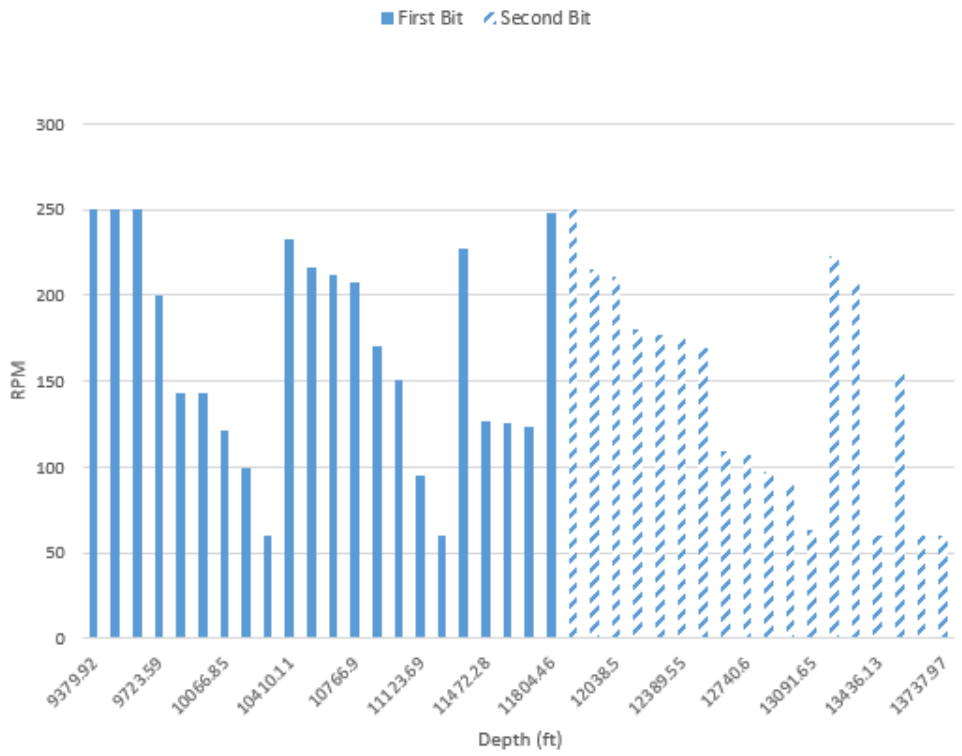


Figure 51: Optimal RPM for field case WOB and RPM Optimization

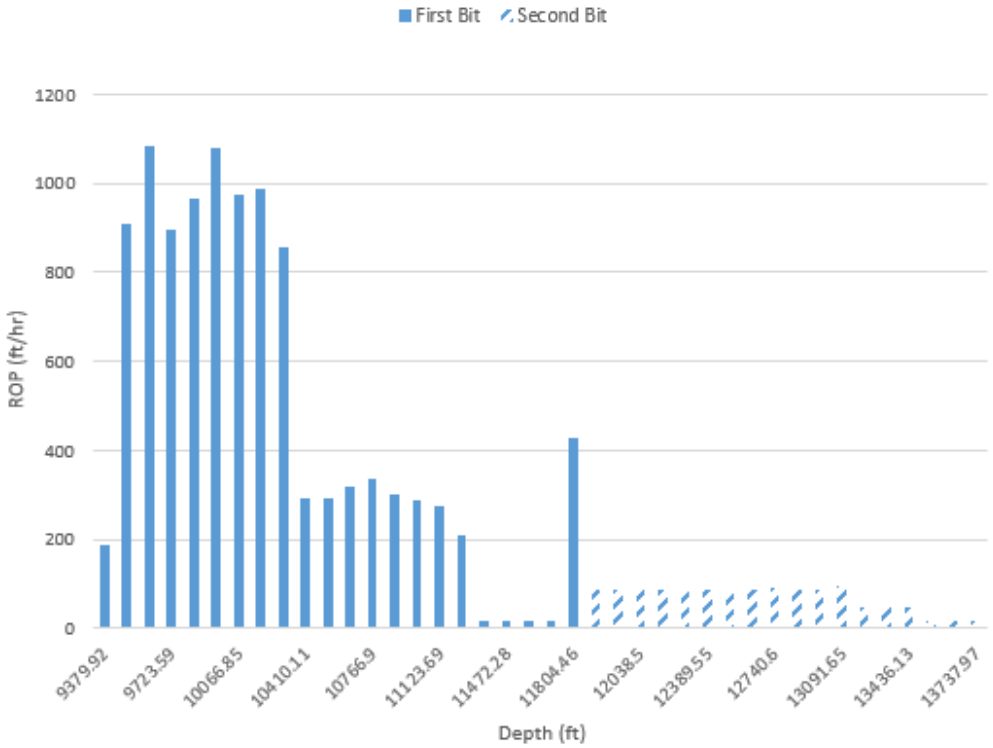


Figure 52: Optimal ROP for field case WOB and RPM Optimization

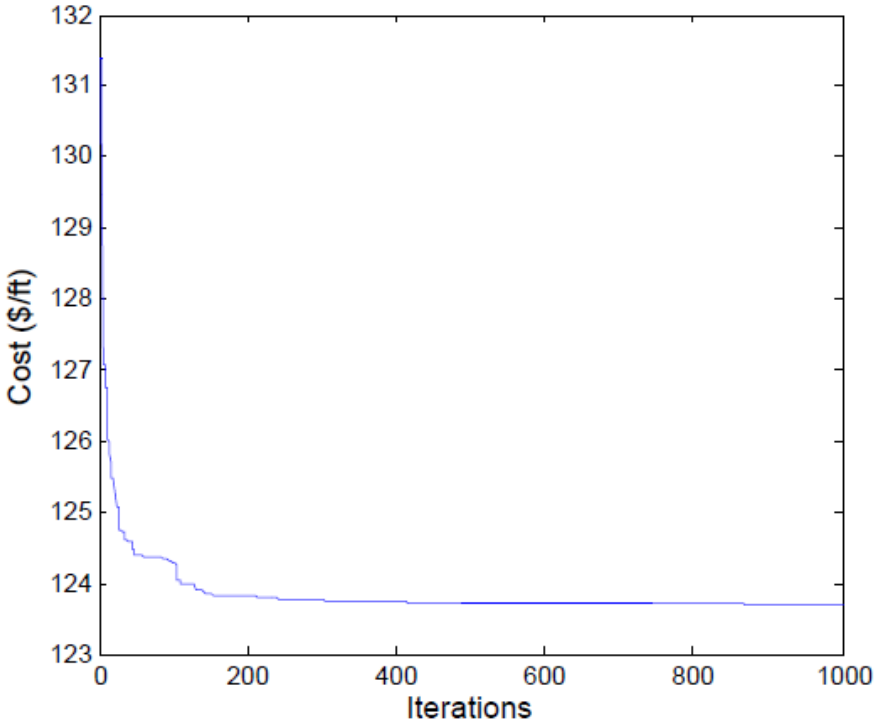


Figure 53: Learning curve for field case WOB and RPM Optimization

4.3.2 WOB, RPM, and Pull Depth Optimization

The next optimization performed was done on WOB and RPM combinations, along with optimal pull depth for changing the bits. The final bit wear out for both bits were changed to 0.5, however, the bit combination was held the same. Below are the graphs showing the results for WOB, RPM, ROP, and the learning curve, Fig. 54 – Fig. 57.

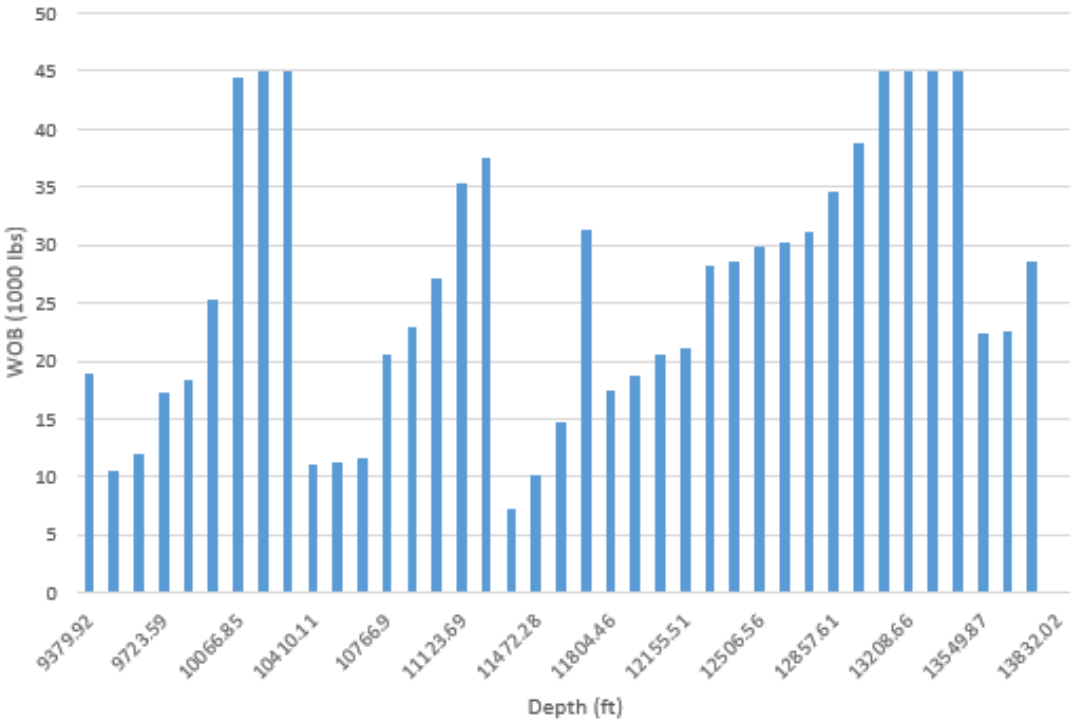


Figure 54: Optimal WOB for field case WOB, RPM, and Pull Depth Optimization

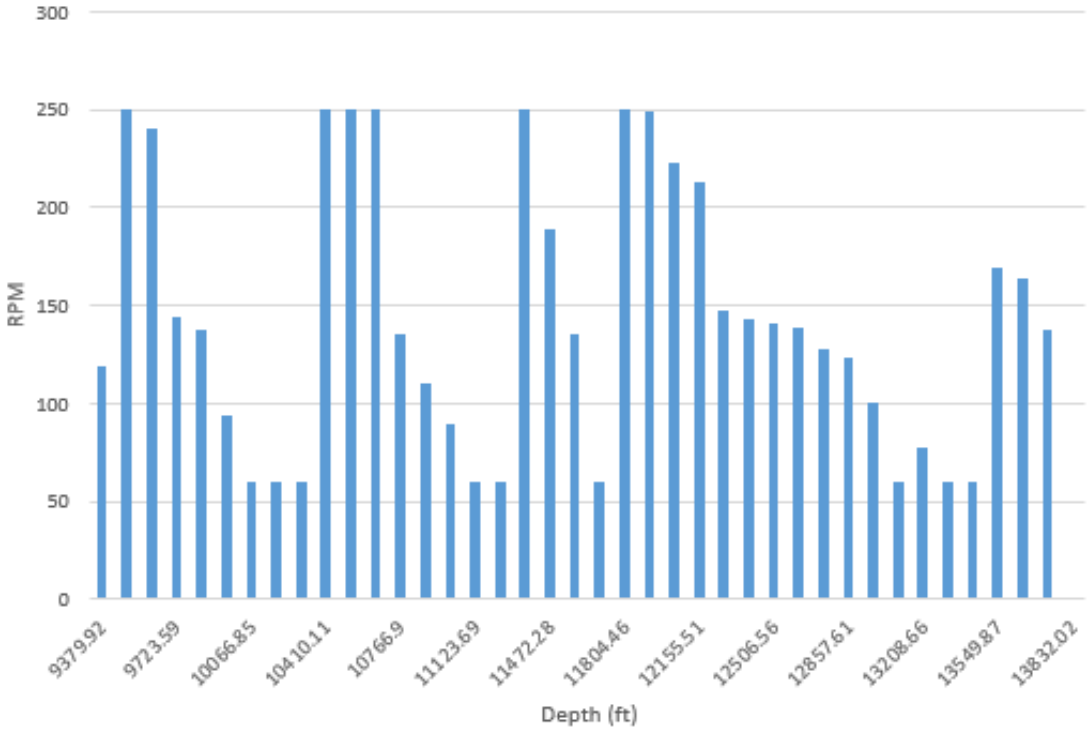


Figure 55: Optimal RPM for field case WOB, RPM, and Pull Depth Optimization

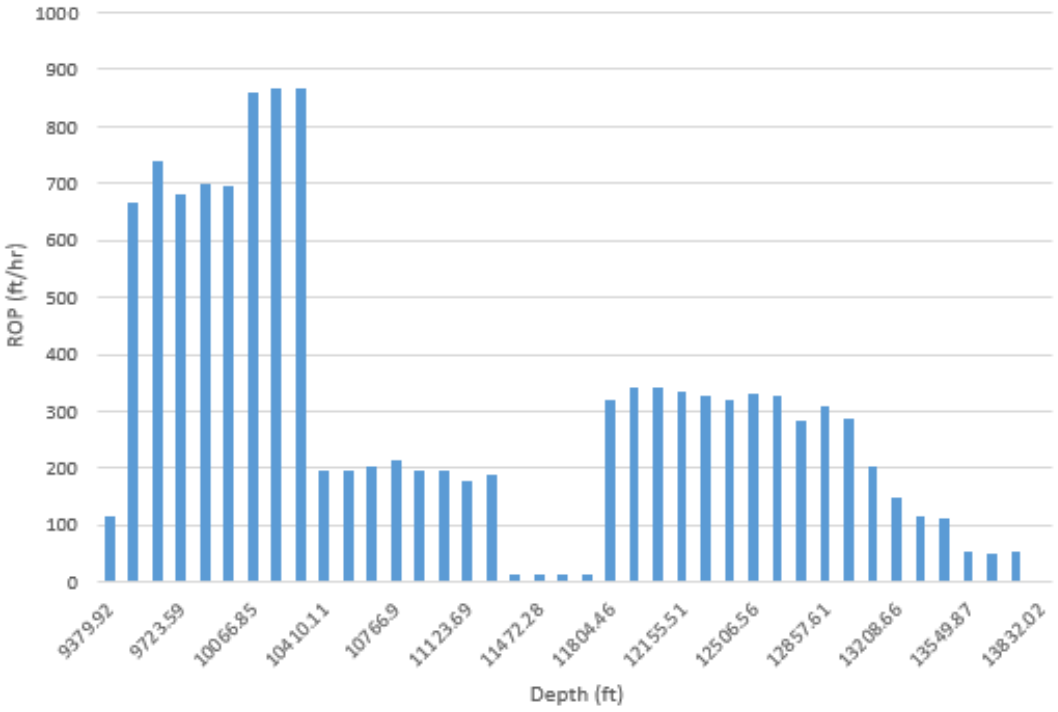


Figure 56: Optimal ROP for field case WOB, RPM, and Pull Depth Optimization

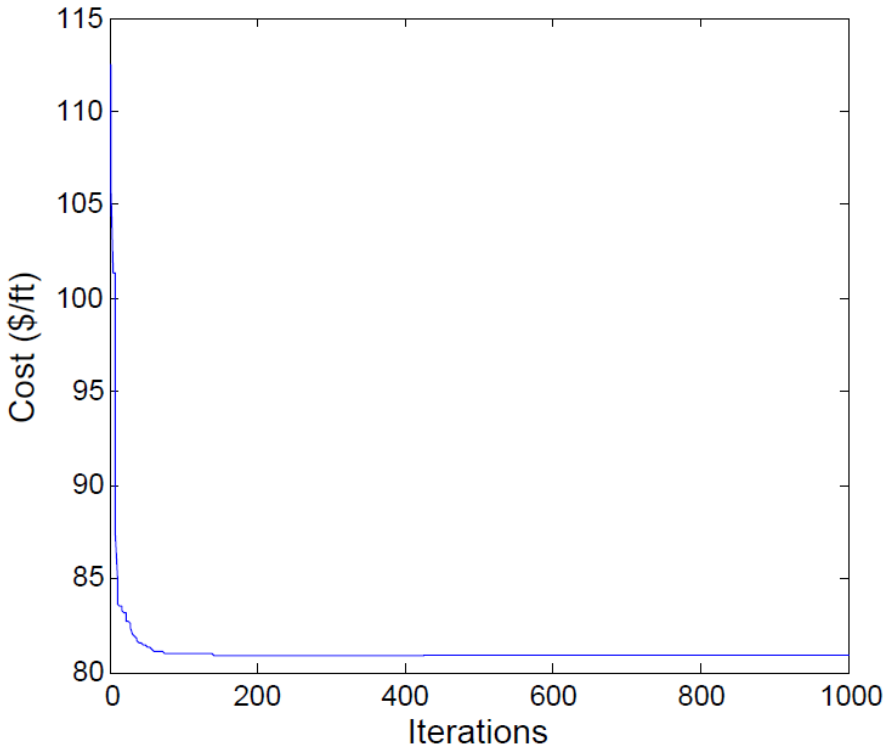


Figure 57: Optimal learning curve for field case WOB, RPM, and Pull Depth Optimization

4.3.3 WOB, RPM, Pull Depth, and Bit Selection Optimization

The last optimization done on the 12.25 well data was a complete optimization. The PSO algorithm optimized WOB, RPM, bit pull depth, and bit combination. The algorithm was allowed to select either order of using bit 1 and bit 2, or simply using the same type of bit twice. The solution from the optimization are shown below in Fig. 58 – Fig. 61.

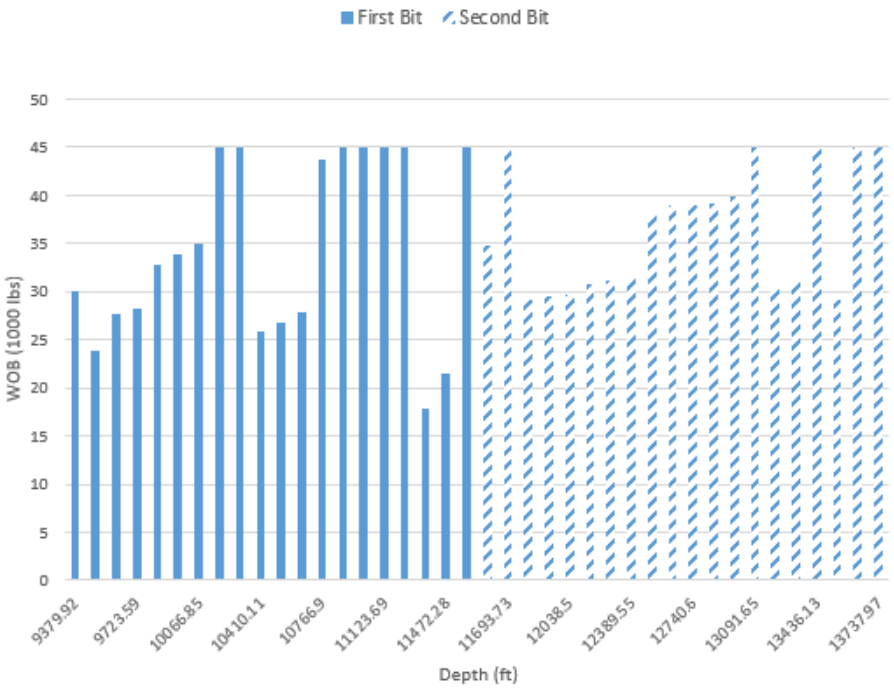


Figure 58: Optimal WOB for field case WOB, RPM, Pull Depth, and Bit Combination Optimization

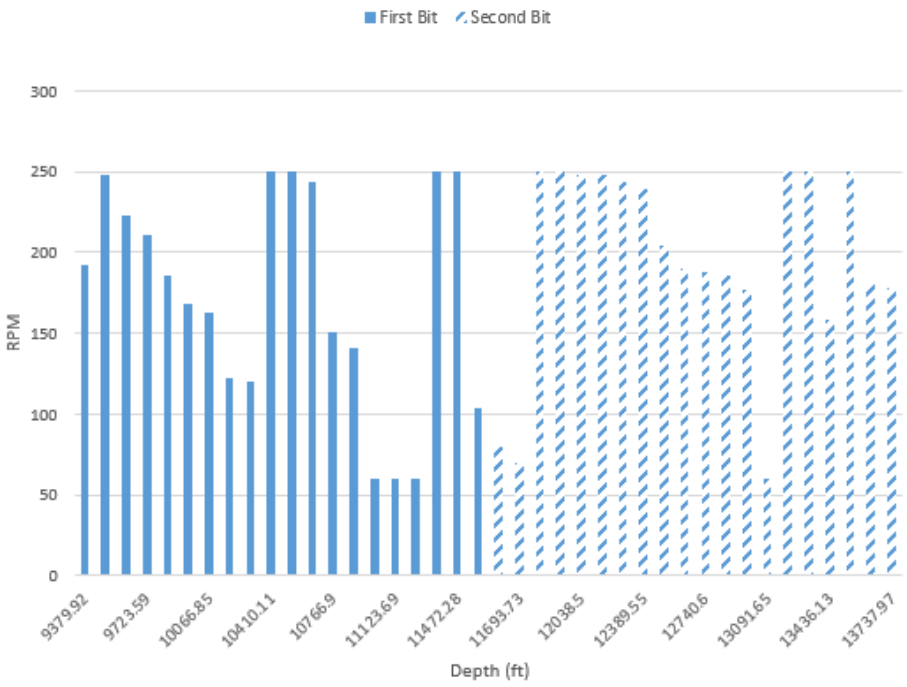


Figure 59: Optimal RPM for field case WOB, RPM, Pull Depth, and Bit Combination Optimization

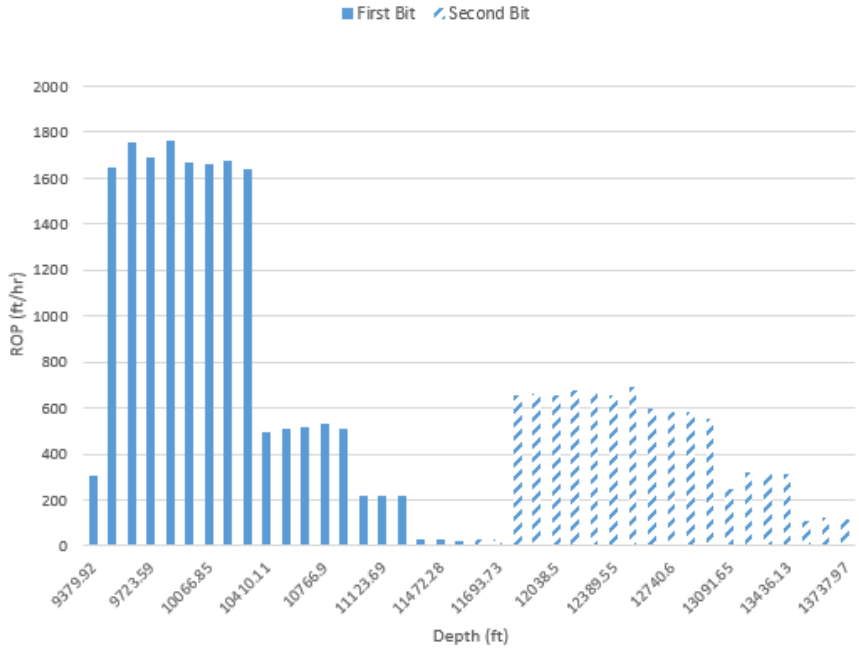


Figure 60: Optimal ROP for field case WOB, RPM, Pull Depth, and Bit Combination Optimization

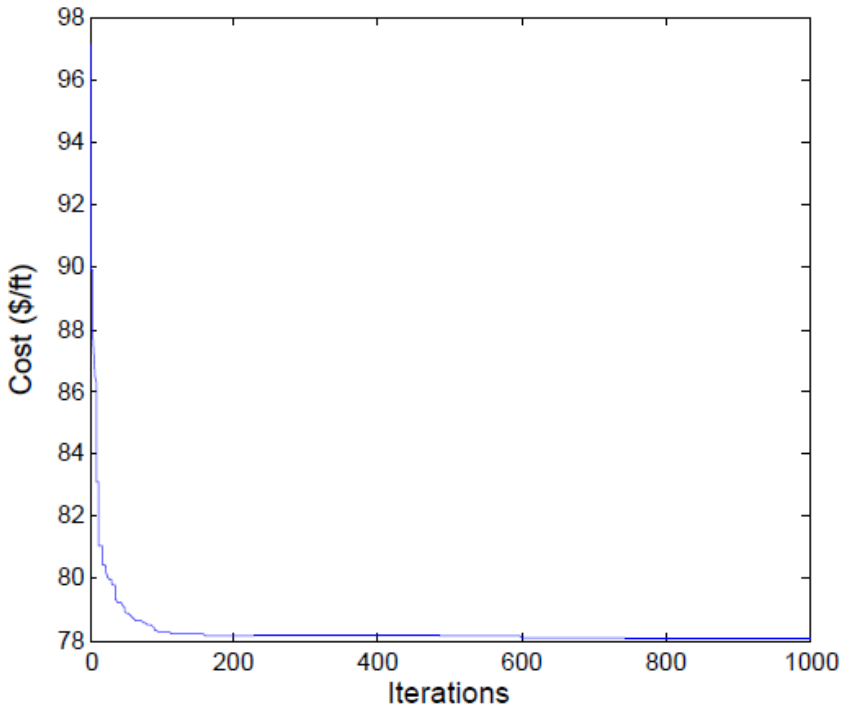


Figure 61: Optimal learning curve for field case WOB, RPM, Pull Depth, and Bit Combination Optimization

4.3.4 Field Case Results

Below are tables showing the rotating times and costs associated with each bit for all the simulations.

Table 11 below shows the data calculated using the real well data. The overall ROP through this section was 51.55 ft. /hr.

| | Depths Drilled | Rotating Time | Cost /ft. | Total Cost for Section Drilled |
|---|---|---|---|---|
| Bit 1: | 9379.92 – 11814.30 ft. | 39.59 hr. | 114.71 ($/ft.) | $ 279,242.13 |
| Bit 2: | 11814.30 – 13832.02 ft. | 46.78 hr. | 165.01 ($/ft.) | $ 332,953.20 |
| Total: | 4452.10 ft. | 86.37 hr. | 137.51 ($/ft.) | $ 612,195.33 |

Table 11: Rotating time and cost for real field case data

Table 12 shows the data from Section 4.3.1. This simulation used the same pull depth and final bit wear determined from the data, 0.45 for bit 1 and 0.825 for bit 2. As seen from the table below, only optimizing on WOB and RPM, the cost of drilling the well was reduced 13.81 $ /ft. and a total cost of $ 61,483.50. The overall ROP calculated was 62.17 ft. /hr.

| | Depths Drilled | Rotating Time | Cost /ft. | Total Cost for Section Drilled |
|---|---|---|---|---|
| Bit 1: | 9379.92 – 11814.30 ft. | 30.19 hr. | 98.63 ($/ft.) | $ 240,093.03 |
| Bit 2: | 11814.30 – 13832.02 ft. | 41.42 hr. | 153.94 ($/ft.) | $ 310,616.43 |
| Total: | 4452.10 ft. | 71.61 hr. | 123.70 ($/ft.) | $ 550,709.46 |

Table 12: Rotating time and cost for WOB and RPM Optimization

Table 13 represents the data from Section 4.3.2. The PSO code was allowed to select the WOB and RPM combinations, along with the optimal pull depth. The final bit wear for both bits were chosen as 0.5. Looking at the data in the table, the algorithm determined that the optimal solution was to drill the entire interval with the first bit. This increased the rotating time for the first bit, but this reduced the cost by not having to trip twice and not including the cost of the second bit. These solutions reduced the cost from the original well, as well as Table 12, resulting in an overall ROP of 77.51 ft. /hr.

| | Depths Drilled | Rotating Time | Cost /ft. | Total Cost for Section Drilled |
|---|---|---|---|---|
| Bit 1: | 9379.92 – 13832.02 ft. | 57.44 hr. | 80.85 ($/ft.) | $ 359,938.70 |
| Bit 2: | NA | 0.00 | 0.00 ($/ft.) | $ 0.00 |
| Total: | 4452.10 ft. | 57.44 hr. | 80.85 ($/ft.) | $ 359,938.70 |

Table 13: Rotating time and cost for WOB, RPM, and Pull Depth Optimization

The table below, Table 14, shows the results from Section 4.3.3. This simulation was a full optimization, allowing WOB, RPM, pull depth, and bit selection. The final wear for both bits was 0.5. For this simulation, the algorithm selected to pull the bit sooner than what was originally

done when drilling the well. It was also determined that the optimal bit selection was to use the first bit selection twice, instead of using bit 2. As expected, this simulation resulted in the lowest cost since all of the allowable variables were optimized. The overall ROP for the well was 174.11 ft. /hr. and this resulted in an overall savings in $ 264,527.72.

| | Depths Drilled | Rotating Time | Cost /ft. | Total Cost for Section Drilled |
|---|---|---|---|---|
| Bit 1: | 9379.92 – 11594.39 ft. | 11.41 hr. | 72.77 ($/ft.) | $ 161,155.18 |
| Bit 1: | 11594.39 – 13832.02 ft. | 14.16 hr. | 83.35 ($/ft.) | $ 186,512.43 |
| Total: | 4452.10 ft. | 25.57 hr. | 78.09 ($/ft.) | $ 347,667.61 |

Table 14: Rotating time and cost for WOB, RPM, Pull Depth, and Bit Combination Optimization

Below is a graph, Fig. 62, showing all three field case learning curves, along with the real field case data.

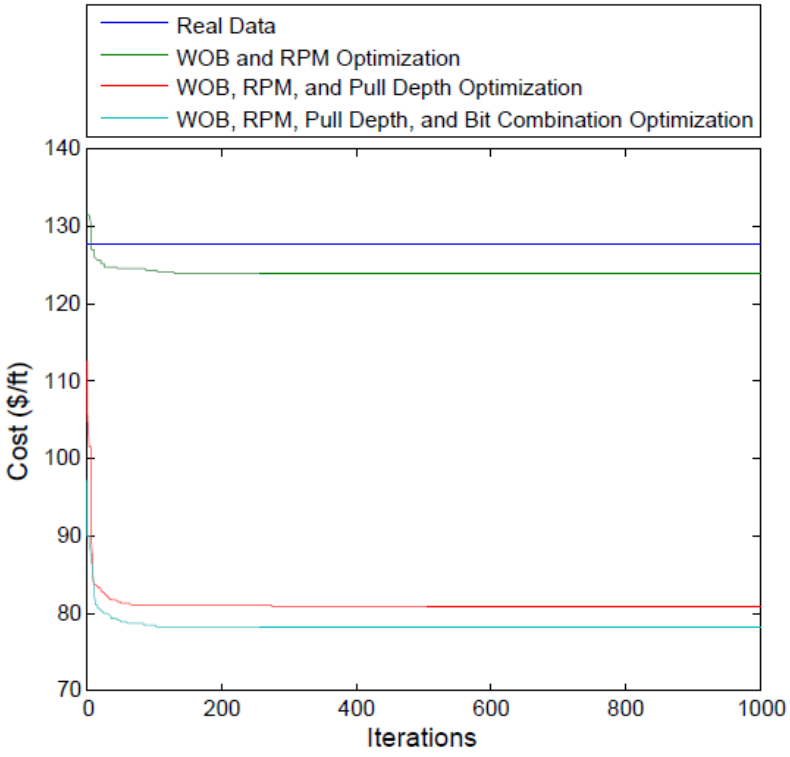


Figure 62: Learning curve showing all three field case optimizations, along with the real data

# CHAPTER V

# DISCUSSION

This study demonstrates a new approach to help find optimal combinations for WOB and RPM for both single bit runs and multiple bits, in addition to bit selection and optimal pull depths. Due to the drilling process having such an inherent sequential nature to it, caused by the bit wear in Eq. 5, there are an infinite possibilities of combinations. The research presented herein helps assist the user search the infinite combination space, and focus down on the optimal drilling point. Shown in the best solutions, the ideal point is not maximizing the instantaneous ROP for each depth point, but rather the overall time or cost to drill the section. If maximizing the ROP was incorporated in the drilling OF, the maximum allowable values for WOB and RPM would be used and the bit would be worn down to a set value before the goal depth was reached. In actuality, the optimal ROP values were found to maintain a constant ROP through a constant rock strength. The results do agree with the knowledge that the ROP decreases as the rock strength increases.

As seen in the results section, the optimal WOB and RPM values are shown, and these results reveal the WOB and RPM have opposite trends through a single rock formation. The WOB begins at a lower value and trends upwards until a new rock strength is reached. In contrast, the RPM values begin higher and gradually lowers through the rock. If the code was run iteratively by decreasing the depth step sizes over one drilling interval, i.e. 3600 – 4000 ft., the exact values

for WOB and RPM found would be representative for the average operational drilling parameters for that interval. The WOB and RPM results also show how large changes in rock strength affect the solutions for RPM and WOB. Analyzing the rock scenarios, both RPM and WOB trends adjust to account for the change in the rock strengths. Another outcome can be seen by comparing the average values for WOB and RPM for each rock strength. While holding abrasiveness constant, Section 4.1.5, the average WOB and RPM ranges increase as the rock strength increases. Conversely, changing abrasiveness values shown in Section 4.1.6, the average WOB and RPM decrease as the rock strength increases. A possible reason may be a combination of the two variables; rock strength and abrasiveness, increasing in Eq. 5. If the average WOB and RPM values increased as the rock got harder, the overall ROP would decrease, and potentially result in the bit getting worn down before the goal depth is reached.

Analyzing all solutions from the results section, it can be seen that every scenario used the full potential life of the bit. Meaning, for all the tests, the final wear out was 0.5, which matches the lowest bit wear value specified. This result is true for both one bit and two bit optimizations. The result agrees with common knowledge that the most efficient drilling would be to maximize the allowable bit wear. If the final wear of a bit was not equal to 0.5, this would imply that the algorithm did not maximize the results, meaning the optimal value was not found and leaving potential bit life unused.

In addition to the WOB and RPM trends, the PSO selected the second bit proposal for all bits used for both two bit rock strength scenarios, Section 4.2. This is potentially a result of the higher wear resistance for bit 2. Regarding the optimal pull depth, the swarm algorithm selected for the bit to be pulled in the hardest rock. A likely reason to change bits during the hardest rock section is to help ensure that ROP does not significantly drop off as the bits wear.

Analyzing the field case scenario, it can be seen as the number of allowable parameters optimized

increase, the overall cost reduced, while the overall ROP increased. This result can be shown in Section 4.3.4. When just optimizing on WOB and RPM, the cost for the well reduced by $ 61,483.50. Once bit pull depth was allowed to be optimized, the overall cost for the well was reduced by $ 252,256.63, even while using less life of bit 1 and using none of bit 2. Finally, when the well was fully optimized, the cost was reduced by $ 264,527.72, and this results in a total cost reduction of 43%. These results show tremendous potential for the use of this optimization approach, and should produce better findings with an increase in more optimized parameters.

Since the solution of PSO results in a discrete output, incorporating a line fit technique could be very beneficial. This could be done by using the midpoints from each step and applying a line of best fit for the output data, allowing it to be transformed from the discrete space to a continuous space. If multiple rock strength sections or multiple bits are included, there will be different continuous functions for each. These continuous outputs would be useful in the future for integrating the results into the drilling process. Below are two examples, Fig. 63 – 64, using the results from Section 4.2.1.


Figure 63: Optimal WOB for the three rock strength, multiple bit scenario; 10,000, 15,000, and 20,000 psi with continuous trends

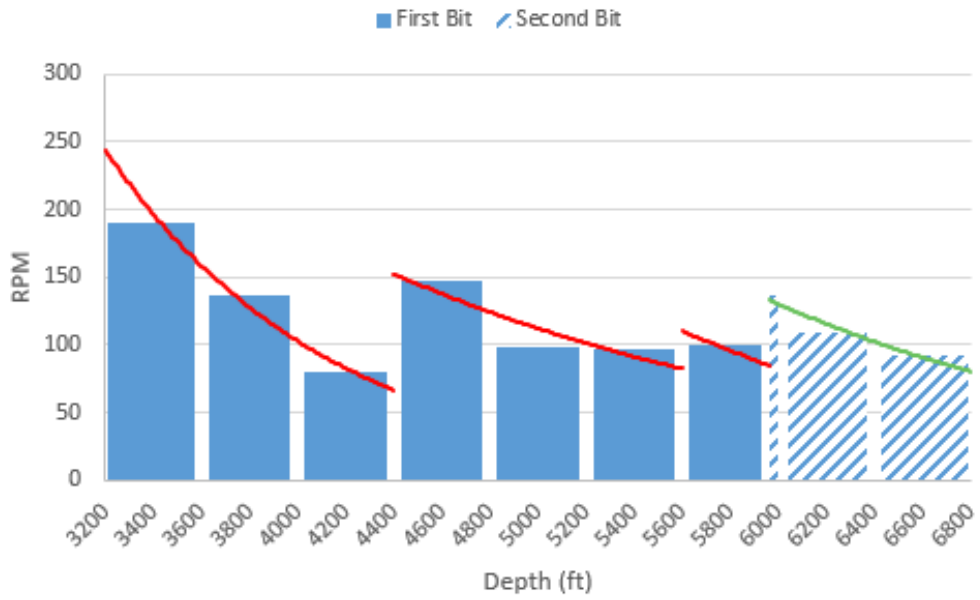


Figure 64: Optimal RPM for the three rock strength, multiple bit scenario; 10,000, 15,000, and 20,000 psi with continuous trends

During drilling there are many factors that are some common problems, such as stick-slip and bit instability, which can affect the drilling efficiency and cause increased drilling costs. To avoid such problems, the PSO algorithm can be modified to filter potential solutions which are considered unacceptable by the additional required criteria. This helps decrease the chances of these problems occurring during the drilling process.

In addition to these issues, in general when drilling a well, there are limitations on maximum ROP values. These restrictions could be due to limitations on the solids control system, annular solids loading and equivalent circulation density (ECD) issues, hole and bit cleaning, wellbore and particle settling, and in directional wells, a larger cuttings bed on the lower side of the annulus. Analyzing the field case validation scenarios, Section 4.3, the solutions do not have a limitation on ROP values since the results are to analyze theoretical optimal drilling solutions. Some of the results have very high ROP values, especially in the second rock strength section. These high ROP values will result in a lower theoretical drilling time and cost, however, the rig

solids control system might not be able handle such high drilling rates. This could easily be addressed in the future by adding an additional criteria to the objective function for maximum ROP. This would lower the high ROP values and the swarm algorithm would adjust the rest of the well to compensate for the change.

# CHAPTER VI

# CONCLUSION

## 6.1 Summary

This study was done to see if drilling optimization could be achieved through an advanced swarm algorithm by introducing a procedure in determining optimal WOB and RPM combinations, in addition to, ideal bit choices and pull depths. The technique used, incorporated a step by step approach into analyze how altering different variables affected the simulation results. Since the drilling process is naturally sequential because of bit wear, Eq. 5, an advanced optimization algorithm was required to find optimal solutions. The analysis in this study, analyzed the effects of rock strength, abrasiveness, bit selection, pull depth, and bit wear. Applying the approach and algorithm to an actual filed case showed potential for substantial reduction in drilling cost. For the actual field case of a 12.25 in. hole section in the North Sea optimized a potential cost reduction of 43% was seen. The findings from this algorithm show potential, and are very encouraging that this research could eventually fully optimize the entire drilling process.

## 6.2 Future Work

This research will be developed further in the future by incorporating torque and drag analysis, which would transform the algorithm's output to produce surface variables. In addition to torque and drag analysis, the algorithm will generically create bit designs for optimization, along with

incorporating both PDC bits and roller cone bit combinations for optimization.

# REFERENCES


Arabjamaloei, R., & Shadizadeh, S. (2011). Modeling and optimizing rate of penetration using intelligent systems in an Iranian southern oil field (Ahwaz oil field). Petroleum Science and Technology, 29(16), 1637-1648.

Atashnezhad, A., Wood, D. A., Fereidounpour, A., & Khosravanian, R. (2014). Designing and optimizing deviated wellbore trajectories using novel particle swarm algorithms. Journal of Natural Gas Science and Engineering, 21, 1184-1204.

Bangerth, W., Klie, H., Wheeler, M. F., Stoffa, P. L., & Sen, M. K. (2006). On optimization algorithms for the reservoir oil well placement problem. Computational Geosciences, 10(3), 303-319.

Blum, C., & Li, X. (2008). Swarm intelligence in optimization (pp. 43-85). Springer Berlin Heidelberg.

Bourgoyne Jr, A. T., & Young Jr, F. S. (1974). A multiple regression approach to optimal drilling and abnormal pressure detection. Society of Petroleum Engineers Journal, 14(04), 371-384.

Bourgoyne, A. T., Millheim, K. K., Chenevert, M. E., & Young, F. S. (1986). Applied drilling engineering.

Bratli, R. K., Hareland, G., Stene, F., Dunsaed, G. W., & Gjelstad, G. (1997, January). Drilling optimization software verified in the North Sea. In Paper SPE 39007 presented at SPE LACPEC Conference in Rio De Janeiro, Brazil, August.

Charlez, P. A. (1999, January 1). The Concept of Mud Weight Window Applied to Complex Drilling. Society of Petroleum Engineers. doi:10.2118/56758-MS

Cormen, T. H. (2009). *Introduction to algorithms.* MIT press.

Elbeltagi, E., Hegazy, T., & Grierson, D. (2005). Comparison among five evolutionary-based optimization algorithms. *Advanced engineering informatics*, *19*(1), 43-53.

Eren, T. (2010). Real-time-optimization of drilling parameters during drilling operations (Doctoral dissertation, Middle East Technical University).

Galle, E. M., & Woods, H. B. (1963, January). Best Constant Weight and Rotary Speed for Rotary Rock Bits. In Drilling and Production Practice. American Petroleum Institute.

Gjelstad, G., Hareland, G., Nikolaisen, K. N., & Bratli, R. K. (1998, January). The method of reducing drilling costs more than 50 percent. In SPE/ISRM Rock Mechanics in Petroleum Engineering. Society of Petroleum Engineers.

Graham, J. W., & Muench, N. L. (1959, January). Analytical determination of optimum bit weight and rotary speed combinations. In Fall Meeting of the Society of Petroleum Engineers of AIME. Society of Petroleum Engineers.

Hamrick, T. R. (2011). Optimization of Operating Parameters for Minimum Mechanical Specific Energy in Drilling (Doctoral dissertation, West Virginia University).

Hareland, G. (1988). *Shale and Limestone drill off tests*. [data file]. Amoco Drilling Research Laboratory. Tulsa, OK.

Hareland, G., & Hoberock, L. L. (1993, January). Use of drilling parameters to predict in-situ stress bounds. In SPE/IADC Drilling Conference. Society of Petroleum Engineers.

Hareland, G., & Rampersad, P. R. (1994, January). Drag-bit model including wear. In SPE Latin America/Caribbean Petroleum Engineering Conference. Society of Petroleum Engineers.

Hareland, G., Wu, A., & Rashidi, B. (2010, January 1). A Drilling Rate Model for Roller Cone Bits and Its Application. Society of Petroleum Engineers. doi:10.2118/129592-MS

Helms, L. Horizontal drilling. 2008. DMR newsletter, 35(1):1–3.

Kaiser, M. J. (2009). Modeling the time and cost to drill an offshore well. Energy, 34(9), 1097-1112.

Kennedy, J. (2011). Particle swarm optimization. In Encyclopedia of machine learning (pp. 760-766). Springer US.

Kerkar, P. B., Hareland, G., Fonseca, E. R., & Hackbarth, C. J. (2014, January). Estimation of Rock Compressive Strength Using Downhole Weight-on-Bit and Drilling Models. In IPTC 2014: International Petroleum Technology Conference.

Onwunalu, J. E., & Durlofsky, L. J. (2010). Application of a particle swarm optimization algorithm for determining optimum well location and type. Computational Geosciences, 14(1), 183-198.

Rashidi, B. (2011). Performance, Simulation and Field Application Modeling of Rollercone and PDC Drill Bits (Doctoral dissertation, University of Calgary).

Rastegar, M., Hareland, G., Nygaard, R., & Bashari, A. (2008, January). Optimization of multiple bit runs based on ROP models and cost equation: a new methodology applied for one of the Persian Gulf carbonate fields. In IADC/SPE Asia Pacific Drilling Technology Conference and Exhibition. Society of Petroleum Engineers.

Reed, R. L. (1972). A Monte Carlo Approach to Optimal Drilling. Society of Petroleum Engineers Journal, 12(05), 423-438.

Rejeb, L., Guessoum, Z., & M'Hallah, R. (2005, March). The exploration-exploitation dilemma for adaptive agents. In Proceedings of the Fifth European Workshop on Adaptive Agents and Multi-Agent Systems.

Self, R., Atashnezhad, A., and Hareland, G. (2016A, September). Reducing Drilling Cost by finding Optimal Operational Parameters using Particle Swarm Algorithm. Presented at the Society of Petroleum Engineers (SPE) Deepwater Drilling & Completions Conference, Galveston, Texas, 14 – 15 September. SPE-180280-MS.

Self, R., Atashnezhad, A., and Hareland, G. (2016B, June). Use of a Swarm Algorithm to Reduce the Drilling Time through Measurable Improvement in Rate of Penetration. Presented at the American Rock Mechanics Association (ARMA) Symposium, Houston, Texas, 26 – 29 June. ARMA 16-456.

Speer, J. W. (1958, January). A method for determining optimum drilling techniques. In Drilling and Production Practice. American Petroleum Institute.

Teale, R. (1965, March). The concept of specific energy in rock drilling. In International Journal of Rock Mechanics and Mining Sciences & Geomechanics Abstracts (Vol. 2, No. 1, pp. 57-73). Pergamon.

Warren, T. M. (1981). Drilling model for soft-formation bits. Journal of Petroleum Technology, 33(06), 963-970.

Warren, T. M. (1987). Penetration rate performance of roller cone bits. SPE Drilling Engineering, 2(01), 9-18.

Winters, W. J., Warren, T. M., & Onyia, E. C. (1987, January). Roller bit model with rock ductility and cone offset. In SPE Annual Technical Conference and Exhibition. Society of Petroleum Engineers.

Wu, A., Hareland, G., & Fazaelizadeh, M. (2011). Torque & drag analysis using finite element method. Modern Applied Science, 5(6), 13.

# APPENDIX

Data Summary for WOB and RPM Optimization of Field Case

| CCS | ABR | WOB | RPM | MD | $W_f$ | b(x) | h(x) | ROP |
|---|---|---|---|---|---|---|---|---|
| 7,547.00 | 0.0612 | 15.55 | 249.82 | 9379.92 | 0.970 | 0.90 | 1.00 | 186.43 |
| 3,352.80 | 0.0256 | 13.95 | 250.00 | 9494.75 | 0.967 | 0.90 | 1.00 | 907.30 |
| 3,352.80 | 0.0256 | 16.36 | 250.00 | 9609.17 | 0.963 | 0.90 | 1.00 | 1085.68 |
| 3,352.80 | 0.0256 | 16.81 | 199.51 | 9723.59 | 0.960 | 0.90 | 1.00 | 897.44 |
| 3,352.80 | 0.0256 | 23.70 | 143.29 | 9838.01 | 0.957 | 0.91 | 1.00 | 963.80 |
| 3,352.80 | 0.0256 | 26.30 | 143.20 | 9952.43 | 0.954 | 0.91 | 1.00 | 1081.76 |
| 3,352.80 | 0.0256 | 27.74 | 120.98 | 10066.85 | 0.951 | 0.91 | 1.00 | 973.84 |
| 3,352.80 | 0.0256 | 33.11 | 99.70 | 10181.27 | 0.948 | 0.91 | 1.00 | 986.76 |
| 3,352.80 | 0.0256 | 44.96 | 60.00 | 10295.69 | 0.945 | 0.92 | 1.00 | 855.63 |
| 6,037.00 | 0.0447 | 16.82 | 233.17 | 10410.11 | 0.936 | 0.90 | 1.00 | 290.91 |
| 6,037.00 | 0.0447 | 18.26 | 216.66 | 10529.04 | 0.926 | 0.90 | 1.00 | 294.73 |
| 6,037.00 | 0.0447 | 20.16 | 211.66 | 10647.97 | 0.917 | 0.90 | 1.00 | 319.70 |
| 6,037.00 | 0.0447 | 21.64 | 207.92 | 10766.90 | 0.908 | 0.90 | 1.00 | 337.55 |
| 6,037.00 | 0.0447 | 23.47 | 170.47 | 10885.83 | 0.899 | 0.90 | 1.00 | 302.63 |
| 6,037.00 | 0.0447 | 25.05 | 150.65 | 11004.76 | 0.892 | 0.90 | 1.00 | 286.86 |
| 6,037.00 | 0.0447 | 36.10 | 94.59 | 11123.69 | 0.884 | 0.91 | 1.00 | 275.95 |
| 6,037.00 | 0.0447 | 41.70 | 60.00 | 11242.62 | 0.879 | 0.92 | 1.00 | 208.00 |
| 17,399.00 | 0.4750 | 11.24 | 227.61 | 11361.55 | 0.767 | 0.90 | 1.00 | 17.26 |
| 17,399.00 | 0.4750 | 21.91 | 127.04 | 11472.28 | 0.659 | 0.91 | 1.00 | 18.46 |
| 17,399.00 | 0.4750 | 23.48 | 125.89 | 11583.01 | 0.558 | 0.91 | 1.00 | 17.02 |
| 17,399.00 | 0.4750 | 28.21 | 123.56 | 11693.73 | 0.450 | 0.91 | 1.00 | 17.48 |
| 4,889.49 | 0.0352 | 28.81 | 248.21 | 11804.46 | 0.450 | 0.90 | 1.00 | 429.13 |
| 4,889.49 | 0.0352 | 7.29 | 250.00 | 11814.30 | 0.987 | 0.90 | 1.00 | 87.75 |
| 4,889.49 | 0.0352 | 8.48 | 215.41 | 11921.48 | 0.978 | 0.90 | 1.00 | 89.27 |
| 4,889.49 | 0.0352 | 8.98 | 210.65 | 12038.50 | 0.970 | 0.90 | 1.00 | 92.52 |
| 4,889.49 | 0.0352 | 9.78 | 179.87 | 12155.51 | 0.963 | 0.90 | 1.00 | 86.84 |
| 4,889.49 | 0.0352 | 9.90 | 177.04 | 12272.53 | 0.956 | 0.90 | 1.00 | 86.12 |

| | | | | | | | | |
|---|---|---|---|---|---|---|---|---|
| 4,889.49 | 0.0352 | 10.00 | 177.02 | 12389.55 | 0.950 | 0.90 | 1.00 | 86.47 |
| 4,889.49 | 0.0352 | 10.55 | 169.65 | 12506.56 | 0.944 | 0.90 | 1.00 | 87.74 |
| 4,889.49 | 0.0352 | 16.00 | 109.41 | 12623.58 | 0.939 | 0.91 | 0.94 | 86.16 |
| 4,889.49 | 0.0352 | 17.38 | 107.37 | 12740.60 | 0.933 | 0.91 | 0.94 | 92.67 |
| 4,889.49 | 0.0352 | 18.05 | 97.55 | 12857.61 | 0.927 | 0.91 | 0.95 | 88.37 |
| 4,889.49 | 0.0352 | 18.72 | 92.01 | 12974.63 | 0.922 | 0.91 | 0.93 | 85.25 |
| 4,889.49 | 0.0352 | 26.67 | 63.63 | 13091.65 | 0.916 | 0.92 | 1.00 | 95.70 |
| 6,691.57 | 0.0513 | 8.90 | 222.95 | 13208.66 | 0.907 | 0.90 | 1.00 | 46.30 |
| 6,691.57 | 0.0513 | 9.48 | 206.10 | 13322.40 | 0.897 | 0.90 | 1.00 | 45.63 |
| 6,691.57 | 0.0513 | 28.49 | 60.00 | 13436.13 | 0.888 | 0.92 | 1.00 | 48.54 |
| 10,492.50 | 0.1130 | 10.82 | 154.90 | 13549.87 | 0.867 | 0.90 | 1.00 | 15.07 |
| 10,492.50 | 0.1130 | 25.20 | 60.00 | 13643.92 | 0.845 | 0.92 | 0.99 | 15.45 |
| 10,492.50 | 0.1130 | 25.67 | 60.00 | 13737.97 | 0.825 | 0.92 | 1.00 | 15.49 |

Table A-1: Data from WOB and RPM Optimization of Field Case

Data Summary for WOB, RPM, and Pull Depth Optimization of Field Case

| CCS | ABR | WOB | RPM | MD | $W_f$ | b(x) | h(x) | ROP |
|---|---|---|---|---|---|---|---|---|
| 7,547.00 | 0.0612 | 18.99 | 119.26 | 9379.92 | 0.978 | 0.91 | 1.00 | 114.75 |
| 3,352.80 | 0.0256 | 10.59 | 250.00 | 9494.75 | 0.975 | 0.90 | 1.00 | 666.38 |
| 3,352.80 | 0.0256 | 12.04 | 240.13 | 9609.17 | 0.972 | 0.90 | 1.00 | 740.21 |
| 3,352.80 | 0.0256 | 17.26 | 144.32 | 9723.59 | 0.969 | 0.91 | 1.00 | 682.39 |
| 3,352.80 | 0.0256 | 18.43 | 137.51 | 9838.01 | 0.967 | 0.91 | 1.00 | 700.40 |
| 3,352.80 | 0.0256 | 25.37 | 93.75 | 9952.43 | 0.964 | 0.91 | 1.00 | 696.13 |
| 3,352.80 | 0.0256 | 44.47 | 60.00 | 10066.85 | 0.961 | 0.92 | 1.00 | 859.50 |
| 3,352.80 | 0.0256 | 45.00 | 60.00 | 10181.27 | 0.958 | 0.92 | 1.00 | 868.66 |
| 3,352.80 | 0.0256 | 45.00 | 60.00 | 10295.69 | 0.955 | 0.92 | 1.00 | 865.98 |
| 6,037.00 | 0.0447 | 11.10 | 250.00 | 10410.11 | 0.948 | 0.90 | 1.00 | 195.04 |
| 6,037.00 | 0.0447 | 11.30 | 250.00 | 10529.04 | 0.941 | 0.90 | 1.00 | 197.63 |
| 6,037.00 | 0.0447 | 11.63 | 250.00 | 10647.97 | 0.934 | 0.90 | 1.00 | 202.77 |
| 6,037.00 | 0.0447 | 20.61 | 135.50 | 10766.90 | 0.927 | 0.91 | 1.00 | 214.83 |
| 6,037.00 | 0.0447 | 22.86 | 110.21 | 10885.83 | 0.921 | 0.91 | 1.00 | 196.72 |
| 6,037.00 | 0.0447 | 27.15 | 89.72 | 11004.76 | 0.915 | 0.91 | 1.00 | 195.24 |
| 6,037.00 | 0.0447 | 35.33 | 60.06 | 11123.69 | 0.910 | 0.92 | 1.00 | 178.06 |
| 6,037.00 | 0.0447 | 37.54 | 60.00 | 11242.62 | 0.904 | 0.92 | 1.00 | 189.60 |
| 17,399.00 | 0.4750 | 7.31 | 250.00 | 11361.55 | 0.817 | 0.90 | 1.00 | 11.85 |
| 17,399.00 | 0.4750 | 10.09 | 188.56 | 11472.28 | 0.740 | 0.90 | 1.00 | 11.81 |
| 17,399.00 | 0.4750 | 14.63 | 135.81 | 11583.01 | 0.665 | 0.91 | 1.00 | 11.94 |
| 17,399.00 | 0.4750 | 31.36 | 60.00 | 11693.73 | 0.590 | 0.92 | 1.00 | 11.69 |
| 4,889.49 | 0.0352 | 17.49 | 250.00 | 11804.46 | 0.587 | 0.90 | 1.00 | 319.03 |

| | | | | | | | | |
|---|---|---|---|---|---|---|---|---|
| 4,889.49 | 0.0352 | 18.66 | 249.28 | 11921.48 | 0.584 | 0.90 | 1.00 | 341.25 |
| 4,889.49 | 0.0352 | 20.59 | 223.03 | 12038.50 | 0.581 | 0.90 | 1.00 | 341.36 |
| 4,889.49 | 0.0352 | 21.03 | 213.06 | 12155.51 | 0.578 | 0.90 | 1.00 | 332.83 |
| 4,889.49 | 0.0352 | 28.30 | 147.33 | 12272.53 | 0.575 | 0.90 | 1.00 | 326.03 |
| 4,889.49 | 0.0352 | 28.61 | 143.56 | 12389.55 | 0.572 | 0.91 | 1.00 | 320.31 |
| 4,889.49 | 0.0352 | 29.83 | 141.29 | 12506.56 | 0.569 | 0.91 | 1.00 | 329.26 |
| 4,889.49 | 0.0352 | 30.22 | 138.40 | 12623.58 | 0.567 | 0.91 | 1.00 | 325.88 |
| 4,889.49 | 0.0352 | 31.10 | 128.16 | 12740.60 | 0.564 | 0.91 | 0.91 | 283.56 |
| 4,889.49 | 0.0352 | 34.60 | 123.04 | 12857.61 | 0.561 | 0.91 | 0.92 | 308.02 |
| 4,889.49 | 0.0352 | 38.75 | 100.09 | 12974.63 | 0.558 | 0.91 | 0.92 | 288.10 |
| 4,889.49 | 0.0352 | 45.00 | 60.00 | 13091.65 | 0.556 | 0.92 | 0.91 | 204.41 |
| 6,691.57 | 0.0513 | 45.00 | 77.64 | 13208.66 | 0.550 | 0.92 | 1.00 | 146.80 |
| 6,691.57 | 0.0513 | 45.00 | 60.37 | 13322.40 | 0.546 | 0.92 | 1.00 | 114.03 |
| 6,691.57 | 0.0513 | 45.00 | 60.05 | 13436.13 | 0.542 | 0.92 | 1.00 | 112.57 |
| 10,492.50 | 0.1130 | 22.46 | 169.72 | 13549.87 | 0.528 | 0.90 | 1.00 | 52.41 |
| 10,492.50 | 0.1130 | 22.58 | 163.64 | 13643.92 | 0.515 | 0.90 | 1.00 | 49.60 |
| 10,492.50 | 0.1130 | 28.59 | 137.04 | 13737.97 | 0.500 | 0.91 | 0.97 | 51.81 |

Table A-2: Data from WOB, RPM and Pull Depth Optimization of Field Case

Data Summary for WOB, RPM, Pull Depth, and Bit Combination Optimization of Field Case

| CCS | ABR | WOB | RPM | MD | $W_f$ | b(x) | h(x) | ROP |
|---|---|---|---|---|---|---|---|---|
| 7,547.00 | 0.0612 | 30.07 | 192.45 | 9379.92 | 0.960 | 0.90 | 1.00 | 309.09 |
| 3,352.80 | 0.0256 | 23.81 | 247.71 | 9494.75 | 0.955 | 0.90 | 1.00 | 1643.71 |
| 3,352.80 | 0.0256 | 27.63 | 223.04 | 9609.17 | 0.950 | 0.90 | 1.00 | 1753.12 |
| 3,352.80 | 0.0256 | 28.16 | 210.83 | 9723.59 | 0.945 | 0.90 | 1.00 | 1688.30 |
| 3,352.80 | 0.0256 | 32.69 | 185.29 | 9838.01 | 0.940 | 0.90 | 1.00 | 1759.78 |
| 3,352.80 | 0.0256 | 33.86 | 168.75 | 9952.43 | 0.936 | 0.90 | 1.00 | 1665.84 |
| 3,352.80 | 0.0256 | 34.92 | 162.85 | 10066.85 | 0.932 | 0.90 | 1.00 | 1659.65 |
| 3,352.80 | 0.0256 | 45.00 | 122.04 | 10181.27 | 0.927 | 0.91 | 1.00 | 1672.79 |
| 3,352.80 | 0.0256 | 45.00 | 120.24 | 10295.69 | 0.923 | 0.91 | 1.00 | 1641.53 |
| 6,037.00 | 0.0447 | 25.79 | 250.00 | 10410.11 | 0.910 | 0.90 | 1.00 | 496.90 |
| 6,037.00 | 0.0447 | 26.70 | 249.79 | 10529.04 | 0.897 | 0.90 | 1.00 | 509.09 |
| 6,037.00 | 0.0447 | 27.94 | 243.97 | 10647.97 | 0.884 | 0.90 | 1.00 | 516.72 |
| 6,037.00 | 0.0447 | 43.69 | 150.80 | 10766.90 | 0.872 | 0.90 | 1.00 | 535.00 |
| 6,037.00 | 0.0447 | 45.00 | 140.79 | 10885.83 | 0.860 | 0.91 | 1.00 | 510.54 |
| 6,037.00 | 0.0447 | 45.00 | 60.00 | 11004.76 | 0.854 | 0.92 | 1.00 | 220.81 |
| 6,037.00 | 0.0447 | 45.00 | 60.00 | 11123.69 | 0.849 | 0.92 | 1.00 | 219.36 |
| 6,037.00 | 0.0447 | 45.00 | 60.00 | 11242.62 | 0.843 | 0.92 | 1.00 | 217.94 |
| 17,399.00 | 0.4750 | 17.78 | 250.00 | 11361.55 | 0.676 | 0.90 | 1.00 | 30.72 |

| | | | | | | | | |
|---|---|---|---|---|---|---|---|---|
| 17,399.00 | 0.4750 | 21.48 | 250.00 | 11472.28 | 0.515 | 0.90 | 1.00 | 30.61 |
| 17,399.00 | 0.4750 | 44.94 | 103.57 | 11583.01 | 0.500 | 0.91 | 1.00 | 23.24 |
| 17,399.00 | 0.4750 | 34.71 | 80.23 | 11594.39 | 0.818 | 0.92 | 1.00 | 26.18 |
| 17,399.00 | 0.4750 | 44.89 | 70.40 | 11693.73 | 0.674 | 0.92 | 1.00 | 25.36 |
| 4,889.49 | 0.0352 | 29.09 | 250.00 | 11804.46 | 0.669 | 0.90 | 1.00 | 654.05 |
| 4,889.49 | 0.0352 | 29.58 | 250.00 | 11921.48 | 0.664 | 0.90 | 1.00 | 661.62 |
| 4,889.49 | 0.0352 | 29.60 | 248.38 | 12038.50 | 0.658 | 0.90 | 1.00 | 652.80 |
| 4,889.49 | 0.0352 | 30.80 | 247.53 | 12155.51 | 0.653 | 0.90 | 1.00 | 675.50 |
| 4,889.49 | 0.0352 | 31.15 | 244.03 | 12272.53 | 0.648 | 0.90 | 1.00 | 669.45 |
| 4,889.49 | 0.0352 | 31.40 | 239.06 | 12389.55 | 0.642 | 0.90 | 1.00 | 656.85 |
| 4,889.49 | 0.0352 | 37.85 | 204.73 | 12506.56 | 0.637 | 0.90 | 1.00 | 695.27 |
| 4,889.49 | 0.0352 | 38.89 | 189.89 | 12623.58 | 0.631 | 0.90 | 0.90 | 593.62 |
| 4,889.49 | 0.0352 | 38.89 | 187.93 | 12740.60 | 0.626 | 0.90 | 0.90 | 585.62 |
| 4,889.49 | 0.0352 | 39.21 | 185.25 | 12857.61 | 0.621 | 0.90 | 0.91 | 584.00 |
| 4,889.49 | 0.0352 | 39.80 | 177.34 | 12974.63 | 0.616 | 0.90 | 0.90 | 555.61 |
| 4,889.49 | 0.0352 | 45.00 | 60.00 | 13091.65 | 0.614 | 0.92 | 1.00 | 248.32 |
| 6,691.57 | 0.0513 | 30.24 | 250.00 | 13208.66 | 0.604 | 0.90 | 1.00 | 318.08 |
| 6,691.57 | 0.0513 | 30.88 | 250.00 | 13322.40 | 0.594 | 0.90 | 1.00 | 319.85 |
| 6,691.57 | 0.0513 | 45.00 | 158.61 | 13436.13 | 0.584 | 0.90 | 1.00 | 313.12 |
| 10,492.50 | 0.1130 | 29.16 | 250.00 | 13549.87 | 0.558 | 0.90 | 1.00 | 110.91 |
| 10,492.50 | 0.1130 | 45.00 | 180.01 | 13643.92 | 0.529 | 0.90 | 0.95 | 121.29 |
| 10,492.50 | 0.1130 | 45.00 | 178.43 | 13737.97 | 0.500 | 0.90 | 1.00 | 119.25 |

Table A-3: Data from WOB, RPM, Pull Depth, and Bit Combination Optimization of Field Case

VITA

Ryan Voyd Self

Candidate for the Degree of

Master of Science

Thesis: USE OF PARTCILE SWARM OPTIMIZATION ALGORITHM TO REDUCE DRILLING COSTS BY FINDING OPTIMAL OPERATIONAL PARAMETERS

Major Field: Mechanical and Aerospace Engineering

Biographical:

Education:

Completed the requirements for the Master of Science in Mechanical Engineering at Oklahoma State University, Stillwater, Oklahoma in July, 2016.

Completed the requirements for the Bachelor of Science in Mechanical Engineering at Oklahoma State University, Stillwater, Oklahoma in 2014.

Experience:

Engineering RA, Oklahoma State University, Fall 2014 – Summer 2016
- Developing a drilling parameter optimization algorithm

Engineering TA, Oklahoma State University, Fall 2013 – Spring 2014
- Guiding small groups to successful design and testing of solar collectors

Mechanical Engineering Intern, Ditch Witch®, Summer 2011
- Assisted in designing and assembling a test stand in SolidEdge for both the horizontal directional drill and the comparable competitive machine to evaluate machine performance for comparison purposes

Warehouse Worker, Ditch Witch®, Summer 2010
- Warehouse parts procurement matching parts lists and deliver to assembly

Red Lobster, Nov. 2009 – Dec. 2015

Professional Memberships:

Samson Energy Graduate Student Fellowship in PE, 2014 – Spring 2016
American Association of Drilling Engineers, Spring 2015 – Spring 2016
Society of Petroleum Engineers, Fall 2015
Wild Well Control Certificate, Spring 2015
Pi Tau Sigma Engineering Honors Society, Fall 2013